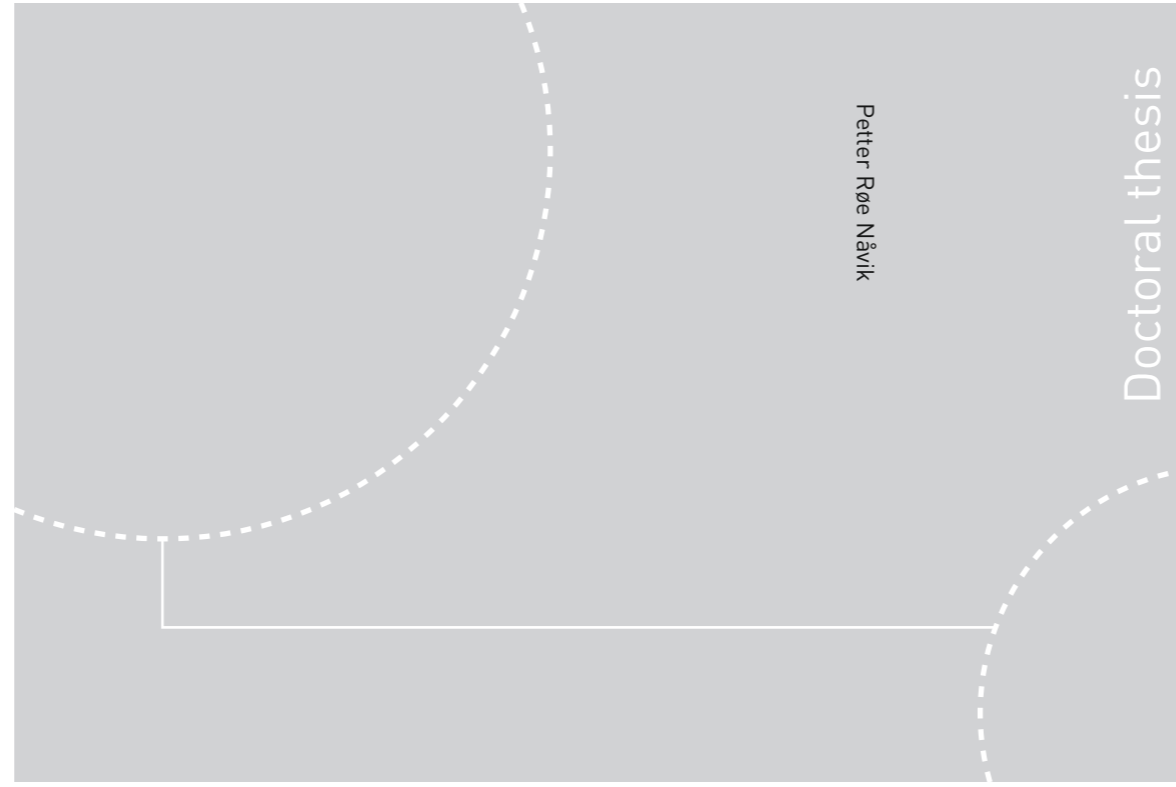


ISBN 978-82-326-1935-1 (printed ver.)  
ISBN 978-82-326-1934-4 (electronic ver.)  
ISSN 1503-8181



Doctoral theses at NTNU, 2016:298

Petter Røe Nåvik

# Dynamic behaviour of existing and new railway catenary systems under Norwegian conditions

Doctoral theses at NTNU, 2016:298

**NTNU**  
Norwegian University of  
Science and Technology  
Thesis for the Degree of  
Philosophiae Doctor  
Faculty of Engineering Science and Technology  
Department of Structural Engineering

 **NTNU**  
Norwegian University of  
Science and Technology

 **NTNU**  
Norwegian University of  
Science and Technology

 NTNU

Petter Røe Nåvik

# Dynamic behaviour of existing and new railway catenary systems under Norwegian conditions

Thesis for the Degree of Philosophiae Doctor

Trondheim, October 2016

Norwegian University of Science and Technology  
Faculty of Engineering Science and Technology  
Department of Structural Engineering



Norwegian University of  
Science and Technology

**NTNU**  
Norwegian University of Science and Technology

Thesis for the Degree of Philosophiae Doctor

Faculty of Engineering Science and Technology  
Department of Structural Engineering

© Petter Røe Nåvik

ISBN 978-82-326-1935-1 (printed ver.)  
ISBN 978-82-326-1934-4 (electronic ver.)  
ISSN 1503-8181

Doctoral theses at NTNU, 2016:298

Printed by NTNU Grafisk senter

**Abstract**

This thesis concerns the dynamic behaviour of railway catenary systems, particularly Norwegian systems. The aim of this PhD study is to increase the knowledge of the dynamic behaviour of these systems. This includes analyses of field measurements sampled during daily train operation and parameter studies by developing and using a detailed and validated numerical model.

A range of field measurements was obtained and analysed during the study. These include displacements, accelerations, rotational velocities, contact forces and geometries. A new and purpose-specific wireless monitoring system designed for field measurements was developed during the thesis and was used for sampling accelerations and rotational velocities. The monitoring system consists of up to ten wireless sensors and one master unit. The sensors can be mounted arbitrarily over a range of 1400 m. Triggering is mainly accomplished by passing trains, but manual triggering is made possible. Time synchronization of the sensors is ensured by a developed scheme. Furthermore, close-range photogrammetry and integrated accelerations were used to estimate and verify the displacement uplift time series. The analysed recorded contact forces were obtained from a database constructed by data from an overhead line recording locomotive. In addition, catenary geometry was measured by laser.

The study develops, presents and uses different methods for assessing the dynamic behaviour of railway catenary systems by evaluating both numerical simulations and field measurements. The methods include the use of power spectral density (PSD), short-time Fourier transforms (STFT), covariance-driven stochastic subspace method (Cov-SSI), histograms, cross-correlation and extreme value probability distributions.

The thesis demonstrates that the dynamic behaviour of railway catenary systems has a high grade of variability. This includes high variability in the frequency content that is shown to be substantially dependent on the position in a span, the properties of the span, the properties of each catenary section and the loading. This demonstrates the importance of establishing system frequencies and position-specific frequencies. The variability of the loading depends on the train speed, static uplift, type of pantograph and wear on pan heads. This makes it favourable to perform both overall analyses, including many train passages, and analyses of single train passages to obtain the full picture. In addition, the importance of the variability in the response at one point in the catenary during a train passage is demonstrated and requires that the analysis should be performed both for segments of the time series and for the whole time series. The study clearly suggests distinguishing pre- and post-

passage parts based on their difference in frequency content. In addition, clear differences found in the lateral and vertical response indicate that both should be included in a frequency investigation to improve interpretations.

The dynamic response was demonstrated to be a good tool for parameter study. It was used to evaluate changes in tension forces, the effect of rapid changes in contact wire height and differences depending on curvature. A damping study including analysis of data from three different catenary sections and several train passages resulted in proposed Rayleigh damping coefficients for numerical models.

Above all, this study highlights the complexity of the pantograph–catenary interaction.

**Preface**

This thesis is submitted in partial fulfilment of the requirements for the degree philosophiae doctor. The work for the thesis was carried out at the Department for Structural Engineering at the Norwegian University of Science and Technology (NTNU) with Anders Rønnquist, NTNU, as main supervisor and Sebastian Stichel, KTH Royal Institute of Technology, and Ole Øiseth, NTNU, as co-supervisors. Jernbaneverket (The Norwegian National Rail Administration) has funded the work. The thesis is based on journal papers that are either published or submitted. The thesis contains two parts. The first is an introductory section including the chapters introduction, railway catenary systems, numerical modelling, field measurements, measurement system, and summary of present investigations with concluding remarks. The second contains seven published or submitted journal papers.



## **Acknowledgements**

I take this opportunity to gratefully acknowledge those who have given me assistance and contributed to the work I have done during my PhD work.

I would like to express my deepest gratitude to my main supervisor Professor Anders Rønquist, who set the spark of my interest for railway catenary systems in the autumn of 2012, for making the PhD project a reality, for all assistance, for all collaboration and for many interesting conversations.

To my co-supervisor Sebastian Stichel for all discussions, guidance, assistance and collaboration.

To my co-supervisor Ole Øiseth for assistance when it has been needed.

To all the help I have received from Jernbaneverket. This thesis could not have been completed without it. To Sverre Kringtrø, Martin Rosvold and Stig Morten Myran for all the help with mounting the sensor system and being available for all sorts of questions. To Turgut Senuysal for help with the contact force database, for assistance regarding the data and for allowing me on board the overhead line recording train. To Thorleif Pedersen, Thor Egil Thoresen and Jomar Bredesen for help with general knowledge about Norwegian railway catenary systems. To Ragnhild Wahl for believing in the project and funding.

To Per Anders Jönsson for interesting discussions and help with the numerical model.

To Elektromotus at Rytis Karpuška, Karolis Tarasauskas and Gintautas Paluckas for our collaboration in developing the monitoring system.

To Einar Gotaas for helping in the development of the monitoring system.

To Knut Andreas Kvåle for many discussions and valuable input and for being able to stand sharing an office with me for these three years.

To Gunnstein Thomas Frøseth for valuable discussions, input and collaboration.

To Zhendong Liu, fellow PhD in railway catenary systems at KTH, for valuable discussions.

To my fellow PhDs and postdocs at the structural dynamics group, Øyvind Wiig Petersen, Torodd Skjerve Nord, Bartosz Siedziako, Aksel Fenerci, Yuwang Xu and Daniel Cantero Lauer for comments and discussions and for facilitating a good working environment.

Last, but not least, I want to express my gratitude to my family, particularly to Rosie for encouraging me to take on this project, for encouraging me during the project and for just being there for me.





---

## Contents

Abstract .....	I
Preface .....	III
Acknowledgements.....	V
Contents.....	VII
List of papers.....	IX
Other publications.....	XI
1. Introduction.....	1
2. Railway catenary systems.....	7
3. Numerical modelling.....	13
4. Monitoring system.....	15
5. Field measurements .....	19
6. Summary of present investigations with concluding remarks .....	23
7. Suggestions for future works .....	27
References .....	29
Further readings.....	33
Paper I.....	35
Paper II.....	47
Paper III.....	69
Paper IV .....	81
Paper V .....	93
Paper VI .....	115
Paper VII .....	139



---

## List of papers

The following journal papers are included in the thesis.

- I. Nåvik P, Rønnquist A, and Stichel S. The use of dynamic response to evaluate and improve the optimization of existing soft railway catenary systems for higher speeds. Proceedings of the Institution of Mechanical Engineers Part F Journal of Rail and Rapid Transit 2016;230(4):1388-1396 (Online 2015). DOI:10.1177/0954409715605140
- II. Rønnquist A, Nåvik P. Dynamic assessment of existing soft catenary systems using modal analysis to explore higher train velocities: A case study of a Norwegian contact line system. Vehicle System Dynamics 2015;53(6):756-774. DOI:10.1080/00423114.2015.1013040
- III. Nåvik P, Rønnquist A, and Stichel S. Identification of system damping in railway catenary wire systems from full-scale measurements. Engineering Structures 2016;113:71-78. DOI:10.1016/j.engstruct.2016.01.031
- IV. Nåvik P, Rønnquist A, and Stichel S. A wireless railway catenary structural monitoring system: Full-scale case study. Case Studies in Structural Engineering 2016;6:22-30 (Online 2016). DOI:10.1016/j.csse.2016.05.003
- V. Frøseth G T, Nåvik P, Rønnquist A. Operational displacement estimations of railway catenary systems by photogrammetry and the integration of acceleration time series. 2016. Submitted for journal publication.
- VI. Rønnquist A, Nåvik P. Vertical vs. lateral dynamic behaviour of soft catenaries subject to regular loading using field measurements. 2016. Submitted for journal publication.
- VII. Nåvik P, Rønnquist A, and Stichel S. Variation in predicting pantograph-catenary interaction contact forces, numerical simulations and field measurements. 2016. Submitted for journal publication.



---

## Other publications

The following publications resulted from the work carried out by the candidate during the PhD study, in addition to papers I–VII.

1. Nåvik P, Rønnquist A, 2016, Estimating the Damping of Existing Railway Catenary Sections from Full-Scale Measurements. Proceedings of the Third International Conference on Railway Technology: Research, Development and Maintenance, ed. J. Pombo. Civil-Comp Press, Stirlingshire, UK, Paper 103. DOI: 10.4203/ccp.110.103
2. Frøseth G T, Nåvik P, Rønnquist A, 2016, Close Range Photogrammetry for Measuring the Response of a Railway Catenary System. Proceedings of the Third International Conference on Railway Technology: Research, Development and Maintenance, ed. J. Pombo. Civil-Comp Press, Stirlingshire, UK, Paper 102. DOI: 10.4203/ccp.110.102
3. Rønnquist A, Nåvik P, 2016, Exploring Dynamic Behaviour of Soft Catenaries subject to Regular Loading using Full Scale Measurements. Proceedings of the Third International Conference on Railway Technology: Research, Development and Maintenance, ed. J. Pombo. Civil-Comp Press, Stirlingshire, UK, Paper 101 DOI: 10.4203/ccp.110.101
4. Rønnquist A, Nåvik P, 2016, Wireless Monitoring of the Dynamic Behavior of Railway Catenary Systems. Structural Health Monitoring, Damage Detection & Mechatronics, Volume 7: Proceedings of the 34th IMAC, A Conference and Exposition on Structural Dynamics
5. Nåvik P, Rønnquist A, 2015, Uplift-Monitoring for Dynamic Assessment of Electrical Railway Contact Lines. Dynamics of Civil Structures, Volume 2 Proceedings of the 33rd IMAC, A Conference and Exposition on Structural Dynamics. DOI: 10.1007/978-3-319-15248-6\_25
6. Nåvik P, Rønnquist A, 2014, Dynamic behaviour of an existing railway catenary system for extreme low passage at exceeding design velocities. Proceedings of the 9th International Conference on Structural Dynamics, EURODYN 2014
7. Rønnquist A, Nåvik P, 2014, Dynamic implications for higher speed in sharp curves of an existing Norwegian overhead contact line system for electric railways. Proceedings of the 9th International Conference on Structural Dynamics, EURODYN 2014
8. Nåvik P, Rønnquist A, 2014, Dynamic Optimization of an Existing Catenary System when Exceeding Design Speed. Proceedings of the Second International Conference on Railway Technology: Research, Development and Maintenance, ed. J. Pombo. Civil-Comp Press, Stirlingshire, UK, Paper 138. DOI:10.4203/ccp.104.138
9. Rønnquist A, Nåvik P, 2014, Dynamic Assessment of a Norwegian Contact Line: Exploring Higher Speed in Sharp Curves. Proceedings of the Second International Conference on Railway Technology: Research, Development and Maintenance, ed. J. Pombo. Civil-Comp Press, Stirlingshire, UK, Paper 139. DOI: 10.4203/ccp.104.139



## 1. Introduction

The railway catenary system, together with the pantograph, is responsible for ensuring an uninterrupted power supply to trains. The interaction between these two nonlinear dynamic systems, called the pantograph-catenary interaction, is dependent on the dynamic behaviour of both parts, separately and as a coupled system. Thus, the dynamic behaviour of railway catenary systems is essential for running electrical locomotives. In general, a good structural understanding is always important, for both assessing and improving the behaviour of existing structures and for designing new structures and understanding this complex interaction [1]. Assessment of the dynamic behaviour of existing structures is important. This is because they are already in use under conditions that differ from that for which they were initially designed, and an aim is to exploit them even more to further increase the train speed. An increase in speed leads to different and larger loads, which results in more rapid wear and shortening of the lifespan. The dynamic assessment is therefore important to estimate how fast the trains can travel with these catenary systems and the effects in terms of maintenance and lifespan reduction of the structures. In addition, the assessment is important for creating a basis of knowledge for evaluating suggestions for improvement through numerical analysis. It is also of utmost importance that knowledge gained through field measurements and assessment of existing structures is passed on to designers so that this knowledge is used in new catenary sections.

The design of railway lines and catenary sections is, among others, dependent on topography and weather conditions. This is especially important in Norway where valleys, hills, rivers, mountains etc., result in numerous and sharp curves and large variation in elevation. Approximately 40% of the Norwegian railway network consists of curves with radius below 1100 m. It is difficult to obtain a perfect catenary geometry when the catenary section changes from curve to curve with different radii. The span lengths vary in some places between 40 m and 60 m within one catenary section, which in turn leads to further challenges regarding the dynamics, despite functioning as a quasi-static system. Wind is one of the major weather challenges because the catenary is a quite flexible structure. Mountain crossings and valleys can result in high wind speeds, which in turn may necessitate shortening the span lengths.

An effect of the topography is that only 35% of the existing rail lines in Norway allow velocities above 100 km/h [2]. To further illustrate the train speeds in Norway, the speed distribution along the 475 km long Dovrebanen rail line, a major railway line between Oslo and Trondheim, shows that 46% is between 75 and 100 km/h, as presented in Figure 1. The demand for even higher speeds, combined with the fact that there is presently no plan for any major upgrades of the whole railway



line, has resulted in the need to investigate how the dynamic behaviour can be reduced for higher speeds. This should preferably be achieved by applying only small changes to the existing catenary system. The dynamic component of the response is generally assumed to increase significantly above 200–220 km/h. However, under special conditions, it may also occur at relatively low speeds [3]. At present, the rail network consists of both railway lines that are electrified and railway lines that are not electrified. The electrified lines are mostly non-electrical lines that have been upgraded with a catenary system to supply electrical power. Advances in the technology of trains and locomotives—for instance, tilting trains—have led to the ability for trains to run faster in curves on existing rail tracks [4]. An increase in the train speed will lead to changes in loading on all parts of the existing infrastructure. Investigations are therefore needed to ensure that all parts of the infrastructure can handle this increase in velocity. One of the parts that needs thorough investigation and changes to its properties is the catenary system [5]. Several different catenary systems are in use in Norway at present, and they are designed for different speeds and geometry. The major part of the existing railway catenary sections in Norway is old and was originally designed for travel at low speeds, approximately 80–90 km/h. Changes have later been applied to allow higher speeds, especially on straight parts of the railway. The changes applied to the catenary have in retrospect led to both positive and negative effects observed by Jernbanverket (the Norwegian National Rail Administration). One of the obvious positive effects of increased speed is a decrease in travel time. However, one has observed that the changes have in several catenary sections led to poorer behaviour of the system. This has in turn led to the need for a more thorough understanding of the behaviour of existing and new contact wire systems at high speeds under Norwegian conditions.

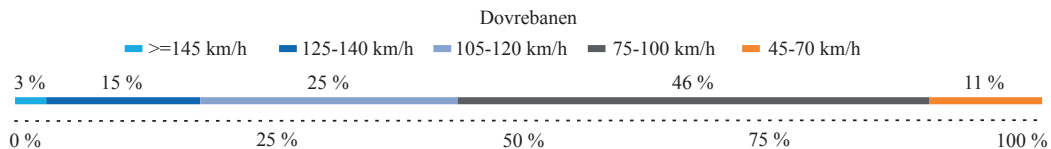


**Figure 1. Distribution of possible train speed along the Dovrebanen rail line in Norway**

The pantograph-catenary interaction will, as the train moves along the railway line, result in a contact force between the contact wire and the pan head. The contact force varies along the line and renders static and dynamic response in both systems. The increasing complexity of the system and the importance of the dynamic response become progressively more significant as the velocity of the train increases [6]. Excessively low contact force cause interruptions in the electric supply [1], and excessively high contact force will result in an undesirably high degree of wear [7]. Poetsch, et al. [1] present five critical parameters for the performance of a catenary system: contact wire tension,

---

messenger wire tension, contact wire sag, errors in setting the contact wire height, and static and dynamic uplift forces. Railway catenary systems are generally considered to have low damping [1], [5], [8]. Thus, oscillations appear in a large region both in front of and behind the contact point [1]. It becomes increasingly important to study the dynamic response of the catenary as the train speed is increased above the design speed [9]. Problems caused by oscillations may include loss of contact between the pantograph and the contact wire and undesirable wear. This is especially true for trailing pantographs owing to the large oscillations induced by the leading pantograph, which do not die out rapidly enough before the trailing pantograph passes. This in turn may lead to higher contact forces, higher wear and/or contact losses [10].

A natural step for the investigation of the parameters and behaviour of catenary systems is to establish a numerical model that can be used for simulations of trains passing under catenary systems. A thorough understanding of the complex pantograph-catenary interaction is therefore required to establish a trustworthy numerical model. The numerical model allows one to investigate the properties of the current design and study possibilities of optimizing the existing systems where an increase in the speed is desirable [11]. The aim for an optimization should be to preserve low dynamic forces, minimise wear, and ensure reliable contact as the speed is increased [1]. Numerical modelling capabilities for dynamic systems have generally improved as computational power has increased. At present, the most common approach for simulation of the interaction between the pantograph and the catenary is the finite element method (FEM) [8]. Other approaches found in the literature are the finite difference method and modal analysis [1]. The elements normally used to describe the catenary components are either string, bar or beam elements. Beam elements are considered preferable, especially for the contact wire, owing to the quality of the results. However, they are also the most computer time expensive [1]. The importance of the bending stiffness term in the beam element formulation increases as the speed is increased [12]. The contact between the contact wire and the pantograph has in the literature been modelled with the Lagrange multiplier method [13], the penalty method [5] or a combination of these two called the augmented Lagrange method [14]. Ambrósio et al. [5] conclude that the penalty method is sufficient for describing all relevant features in this contact interface. The numerical models of the pantograph used are mostly multi-degree-of-freedom lumped mass models with springs and dampers between the masses [8]. More recently, multi-body pantograph models have been used by some [5], [8]. Some studies have investigated particular characteristics of the catenary systems—i.e., how to obtain the correct initial geometry of the catenary [15]–[17] and the slackening of a dropper in compression [18]. Damping is included in the literature as either modal or proportional damping [8].

The validation of numerical models is crucial. This can either be accomplished by comparison with existing numerical models as a benchmark or by measuring data on the existing infrastructure [19]. Many different models are used around the world by different research groups and are well documented [8]. Several publications have focused on measurements on the pantograph for identification of its parameters and for evaluation of the dynamic interaction—for instance, [20]–[22]. Sampling on a pantograph in a laboratory is typically performed to establish the numerical model of the pantograph, whereas continuous sampling of forces in the pan head while the train runs is used to assess the pantograph-catenary interaction, [23]. Kiessling et al. [6] show some techniques used to measure the behaviour of the catenary, but little has been published on measurements taken on the catenary system or how to assess its behaviour. Drugge [24] measured the movement of the contact wire in five different places along a span for verification of computer simulations of the pantograph-catenary system and to examine the possibility of using multiple pantographs on the Swedish system ST15/15. Usuda [21] employed several accelerometers in a contact wire span to identify the contact force between the pan head and the contact wire, which ultimately can be used for monitoring. This setup was later used as part of a study on contact wire wear [25]. Stickland et al. [26] used drawstring potentiometers to measure the displacement of the contact wire and the messenger wire. The data were then used to calculate the damping ratio of the system. Cho et al. [27] and Cho [28] used a strain-gauge accelerometer fastened to the contact wire to sample acceleration time series.

More detailed knowledge of the dynamic behaviour is a constant aim for improving the pantograph-catenary interaction. This is shown by the focus in recent studies on details regarding and influencing this interaction. Examples are an increasing focus on the wear resulting from this interaction [7], [25], [29]–[32], effects of multiple pantograph operation [3], [10], [33]–[36], and effects of wind [26], [37]. These are mostly numerical and experimental studies. More thorough field measurements sampled directly on the catenary systems are required to further explore and understand their dynamic behaviour and improve numerical models to study the response in greater detail. This can be divided into two separate parts. First, the dynamics of the existing system must be assessed only by analysing field measurements directly. This is essential for establishing knowledge about the nature of the particular structure, and it is also of importance to assess different types of catenaries to gain both general and specific knowledge. Different types of catenaries, types of pantographs, train speeds, vertical and horizontal geometry and numbers of pantographs will all make an important difference in the response. Second, the knowledge and results from the assessment of the measurements are needed to establish important structural parameters and validate and develop more detailed numerical

models. These models can be used for more detailed analyses—e.g., to study the contact force for identification of point wear and other local effects, which are very important to locate for identifying limiting factors and for optimization. This is important for both existing and new catenary systems. The maintenance of existing systems can be better planned, and optimizations can be suggested and verified. The design of new sections can be improved based on the findings and studies using the numerical models. Field measurements can be time consuming, costly and difficult to execute, so many considerations must be made regarding the aim of measurements. Suitable types of measurements must be determined along with how to analyse these to optimally utilize the measurements. Deciding on the positions and procedures for sampling is very important.

The PhD study is divided into three parts. The first part is based on numerical models. It focuses on establishing methods to assess the dynamic properties of railway catenary systems and uses this to explore different parameters to better understand the dynamic behaviour of railway catenary systems (Papers I and II). The second part is the assessment of field measurements sampled during daily train operations, primarily using methods proposed in the first part (Papers III–VI). This is to extend the knowledge about the catenary systems—e.g., frequency content, damping and the effect of different parameters on the dynamic parameters. The third part uses the results from parts one and two to improve the numerical model and validate and use the improved model to further explore properties of railway catenary systems, such as the variation in contact force (Paper VII).

### 1.1 Objectives and limitations

The main objective of this PhD project was to increase the knowledge and improve the structural behaviour of existing catenary systems. It is important to note that the perspective is as the owner of the infrastructure. Several subsidiary objectives have been set to accomplish this:

- Develop three-dimensional numerical models of full-length railway catenary sections
- Develop assessment methods
- Expand the knowledge about how railway catenary systems behave

Although an important part of the pantograph-catenary interaction is electrical, it is outside the scope of this thesis.



## **2. Railway catenary systems**

Railway catenary systems, or overhead contact lines, are systems of wires located above the electrical trains supplying electrical energy to passing trains through a pantograph, a roof-mounted current collector device. The main structural components are a contact wire, a messenger wire, droppers, registration arms, brackets and poles, and occasional stitch wires, as shown in Figure 2. The contact wire is the part in contact with the pantograph and, thus, the part that transfers the electricity to the train. The contact wire is carried by the messenger wire, or catenary wire, through the droppers. The poles carry the wire system by fastening the messenger wire to the support by the brackets. The registration arms mainly ensure the correct horizontal geometry of the contact wire. Stitch wires are used to achieve more even elasticity throughout each span. This minimises the vertical movement of the pantograph. Other important properties influencing the vertical geometry of the contact wire include the length and position of the droppers and the length and tension in the stitch wires. A small sag in the vertical height of the contact wire in the middle of each span is often desirable for the quality of the pantograph-catenary interaction. One catenary section stretches over several spans and can be up to 1600 meters in the Norwegian railway network. The contact wire and messenger wire are continuous over a section and are pre-tensioned to obtain the desired elasticity and vertical geometry. The tension is typically introduced by mounting weights on the ends of the section, as illustrated in Figure 3. For more details on railway catenary systems, see Kiessling et al. [6]. For completion, a train with a pantograph passing under a catenary section is shown in Figure 4.



Figure 2. The placement of the structural components of railway catenary systems [38]

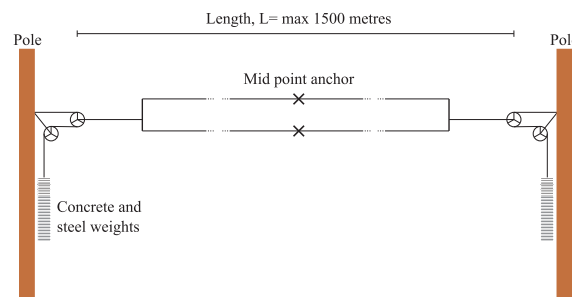


Figure 3. Illustration of pre-tensioning the contact and messenger wire



**Figure 4. A train passing a catenary section. Photograph: NTNU/Petter N avik**

### 2.1 Norwegian catenary systems

There are several different railway catenary systems in use in Norway. The four base types are Tabell 54, System 35, System 20 and System 25, which all can be found with different alterations around the Norwegian rail network. These systems are meant for different train speeds and locations. It is the Norwegian National Rail Administration, through technical regulations [39], that indicates which system should be used in particular sections.

Tabell 54 is an old catenary system originally designed for low speeds, with a maximum speed of 130 km/h today. This system is found in two configurations with original tension forces 6.1 kN and 5 kN in the contact and messenger wires, respectively, which were changed to 10 kN and 5 kN to improve the dynamic behaviour at higher speeds. Building it is no longer allowed, but it is still a major part of the rail network, as shown in Figure 5.



System 35 catenary sections can be divided into two major types, with and without stitch wires—System 35 and System 35 MS, respectively. It is designed for speeds of approximately 130 km/h with multiple pantographs. The tension configuration is 7.06 kN in both wires. System 35 is a newer system than Tabell 54, but it is seldom used in new catenary sections. It is also a major part of the rail network, as shown in Figure 5.

System 20 is a much newer system than the previous two. It is mainly divided into four types: Standard A, Standard B, Standard C1 and Standard C2. Their different configurations are shown in Table 1.

System 25 is the catenary system that allows the highest speed in Norway, 250 km/h. It is a new system and only exists in newly built sections.

**Table 1. Catenary system parameters**

Type	Maximum speed [km/h]		Tension [kN]		Stitch wire	Max length [m]	Curvature
	One pantograph	Multiple pantographs	CW	MW			
Tabell 54	80	80	6.1	4.9	No	-	-
Tabell 54 op	130		10	5	No	-	-
System 35 MS	140	120	7.1	7.1	No	1600	-
System 35	150	130	7.1	7.1	Yes	1600	-
System 20 A	200	160	10	10	Yes	1500	>800 m
System 20 B	160	130	10	10	No	1300	<800 m
System 20 C1	200	160	13	13	Yes/No	1500 <sup>1</sup>	>5000 m
System 20 C2	160	130	13	13	No	1500 <sup>1</sup>	-
System 25	250	200	15	15	Yes	1200	>1200 m

<sup>1</sup>up to 3000 m in tunnels if properly documented; loss of tension should be less than 10% along the section

As a catenary designer, it is important to know what to build, but it is equally important to know what already exists along the rail lines. A huge part of the existing catenary in Norway is old and worn, and changes have also been applied during their lifetime. An illustration showing the distribution of catenary systems along the Dovre line demonstrates that although Tabell 54 and System 35 are no longer built in new designs, they dominate the existing infrastructure; see Figure 5.

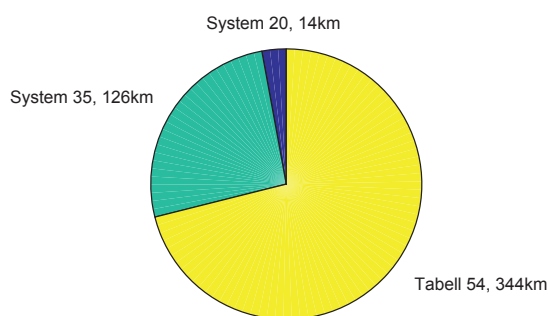


Figure 5. Catenary system distribution along the Dovre line, based on data from BaneData

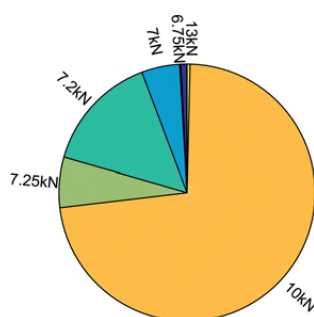


Figure 6. Distribution of tension in the contact wire along the Dovre line, based on data from BaneData

Table 2. A short English – Norwegian pantograph-catenary interaction dictionary

English	Norwegian
railway catenary system	kontaktledningssystem
pantograph	strømvtager (pantograf)
contact wire	kontakttråd
messenger wire (catenary wire)	bæreline
dropper	hengetråd
stitch wire	y-line
registration arm	horisontalstag
light steady arm	lett direksjonsstag
cantilever (pole support)	utligger
pole	mast
train	tog
The Norwegian National Rail Administration	Jernbaneverket
contact force	kontaktkraft
stagger	sikksakk
tensioning device	
midpoint anchor	fikspunkt
pull-off support	strekkutligger
push-off support	trykkutligger



### **3. Numerical modelling**

This chapter presents the procedure for creating railway catenary section numerical models, developed and used during this thesis. Existing railway catenary systems can be very different from section to section. They can have very different vertical and horizontal geometries that result in substantial differences in the response. Some of the reasons for the differences are the actual topography; the fact that some sections have been upgraded, some have not, and various people working with maintenance have improved some sections ad hoc; different sections have been designed by different people and so on. This insight resulted in the aim to develop the numerical models as they are mounted at each section. A detailed description of the final model is presented in Paper VII.

First, the section-specific parameters are filled into a standardized Excel sheet. All parameters can be changed individually, and the changeable parameters are listed below:

- Railway catenary system type
- Type and tension in the contact wire, the messenger wire, and stitch wires
- Start and end kilometre along the rail line and position of the fixed point
- Number of spans
- Horizontal geometry including the number and length of curves, transition parts and straight parts, and curvature and cant
- Length of each span
- Position and length of each dropper
- Whether stitch wires are used
- Length of each stitch wire
- The span in which the pantograph starts

Second, a Python script is developed to develop a numerical model in Abaqus directly from the values given in the Excel sheet. The whole script is written as generally as possible to quickly generate new models of different sections. The script contains all material information about the wire types chosen in the Excel sheet and the geometry of the pan heads. In addition, the script includes some changeable parameters:

- The railway section that will be modelled
- Type of pantograph (new ones can be easily added)
- Train speed

- Sampling frequency
- Rayleigh damping coefficients for the catenary wires
- Element lengths in the separate components
- An iterative step to obtain the correct tension force in the stitch wires individually. This step is very important when working with catenaries that are not on straight lines

Finally, Abaqus runs two initial steps before running the train along the section at the chosen speed.

#### **4. Monitoring system**

A monitoring system to sample accelerations and angular velocities from railway catenary systems has been developed during the PhD study. The need for a monitoring system became evident when working with the numerical models. The accuracy of the numerical models required validation in more detail to be able to study different phenomena more closely. In addition, sampled measurements can be used, and have been used, to directly obtain relevant information about existing railway catenary sections.

The monitoring system was developed in collaboration between the Norwegian University of Science and Technology, Norway, and Elektromotus, Lithuania. Anders Rønnquist, via Einar Gotaas, established contact with Gintautas Paluckas in autumn 2013. The development was a continuous process from late 2013 until August 2015 and was led by Petter Røe Nåvik. The work of Elektromotus developers Rytis Karpuška and Karolis Tarasauskas is gratefully acknowledged.

The system had to be made purpose specific to obtain the necessary measurements and flexibility. First, it was important to decide on wired or wireless sensors. On the one hand, a wired sensor system has some advantages over a wireless sensor system. The main one is time synchronization of the channels. Every sensor in a wireless sensor system has its own analogue-to-digital converter, so specific solutions are needed to ensure proper time synchronization [40]. Wired sensors allow measurements for an unlimited period, whereas a wireless system has limited monitoring time due to battery capacity. On the other hand, a wireless system reduces installation time and costs. In addition, there were several aspects of the railway catenary systems that needed to be considered during the design of the monitoring system. The wires to which the sensors were to be attached transport electric energy—in Norway, 15 kV at 16 2/3 Hz [2]. This results in either using cables not vulnerable to electric noise or using wireless sensors inside a Faraday cage. Those types of cables are normally expensive and heavy, whereas building a Faraday cage for the wireless sensor is inexpensive and easy. Ultimately, it was decided to use a wireless sensor system owing to a desire for flexible sensor positioning, a wide possible positioning range, and a requirement for a short mounting time due to limited track access time. A custom-designed low-power 2.4 GHz radio network was chosen for communication between slave and master units. The master unit was assigned the task of ensuring synchronous sampling, storing data and transferring data remotely through a VPN connection to a remote server. The communication between each individual sensor and the master unit used two different radio antennas to ensure long-range capability. The antenna of the master unit was an Alfa AOA-2049TM antenna, and the one used for the sensors was a Pulse Electronics W1030. The radio

chip and microprocessor used were a Nordic nRF24L01 and a STM32L152, respectively. The range was approximately 700 meters from the master unit under optimal conditions.

A wireless sensor typically consists of a motion processing unit (MPU), a battery pack and a radio antenna. The next step was deciding on the measurement specifications of the individual sensor. To find a suitable MPU, the sampling frequency and magnitude range needed to be defined. The maximum sampling frequency was decided upon based on two pieces of information. First, all measured data must be filtered at least at the Nyquist frequency [41], 50% of the sampling frequency, but to account for the fact that no filter has an infinitely sharp roll-off, it is often set to 80% of this (40% of the sampling frequency) [40]. Second, Collina and Bruni [42] stated that numerical models should be validated to include effects up to at least 100 Hz to describe phenomena related to wear phenomena. These two considerations led to a required sampling frequency of 250 Hz. Based on this, we decided on a maximum sampling frequency of 500 Hz to be able to account for more than what was considered to be the minimum range. Another decision was that the magnitude range for both the gyroscope and accelerometer was important to define according to what was expected on site. The first versions had a maximum limit of  $\pm 8G$  for the accelerometers, but this was later changed to 16 G owing to observations of accelerations above 8G in some tests and train passages. The gyroscope was set with a maximum range of  $2000^\circ/s$ . This was and has since been sufficient. The battery capacity was chosen based on a minimum monitoring period of one week, the expected number of train passages, and the consumption for each passage. In this process, it was equally important that the weight of the sensor should be as low as possible.

The MPU in the final sensors is a commercial unit, MPU-6000 [43], which combines a microelectromechanical system (MEMS) tri-axial gyroscope, an MEMS tri-axial accelerometer and a Digital Motion Processor<sup>TM</sup>. The analogue acceleration and angular velocity data are converted to digital using an inbuilt 16-bit analogue-to-digital converter (ADC). The magnitude range was made user programmable with a full-scale range of  $\pm 2$  g,  $\pm 4$  g,  $\pm 8$  g and  $\pm 16$  g for the accelerometer and  $\pm 250$ ,  $\pm 500$ ,  $\pm 1,000$  and  $\pm 2,000$  deg/sec for the gyroscope [43]. A Boston Power Sonata® 5300 battery was chosen so that the monitoring system could perform measurements for at least one week without charging. It has a nominal capacity of 5300 mAh. A screwed bolt connection ensures a very stiff connection and the freedom to place the sensor wherever one wants. The final weight of a single sensor is 390 g. A sensor is shown with its axis definitions in Figure 7.

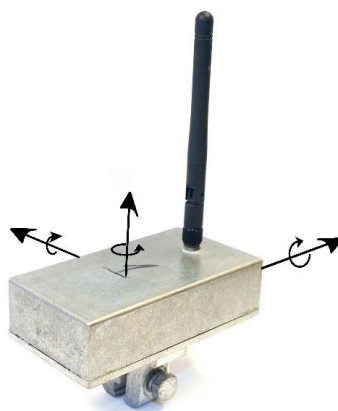


**Figure 7. A single sensor with axis directions. Photo: NTNU/Petter Røe Nåvik [44]**

The next and very important step was to design the actual system as one monitoring system that provides synchronous data. Every sensor samples continuously and records to local flash memory, but data are transferred only when the system is triggered. The system can be triggered either by a train passage or manually. Triggering by train passage is accomplished by setting a threshold value to be exceeded to trigger the system. This value is the same for each sensor but can be set separately for each degree of freedom. The master unit triggers all sensors at the same time when a threshold value is exceeded in any one sensor.

All sensors have an internal timer and run completely unsynchronized. Periodically, the master sends a broadcast packet. When each sensor receives the packet, it stores the ID of the packet together with its own, unsynchronized, timer value in a table. Note that because it is a broadcast packet, all sensors receive this packet at the same time. After a complete sampling, before the measurements are transferred to the master, the tables from each sensor are sent to the master. The master then has local timer values for every sensor for a period before and after the train passage. This was implemented to remove the effects of missing broadcast packets, which might occur owing to the nature of radio communication. A retransmission of the missing data is impossible because this will destroy the time synchronization. The local time value for every sensor corresponding to the same broadcast packet ID is the same point in global time. Linear regression was used between the sensors to obtain global timestamps. The sensor with the lowest timer value was used as a reference to avoid negative timestamps in the other sensors. Linear regression was chosen because it represents quite well the offset of the timer values between sensors and the hardware drift. The master requests the sensors to send the measurements when the linear regression has been completed. The data arrive with local



timestamps. The master recalculates the timestamps according to the linear regression to obtain the time-synchronized data. This process is repeated for every triggering.

The master unit also acts as a server that can be accessed either through a VPN connection or by a local WiFi network. Through these connections, data can be downloaded, measuring parameters can be changed, and the sensors can be manually triggered. The communication setup and transfer of data are presented in Figure 8.

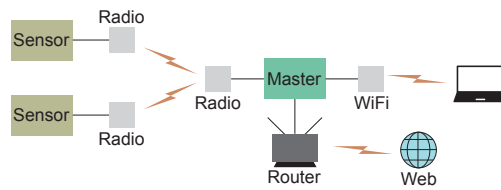


**Figure 8. The monitoring system's communication setup and transfer of data [44]**

The final version of the monitoring system is also described in detail by Nåvik et al. [44] and used for sampling data in Papers III–VII.



**Figure 9. The monitoring system sensors**

## 5. Field measurements

A major part of the thesis has been based on different field measurements performed during the study. This section contains general comments regarding field measurements and a description of the measurements that have been carried out.

It is always important to plan field measurements in detail—mostly to ensure that the correct measurements are sampled but also because of simple practicalities such as reducing mounting time, which is very important on the railways because of limited track access. The five types of measurements used in this thesis are acceleration, angular velocity, displacements, geometry and contact forces.

### 5.1 Acceleration and angular velocity of the catenary

The developed monitoring system, presented in Chapter 4, has been extensively used during the PhD work to sample acceleration and angular velocity. It has been mounted and sampled at six different locations on the Norwegian rail network: Alna, Melhus, Soknedal, Vålåsjø, Fokstua (2 times) and Hovin. Every location has different properties, so the monitoring setup had to be designed specifically for each location. Some important properties of the studied sections are presented in Table 3.

The most important part of the planning is deciding on the positions of the sensors. First, one should ensure that the sensor setup gives enough information to perform the planned assessments. Second, one should attempt to establish the sensor setup for each location such that one can easily compare the results with results from other locations. Third, every new location and setup should include different features so that the result includes new knowledge about the catenary. Fourth, good communication with the workers from the company that owns the structures is required to obtain the best possible results. They know more about the existing structures than anyone else and can help in the decision of where to measure.

The setups used during this thesis have been designed based on the steps above. The main guidelines have been that there should always be a sufficient number of sensors within one span length to be able to identify system frequencies rather than local frequencies. There should also be sensors in several different spans, also for capturing the system frequencies. In addition, for the same reason, there should always be sensors placed on the messenger wire and the contact wire. For optimal cross-correlation, one should have at least two sensors in the same position in a span but positioned in different spans. The overall distance between the first and last sensor should be of sufficient length to be able to well estimate the train speed.

**Table 3. Important properties of the railway catenary sections investigated in the PhD study. The data are based on Jernbaneverket's database "BaneData Innsyn"**

<b>Section</b>	<b>Alna</b>	<b>Melhus</b>	<b>Soknedal</b>	<b>Vålåsjo</b>
Name	KM7,185H	Wire 191	Wire 152	Wire 12
Measurement period	24.-26.06.14	06.-14.03.15	30.03-07.04.15	26.05-02.06.15
Catenary system	System 35 MS	System 35	Table 54	System 20 C1
Length [m]	533	528	1451	1265
Tension CW [kN]	7.06	7.06	10	13
Tension MW [kN]	7.06	7.06	5	13
Area CW [mm <sup>2</sup> ]	100	100	100	120
Area MW [mm <sup>2</sup> ]	50	50	50	70
Stitch wire (Yes/No)	No	Yes	No	Yes
Start [KM]	7.185	532.68	486.939	372.202
End [KM]	7.718	533.208	488.39	373.467
Curves	1	0	4	1
JBV Object (EH-KTL)	000024	001139	001092	000966
JBV Location	0210-00003	1120-11200	1111-11120	1100-11015
<b>Section</b>	<b>Fokstua</b>	<b>Hovin</b>	<b>Fokstua 2</b>	
Name	Wire 24	Wire 1	Wire 21	
Measurement period	23.-25.06.15	24.08-02.09.15	30.11-05.12.15	
Catenary system	System 35	System 35	System 20 C1	
Length [m]	705	1411	1295	
Tension CW [kN]	7.06	7.06	13	
Tension MW [kN]	7.06	7.06	13	
Area CW [mm <sup>2</sup> ]	100	100	120	
Area MW [mm <sup>2</sup> ]	50	50	70	
Stitch wire (Yes/No)	Yes	Yes	Yes	
Start [KM]	363.85	507.137	363.817	
End [KM]	364.555	508.548	365.112	
Curves	0	1	0	
JBV Object (EH-KTL)	001806	001110	-	
JBV Location	1100-00002	1120-00001	-	

During planning, it is very important to consider limited track access. A detailed description of the mounting procedure including a detailed train schedule, the position of every sensor, the schedule for mounting and the schedule for testing should be formulated in advance.

### 5.2 Displacements of the catenary

Two methods have been used for estimating the displacement of railway catenary systems: photogrammetry and integrated accelerations. The measurement procedure for accelerations is described in Chapter 5.1. A close-range photogrammetry scheme for use on railway catenary systems was developed and used for estimations of displacement time series by Gunnstein Thomas Frøseth and is thoroughly described in Paper V.

### 5.3 Geometry

The actual geometry of the railway catenary sections is often different from the design. The differences may be significant for the response. Thus, it is important to gain knowledge about these differences. Measurements have been taken to find the actual pre-sag, contact wire height and stagger. The measurements have been performed using a laser mounted on a holder specifically designed for the purpose; see Figure 10.



**Figure 10. Measurement of contact wire height and stagger using a laser. Photograph: NTNU/Petter N avik**

### 5.4 Contact forces

The contact force measurements used in the thesis are all from the same database at Jernbaneverket. The database is from their own measurement program that includes a track and overhead line recording car, Mermec Roger 1000 [45], that travels all lines in Norway twice a year. The measurement program includes many different measurements, but for this work, only a select few

have been used. The used measurements are the contact forces, at four locations, and the train speed. All sampling is performed every 0.5 meters along the track. The contact forces are taken directly from the force transducers located just beneath the collector strips; thus, the inertia correction described in EN50317:2012 is not included in the values.

---

## 6. Summary of present investigations with concluding remarks

The focus of this PhD study has been to increase knowledge about the dynamic behaviour of railway catenary systems by numerical studies and analysis of field measurements. First, numerical models were developed and used to establish suitable methods for assessing the dynamic response and to study dynamic and structural properties in Paper I [46] and Paper II [47]. Paper I uses the dynamic response as a tool to evaluate and improve an optimization of existing railway catenary systems for higher speeds. The methods used were interpretations of differences in the power spectral density (PSD) of different pretension force configurations and different speeds by comparing the shape and peak values of the PSDs and maximum uplift values. A successful evaluation of the railway catenary section was performed using these methods. This resulted in identified speed limits for the different configurations, confirming the hypothesis in the variation of uplift response at mid-span and pole support. It showed that studying the dynamic response in addition to only peak uplifts is invaluable, confirming that tension forces can be used to change the response sufficiently to allow for higher speeds [48], [49]. The same methods were used with success in [50] to assess the dynamic response for extremely low-contact wire height passages in excess of design velocities and the effect of different gradients on the dynamic response. Paper II contributes with other methods to the assessment of the dynamic behaviour of railway catenary systems and gives new insight into the response nature of such structures. Two numerical models were used for a case study: one reference model, a straight section with equal span lengths, and one of an existing railway catenary section containing three different curves and span lengths ranging from 40 to 60 m. The variability of the section was important for testing the following assessment methods as thoroughly as possible. The investigation can be divided into two parts. First, cross-correlation coefficients calculated from sampled time displacement series from successive spans along the catenary in the numerical model have been used to quantify the dynamic predictability of the system. Spans close to each other and with similar span lengths had high correlation, close to 1.0, whereas spans with quite different span lengths that were close to each other had much lower correlations, 0.5-0.8. This demonstrates that it is beneficial to perform local investigations for large changes in the response. Second, a thorough frequency analysis using both PSDs and short-time Fourier transforms (STFT) was performed. Frequency analyses are vital for understanding any dynamic system. The results demonstrate that different information can be extracted from different parts of the response time series, which has been shown by comparing PSDs from the pre- and post-passage parts. The pre-passage contains information about the load frequencies, and the post-passage typically reveals the fundamental system frequencies, motion-induced harmonic components and structural damping. In addition, STFTs

include important information about when and how energy transfers occur between the pre-passage frequencies and the post-passage frequencies. Combinations of the methods in Papers I and II are used in [51] to assess the difference in response in curves with different radii. This was assessed using sampled data from the same numerical model as in Paper II with three curves. A clear difference in both peak uplift and dynamic content was shown, which signifies that sections with varying geometry will not have optimal dynamic behaviour.

Second, field measurements performed during normal train operations were planned and conducted based on the results and knowledge gained from numerical analyses. These were analysed using both previously suggested methods and newly developed methods to further increase the knowledge of the dynamic response of railway catenary systems. The results are presented in detail in Papers III–VI [38], [44], [52], [53]. Paper III analyses acceleration time series sampled by a sensor system, developed during the PhD study, from three different existing railway catenary sections using the covariance-driven stochastic subspace identification method to identify the system damping. The importance of studying the damping is highlighted in the review paper by Ambrosio et al. [5], who recognize that estimating damping is still a considerable challenge; Bruni et al. [8] demonstrate that damping is critical in numerical models and that small differences in its description may significantly affect the simulation result, and a paper on determining damping in railway catenary systems by experimental and numerical methods [55] was published soon after Paper III. The important difference between Paper III and the previous papers on damping [26], [54], as well as the one published soon after [55], is that it identifies the Rayleigh damping coefficients by using damping ratios identified over the range of frequencies between 0 and 20 Hz rather than using only the damping ratio identified at the first natural frequency. In addition, this study uses data from several sensors sampled simultaneously during daily train operation and from three different railway catenary systems. The result recommended Rayleigh mass and stiffness proportional damping coefficients,  $\alpha=0.062$  and  $\beta=6.13e-06$ , respectively. Paper IV presents and uses the abovementioned sensor system for a full assessment of the frequency content in the response of an existing railway catenary system, mostly by methods presented and used in the numerical analyses. An additional method was necessary to be developed for assessing the system frequencies from many passages rather than single passages to capture the variety in the many passing train passages and for including information from all sensors at once. The developed method is to add the PSD of acceleration time series from all sensors and all passages together, pick the peaks from each of these PSDs to produce an overall histogram, and study them together. This then represents both the energy and peak distribution. The PSD is typically dominated by the post-passage result, so including the histogram distribution highlights

natural frequencies that are often excited but with low energy content under the current loading situation. Identifying all of these frequencies is important when considering changes to both the catenary and the pantograph that may lead to load changes, which in turn may lead to other energy-dominant frequencies than those seen today. It is also shown that the STFT works well with field measurements and that changes in the energy content during the train passage can be evaluated. The paper clearly shows that the developed sensor system can be used for operational modal analysis on railway catenary systems. Paper V presents and uses two techniques for estimating displacement of the catenary under daily operation. The first method is by close-range photogrammetry, and the second uses an acceleration integration procedure. Because major differences between the methods exist, the paper focuses on the prediction and validation of the estimated time series. That is, the displacements estimated using the acceleration procedure are compared to those obtained by photogrammetry. The study shows that both methods provide good estimates of the displacement. Although uncertainties are tied to the acceleration procedure, the acceleration time series are easy collected, and the results can be used for assessment of a single passage and evaluation of the safety of daily operations by statistical means using estimations from many passages. Paper VI refocuses on the frequency content of the response in the railway catenary systems as a train passes using field measurements from two different existing catenary sections. In addition to previous studies, it includes a study on the frequency content in the lateral direction, compares it to the vertical direction, and emphasises the importance of including both directions when identifying important frequencies. The study includes identification of system frequencies by full sensor system analyses by PSDs and histograms, as well as frequency studies for separate sensors using histograms and STFTs. The study demonstrates that it is important to assess several points on the catenary to identify important system frequencies because not all sensors display every important frequency.

Third, the two previous parts were used in the work of creating better numerical models: the first part as a basis for new numerical models and the second for validation of the models. Paper VII [56] focuses on the variation in the pantograph-catenary interaction force prediction. The investigation consists of both numerical simulations and field measurements. It presents and validates a numerical model that is developed based on knowledge gained during this PhD study, especially the previous papers, Papers I–VI. This model has been used, in addition to field measurements, to explore in detail the variation of contact force prediction. The results demonstrate that variation in contact forces is important. The predicted values are dependent on the prediction method and the level of filtering. In particular, the study demonstrates that the standard deviation and the maximum and minimum values



of the contact force time series are highly influenced by post-processing. These results illustrate the need for better pantograph models and more detailed contact force measurements.

To sum up, this thesis demonstrates that the structural behaviour of a railway catenary section is very complex and dependent on many parameters. It demonstrates that field measurements are required for validating numerical models. It presents self-developed purpose-specific monitoring systems for field measurements. It presents a range of methods for dynamical assessment, both for numerical data and for field measurements. It presents a detailed three-dimensional numerical model shown to give reasonable results compared with field data. It demonstrates high variability in the dynamic response by studying the frequency content from both field measurements and numerical models. In addition, it demonstrates that system frequencies of a catenary section should be identified based on measurements from several spans, several positions within a span and several train passages. Based on analyses of field measurements from several different catenary sections and train passages, it demonstrates low structural damping and suggests Rayleigh damping coefficients for use in numerical models.

## 7. Suggestions for future works

The reason for exploring the dynamic behaviour of railway catenary systems is to improve the interaction between the catenary and the pantograph. This PhD thesis has helped in gaining knowledge to better describe and understand these systems. However, many topics need further investigations. Suggestions for future works are listed below.

**Frequency content.** The frequency content has been studied in detail. Still, many aspects remain undiscovered. A detailed study for identifying what structural parts contribute to which frequencies is important. A universal strategy to state the dynamic quality of a railway catenary section should be developed.

**Contact force.** The contact force is, as presented in the study, broadly used in the literature to evaluate the quality of the pantograph-catenary interaction. A more detailed study about what causes local effects, such as rapid changes in contact force, arching and point wear, is suggested. This needs a more detailed study both in the field and numerically.

**Wear.** Several studies have looked into wear on the pantograph and contact wire. However, a study that identifies why wear occurs at different locations and which parameters actually matter is suggested.

**Numerical models.** The numerical models in the literature are already good. However, to describe the pantograph-catenary interaction in even more detail a more thorough validation is needed along with possibly an improvement of the models. The pantograph models should be improved, the sampling frequency of both measurements and numerical analyses should be increased, and studies involving the catenary system should always include varying geometry. In addition, rules in the standards might need revision, especially regarding validation of the numerical models. A model validated up to 20 Hz cannot and should not be believed to be of high accuracy at much higher frequencies. More details regarding these topics should be a priority in future works.

**Parameter studies.** This study has used the dynamic response as an evaluation tool to study some parameters such as tension forces, contact wire height and curvature. The methods were demonstrated to work well for these systems, and it is therefore only natural to aim for further parameter studies. One of the main topics is the effect of different designs on the dynamic response of the railway catenary. Are there improvements that can be made to the dynamic response by changing the design only by applying simple changes?

**Field measurements.** Several types of field measurements have been performed in this study. However, simultaneous sampling of the contact force from the pantograph and of measurements from the catenary has not been possible but is an aim for future works. This can be used for more detailed investigation of the correlation between load and response and better numerical validation.

Ultimately, I will suggest that a focus for future works should be that everything should be linked to the quality of energy transfer and wear on both catenaries and pantographs. This is what really matters for the infrastructure, train owners, cargo and passengers.

---

## References

- [1] G. Poetsch, J. Evans, R. Meisinger, W. Kortüm, W. Baldauf, A. Veitl, and J. Wallaschek, “Pantograph/Catenary Dynamics and Control,” *Vehicle System Dynamics*, vol. 28, no. 2–3, pp. 159–195, 1997.
- [2] “Slik fungerer jernbanen,” 2011. [Online]. Available: [http://www.jernbaneverket.no/PageFiles/13736/slikfungererjernbanen\\_2011.pdf](http://www.jernbaneverket.no/PageFiles/13736/slikfungererjernbanen_2011.pdf).
- [3] G. Bucca, M. Carnevale, A. Collina, A. Facchinetti, L. Drugge, P.-A. Jönsson, and S. Stichel, “Adoption of different pantographs’ preloads to improve multiple collection and speed up existing lines,” *Vehicle System Dynamics*, vol. 50, no. Suppl. 1, pp. 403–418, 2012.
- [4] R. Persson, R. M. Goodall, and K. Sasaki, “Carbody tilting – technologies and benefits,” *Vehicle System Dynamics*, vol. 47, no. 8, pp. 949–981, Aug. 2009.
- [5] J. Ambrósio, J. Pombo, M. Pereira, P. Antunes, and A. Mósca, “Recent Developments in Pantograph-Catenary Interaction Modelling and Analysis,” *International Journal of Railway Technology*, vol. 1, no. 1, pp. 249–278, Apr. 2012.
- [6] F. Kiessling, R. Puschmann, A. Schmieder, and E. Schneider, *Contact lines for electric railways: planning, design, implementation, maintenance*, 2nd ed. Erlangen: Publicis Publishing, 2012.
- [7] A. W. C. Shing and P. P. L. Wong, “Wear of pantograph collector strips,” *Proceedings of the Institution of Mechanical Engineers, Part F: Journal of Rail and Rapid Transit*, vol. 222, pp. 169–176, 2008.
- [8] S. Bruni, J. Ambrosio, A. Carnicero, Y. H. Cho, L. Finner, M. Ikeda, S. Y. Kwon, J.-P. Massat, S. Stichel, M. Tur, and W. Zhang, “The results of the pantograph–catenary interaction benchmark,” *Vehicle System Dynamics*, vol. 53, no. 3, pp. 412–435, 2015.
- [9] G. A. Scott and M. Cook, “Extending the limits of pantograph/overhead performance,” in *Better Journey Time - Better Business. I. Mech. E. Conference Transactions 1996-8*, 1996, vol. 8, pp. 207–218.
- [10] J. Pombo and J. Ambrósio, “Multiple Pantograph Interaction With Catenaries in High-Speed Trains,” *Journal of Computational and Nonlinear Dynamics*, vol. 7, no. 4, pp. 041008–041008–7, 2012.
- [11] R. J. Gostling and A. E. W. Hobbs, “The Interaction of Pantograph and Overhead Equipment: Practical Applications of a New Theoretical Method,” *Proceedings of the Institution of Mechanical Engineers, Part C: Journal of Mechanical Engineering Science*, vol. 197, no. 1, pp. 61–69, 1983.
- [12] C. N. Jensen and H. True, “DYNAMICS OF AN ELECTRICAL OVERHEAD LINE SYSTEM AND MOVING PANTOGRAPHS,” *Vehicle System Dynamics*, vol. 29, no. Suppl. 1, pp. 104–113, 1998.
- [13] M. Schaub and B. Simeon, “Pantograph-Catenary Dynamics: An Analysis of Models and Simulation Techniques,” *Mathematical and Computer Modelling of Dynamical Systems*, vol. 7, no. 2, pp. 225–238, 2001.
- [14] J. Ambrósio, J. Pombo, F. Rauter, and M. Pereira, “A Memory Based Communication in the

- 
- Co-simulation of Multibody and Finite Element Codes for Pantograph-Catenary Interaction Simulation Multibody Dynamics,” in *Multibody Dynamics Computational Methods and Applications*, vol. 12, C. L. Bottasso, Ed. Springer Netherlands, 2009, pp. 231–252.
- [15] E. Arias, A. Alberto, J. Montesinos, T. Rojo, F. Cuartero, and J. Benet, “A mathematical model of the static pantograph/catenary interaction,” *International Journal of Computer Mathematics*, vol. 86, no. 2, pp. 333–340, 2008.
- [16] O. Lopez-Garcia, A. Carnicero, and V. Torres, “Computation of the initial equilibrium of railway overheads based on the catenary equation,” *Engineering Structures*, vol. 28, no. 10, pp. 1387–1394, 2006.
- [17] M. Such, J. R. Jimenez-Octavio, A. Carnicero, and O. Lopez-Garcia, “An approach based on the catenary equation to deal with static analysis of three dimensional cable structures,” *Engineering Structures*, vol. 31, no. 9, pp. 2162–2170, 2009.
- [18] Y. H. Cho, “Numerical simulation of the dynamic responses of railway overhead contact lines to a moving pantograph, considering a nonlinear dropper,” *Journal of Sound and Vibration*, vol. 315, no. 3, pp. 433–454, 2008.
- [19] NEK, “NEK EN 50318:2002 Railway applications - Current collection systems - Validation of simulation of the dynamic interaction between pantograph and overhead contact line,” no. 1. p. 20, 2002.
- [20] M. Ikeda, S. Nagasaka, and T. Usuda, “A precise contact force measuring method for overhead catenary system,” in *Proceedings of World Congress on Railway Research 2001*, 2001.
- [21] T. Usuda, “The Pantograph Contact Force Measurement Method in Overhead Catenary System,” in *Proceedings of the 8th World Congress on Railway Research*, 2008.
- [22] W. Zhang, Z. Shen, and J. Zeng, “Study on dynamics of coupled systems in high-speed trains,” *Vehicle System Dynamics*, vol. 51, no. 7, pp. 966–1016, 2013.
- [23] M. Carnevale and A. Collina, “Processing of collector acceleration data for condition-based monitoring of overhead lines,” *Proceedings of the Institution of Mechanical Engineers, Part F: Journal of Rail and Rapid Transit*, vol. 230, no. 2, pp. 472–485, 2016.
- [24] L. Drugge, “Modelling and simulation of pantograph-catenary dynamics,” Luleå University of Technology, 2000.
- [25] T. Usuda, M. Ikeda, and Y. Yamashita, “Prediction of Contact Wire Wear in High-speed Railways,” in *Proceedings of the 9th World Congress on Railway Research*, 2011.
- [26] M. T. Stickland, T. J. Scanlon, I. A. Craighead, and J. Fernandez, “An investigation into the mechanical damping characteristics of catenary contact wires and their effect on aerodynamic galloping instability,” *Proceedings of the Institution of Mechanical Engineers, Part F: Journal of Rail and Rapid Transit*, vol. 217, no. 2, pp. 63–71, 2003.
- [27] S.-I. Seo, Y.-H. Cho, J.-Y. Mok, and C.-S. Park, “A study on the measurement of contact force of pantograph on high speed train,” *Journal of Mechanical Science and Technology*, vol. 20, no. 10, pp. 1548–1556, 2006.
- [28] Y. H. Cho, “Numerical simulation of the dynamic responses of railway overhead contact lines to a moving pantograph, considering a nonlinear dropper,” *Journal of Sound and Vibration*,

- 
- vol. 315, no. 3, pp. 433–454, 2008.
- [29] T. Ding, G. X. Chen, X. Wang, M. H. Zhu, W. H. Zhang, and W. X. Zhou, “Friction and wear behavior of pure carbon strip sliding against copper contact wire under AC passage at high speeds,” *Tribology International*, vol. 44, no. 4, pp. 437–444, 2011.
- [30] G. Bucca and A. Collina, “Electromechanical interaction between carbon-based pantograph strip and copper contact wire: A heuristic wear model,” *Tribology International*, vol. 92, pp. 47–56, 2015.
- [31] T. Ding, G. X. Chen, M. H. Zhu, W. H. Zhang, and Z. R. Zhou, “Influence of the spring stiffness on friction and wear behaviours of stainless steel/copper-impregnated metallized carbon couple with electrical current,” *Wear*, vol. 267, no. 5–8, pp. 1080–1086, 2009.
- [32] G. Bucca and A. Collina, “A procedure for the wear prediction of collector strip and contact wire in pantograph–catenary system,” *Wear*, vol. 266, no. 1–2, pp. 46–59, 2009.
- [33] P. Harèll, L. Drugge, and M. Reijm, “Study of Critical Sections in Catenary Systems During Multiple Pantograph Operation,” *Proceedings of the Institution of Mechanical Engineers, Part F: Journal of Rail and Rapid Transit*, vol. 219, no. 4, pp. 203–211, 2005.
- [34] J. Pombo and P. Antunes, “A Comparative Study between Two Pantographs in Multiple Pantograph High-Speed Operations,” *International Journal of Railway Technology*, vol. 2, no. 1, pp. 83–108, 2013.
- [35] Z. Liu, P.-A. Jönsson, S. Stichel, and A. Rønnquist, “Implications of the operation of multiple pantographs on the soft catenary systems in Sweden,” *Proceedings of the Institution of Mechanical Engineers, Part F: Journal of Rail and Rapid Transit*, vol. 230, no. 3, pp. 971–983, 2014.
- [36] Z. Liu, P.-A. Jönsson, S. Stichel, and A. Rønnquist, “On the implementation of an auxiliary pantograph for speed increase on existing lines,” *Vehicle System Dynamics*, vol. 54, no. 8, pp. 1077–1097, 2016.
- [37] Y. Song, Z. Liu, H. Wang, X. Lu, and J. Zhang, “Nonlinear analysis of wind-induced vibration of high-speed railway catenary and its influence on pantograph–catenary interaction,” *Vehicle System Dynamics*, vol. 54, no. 6, pp. 723–747, 2016.
- [38] P. Nåvik, A. Rønnquist, and S. Stichel, “Identification of system damping in railway catenary wire systems from full-scale measurements,” *Engineering Structures*, vol. 113, pp. 71–78, 2016.
- [39] “JD540 Teknisk regelverk, Kontaktledning.” [Online]. Available: <https://trv.jbv.no/wiki/Kontaktledning/Projektering/Kontaktledningssystemer>. [Accessed: 08-Feb-2016].
- [40] C. Rainieri and G. Fabbrocino, *Operational Modal Analysis of Civil Engineering Structures*. New York: Springer, 2014.
- [41] H. Nyquist, “Certain Topics in Telegraph Transmission Theory,” *Transactions of the American Institute of Electrical Engineers*, vol. 47, no. 2, pp. 617–644, 1928.
- [42] A. Collina and S. Bruni, “Numerical Simulation of Pantograph-Overhead Equipment Interaction,” *Vehicle System Dynamics*, vol. 38, no. 4, pp. 261–291, 2002.

- 
- [43] InvenSense Inc., “MPU-6000 and MPU-6050 Product Specification, Revision 3.4,” 2013.
- [44] P. Nåvik, A. Rønquist, and S. Stichel, “A wireless railway catenary structural monitoring system: Full-scale case study,” *Case Studies in Structural Engineering*, vol. 6, pp. 22–30, 2016.
- [45] “ROGER 1000.” [Online]. Available: <http://www.mermecgroup.com/inspect/recording-cars/104/roger-1000.php>. [Accessed: 16-Jun-2016].
- [46] P. Nåvik, A. Rønquist, and S. Stichel, “The use of dynamic response to evaluate and improve the optimization of existing soft railway catenary systems for higher speeds,” *Proceedings of the Institution of Mechanical Engineers, Part F: Journal of Rail and Rapid Transit*, vol. 230, no. 4, pp. 1388–1396, 2015.
- [47] A. Rønquist and P. Nåvik, “Dynamic assessment of existing soft catenary systems using modal analysis to explore higher train velocities: a case study of a Norwegian contact line system,” *Vehicle System Dynamics*, vol. 53, no. 6, pp. 756–774, 2015.
- [48] K. Ikeda, “Optimization of Overhead Contact Lines for Shinkansen Speed Increases,” *JR EAST Technical Review*, no. 12, pp. 64–69, 2008.
- [49] N. Zhou and W. Zhang, “Investigation on dynamic performance and parameter optimization design of pantograph and catenary system,” *Finite Elements in Analysis and Design*, vol. 47, no. 3, pp. 288–295, Mar. 2011.
- [50] P. Nåvik and A. Rønquist, “Dynamic behaviour of an existing railway catenary system for extreme low passage at exceeding design velocities,” in *Proceedings of the 9th International Conference on Structural Dynamics, EURODYN*, 2014.
- [51] A. Rønquist and P. Nåvik, “Dynamic implications for higher speed in sharp curves of an existing Norwegian overhead contact line system for electric railways,” in *Proceedings of the 9th International Conference on Structural Dynamics, EURODYN*, 2014.
- [52] G. T. Frøseth, P. Nåvik, and A. Rønquist, “Operational displacement estimations of railway catenary systems by photogrammetry and the integration of acceleration time series,” *submitted for journal publication*, 2016.
- [53] A. Rønquist and P. Nåvik, “Vertical vs. lateral dynamic behaviour of soft catenaries subject to regular loading using field measurements,” *submitted for journal publication*, 2016.
- [54] Y. H. Cho, J. M. Lee, S. Y. Park, and E. S. Lee, “Robust Measurement of Damping Ratios of a Railway Contact Wire Using Wavelet Transforms,” *Key Engineering Materials*, vol. 321–323, pp. 1629–1635, 2006.
- [55] D. Zou, W. H. Zhang, R. P. Li, N. Zhou, and G. M. Mei, “Determining damping characteristics of railway-overhead-wire system for finite-element analysis,” *Vehicle System Dynamics*, vol. 54, no. 7, pp. 902–917, 2016.
- [56] P. Nåvik, A. Rønquist, and S. Stichel, “Variation in the prediction of pantograph-catenary interaction contact forces, numerical simulations and field measurements,” *submitted for journal publication*, 2016.

---

### Further readings

Andersson, E., Berg, M. and Stichel, S., *Rail Vehicle Dynamics*, Stockholm: Railway Group KTH, 2007. ISBN 978-91-7415-272-2.

Bendat, J. S. and Piersol, A. G., *Random Data: Analysis and Measurement Procedures*, 4<sup>th</sup> ed. Hoboken, New Jersey: John Wiley & Sons, Inc., 2010. ISBN 978-0-470-24877-5.

Broch, J. T., *Principles of experimental frequency analysis*, Barking, Essex, England: Springer Science+Business Media, 1990. ISBN 978-94-010-6840-6.

Chatfield, C., *The Analysis of Time Series: An Introduction*, 6<sup>th</sup> ed. Boca Raton, Florida: CRC Press, 2004. ISBN 1-58488-317-0.

Chopra, A. K., *Dynamics of Structures: Theory and Application to Earthquake Engineering*, 3<sup>rd</sup> ed. Upper Saddle River, New Jersey: Pearson Education, Inc., 2007. ISBN 0-13-156174-X.

Cook, R. D., Malkus, D. S., Plesha, M. E. and Witt, R. J., *Concepts and applications of finite element analysis*, 4<sup>th</sup> ed. Hoboken, New Jersey: John Wiley & Sons, Inc., 2002. ISBN 978-0471356059.

Doyle, J. F., *Wave Propagation in Structures: Spectral Analysis Using Fast discrete Fourier Transforms*, 2<sup>nd</sup> ed. New York: Springer-Verlag New York, Inc., 1997. ISBN 0-387-94940-2.

Ewins, D. J., *Modal testing: theory, practice and application*, 2<sup>nd</sup> ed. Baldock, Hertfordshire, England: Research Studies Press Ltd, 2000. ISBN 0-86380-218-4.

Kiessling, F., Puschmann, R., Schmieder, A. and Schneider, E., *Contact Lines for Electric Railways: Planning, Design, Implementation, Maintenance*, 2<sup>nd</sup> ed. Erlangen: Publicis Publishing, 2012. ISBN 978-3-89578-322-7.

Ljung, L., *System Identification: Theory for the User*, 2<sup>nd</sup> ed. Upper Saddle River, New Jersey: Prentice-Hall, Inc., 1999. ISBN 978-0-13-656695-3.

Madisetti, V. K. and Williams, D. B., *The Digital Signal Processing: Handbook*, Boca Raton, Florida: CRC Press, 1999. ISBN 0-8493-8572-5.

Maia, N. and Silva, J., *Theoretical and Experimental Modal Analysis*, Baldock, Hertfordshire, England: Research Studies Press Ltd, 1998. ISBN 0-86380-208-7.

Rainieri, C. and Fabbrocino, G., *Operational Modal Analysis of Civil Engineering Structures: An Introduction and Guide for Applications*, New York: Springer Science+Business Media, 2014. ISBN 978-1-4939-0766-3.





## Paper I

Petter Nåvik, Anders Rønnquist, Sebastian Stichel


The use of dynamic response to evaluate and improve the optimization of existing soft railway catenary systems for higher speeds

Proceedings of the Institution of Mechanical Engineers Part F Journal of Rail and Rapid Transit  
2016;230(4):1388-1396

DOI:10.1177/0954409715605140



# The use of dynamic response to evaluate and improve the optimization of existing soft railway catenary systems for higher speeds

Proc IMechE Part F:  
*J Rail and Rapid Transit*  
 2016, Vol. 230(4) 1388–1396  
 © IMechE 2015  
 Reprints and permissions:  
[sagepub.co.uk/journalsPermissions.nav](http://sagepub.co.uk/journalsPermissions.nav)  
 DOI: 10.1177/0954409715605140  
[pif.sagepub.com](http://pif.sagepub.com)  


Petter N avik<sup>1</sup>, Anders R onnquist<sup>1</sup> and Sebastian Stichel<sup>2</sup>

## Abstract

An increasing demand for reduced travel times requires the exploitation of the full capacity of existing overhead railway catenary systems. This need has become an issue in Norway, as the majority of existing catenary systems are designed for a maximum speed of 130 km/h. In many regions, plans to reconstruct the railway line do not exist. Therefore, existing catenary sections must be optimized to increase a train's velocity and reduce the total travel time. In this paper, the dynamic response is evaluated in an optimization investigation of an existing soft catenary system. A dynamic investigation that considers finite element models of existing soft railway catenary sections with original tension forces, current tension forces and suggested new tension forces for velocities at and above the design speed is conducted. The dynamic response is quantified by the interpretation of spectral densities and variations in their peak values. Due to more movement at mid-span than at the pole support, the effects from altering the tension forces and increasing the speed can be more accurately described and estimated by considering the dynamic content of the response at mid-span instead of the peak uplift at the pole support. A 23% increase in speed is possible for the system with the best tested new tension force setting, in which only the dynamic response and uplift at the pole support are considered.

## Keywords

Catenary system, soft catenary system, numerical analyses, finite element model, uplift, dynamic response, optimization, existing catenary lines, Norwegian railways

Date received: 8 October 2014; accepted: 5 August 2015

## Introduction

The improvement of the extent of structural understanding over the lifespan of essential infrastructure has become an important problem to address. This problem is partially attributed to the finding that an increasing amount of infrastructure is nearing the end of its design life and is partially attributed to changing loads and the non-fulfilment of maintenance, which causes physical signs of wear and tear. Increased train velocities that enable existing railway lines to satisfy the demand for reduced travel time contribute to significant changes in the loading of the railway catenary system. This load change requires changes in the catenaries.<sup>1</sup>

An essential property of the pantograph/catenary interaction is the uninterrupted and reliable supply of electrical energy to the train.<sup>2</sup> As the train moves along the railway line, this interaction creates a contact force between the contact wire and pan head. The contact force, which varies along the line, produces static and dynamic responses in both systems. For higher-velocity railways, this contact force results

from the interaction between two nonlinear dynamic systems.<sup>2</sup> The complexity of the systems and the importance of the dynamic response progressively increase as the velocity of the train increases.<sup>3</sup> Thus, a thorough understanding of the systems is required to establish a trustworthy numerical finite element (FE) model. The application areas for such a model include the investigation of the performance of current designs and the possibilities for optimizing existing systems, for which an increase in speeds is desirable.<sup>4</sup> Poetsch et al.<sup>2</sup> presented five critical

<sup>1</sup>Department of Structural Engineering, Norwegian University of Science and Technology, Norway

<sup>2</sup>Department of Aeronautical and Vehicle Engineering, KTH Royal Institute of Technology, Sweden

### Corresponding author:

Petter N avik, Department of Structural Engineering, Norwegian University of Science and Technology, Rich. Birkelandsvei 1A, 7491 Trondheim, Norway.  
 Email: [petter.r.navik@ntnu.no](mailto:petter.r.navik@ntnu.no)

parameters for the performance of a catenary system: contact wire tension, messenger wire tension, contact wire sag, errors in setting the contact wire height, and static and dynamic uplift forces.

The FE method is the most common approach for simulation of a catenary system and the interaction between the pantograph and catenary.<sup>5</sup> Alternative approaches include the finite difference method and modal analysis.<sup>2</sup> The elements that are typically used to describe the catenary components are string, bar or beam elements. The beam elements are the best elements to use, especially for the contact wire, based on the quality of the obtained results.<sup>2</sup> The contact between the contact wire and pantograph has been modelled using the Lagrange multiplier method,<sup>6</sup> the penalty method<sup>1</sup> or a combination of these two methods, which is referred to as the augmented Lagrange method.<sup>7</sup> Ambrósio et al.<sup>1</sup> concluded that the penalty method is a suitable approach to describe all relevant features of this contact interface. In most cases, the numerical models of the pantograph are multi-degree-of-freedom lumped mass models with springs and dampers between the masses.<sup>5</sup> Some recent studies have also used multi-body pantograph models.<sup>5</sup>

The dynamic response of the catenary system becomes an important problem as the speed of a train is increased above the original design speed.<sup>8</sup> Catenary systems are generally lowly damped systems. Thus, oscillations appear in a large region, both in front of and behind the contact point, due to the low damping.<sup>2</sup> A problem caused by excessively large oscillations in the catenary is the loss of contact between the pantograph and contact wire, especially for trailing pantographs as they run into the oscillations from the previous pantograph.

A natural step toward a more optimal catenary system is to alter the tension forces in the contact wire and messenger wire. Ikeda<sup>9</sup> employed this approach to optimize a catenary system and obtained a higher train speed. The running speed was increased from 275 to 320 km/h by increasing the tension in the contact wire from 17.6 to 19.6 kN. That study did not change the total combined tension force of the messenger wire, auxiliary catenary wire and contact wire to prevent necessary modifications in the supporting structures. Furthermore, no adjustments in the length of the droppers were necessary, due to the changes in the applied tension force and a change of the cross-sectional area of the contact wire resulting in a desirable geometry. This approach simplified the upgrading process. Zhou and Zhang<sup>10</sup> found that an increase in the tension force in the contact wire significantly improved the minimum, maximum and standard deviation of the contact force, which significantly improved the ratio of contact loss. The effect of these changes on wear is an important consideration. The literature has demonstrated that the results regarding the effect on wear are dependent on the

system on which the change in tension is applied. Bucca and Collina<sup>11</sup> found that an increase in the tension force from 17 to 20 kN yielded a 50% decrease in wear of the contact wire. Shing and Wong<sup>12</sup> noted that an increase in the height of the contact wire at mid-span due to an increase in the resultant tension force can cause increased wear and tear of the collector strips. Thus, an increase in the tension forces may alter the magnitude of wear, and the wear may increase in some locations and decrease in other locations. Additional effects of increased tension forces include low levels of elasticity, negative pre-sag and special effects due to the non-optimal geometry of the catenary in curved railway sections.

The catenary system called Tabell 54 has been investigated. A major part of the existing catenary systems along one of the most important railway lines in Norway, 'The Dovre line', is constructed based on this system. This line is part of the main railway line between Oslo and Trondheim. Tabell 54 was originally designed for maximum train speeds of 90 km/h. The original tension forces in the contact wire and messenger wire were 6.1 and 4.9 kN, respectively.<sup>13</sup> These tension forces have been changed in some portions of the Norwegian railways. In the specific sections studied, they have been changed to 10 and 5 kN, respectively, to enable an increase in the maximum train velocity to 130 km/h. This change in tension forces, which is partially achieved in an ad hoc manner, has been examined to determine whether it improved the dynamic situation. The demand for even higher speeds has resulted in the need to investigate how the dynamic behaviour can be improved at these speeds by applying small changes to the existing catenary system. The dynamic behaviour is the dynamic movement of the wires in the catenary before the train passes, as the train passes and after it has passed. This is evaluated in terms of the displacement of the catenary wires. The dynamic component of the response is generally assumed to significantly increase at speeds above 200–220 km/h. However, in special conditions, an increase may be observed at relatively low speeds.<sup>14</sup> The investigated catenary system is designed for speeds significantly less than 200 km/h. At the original design speed of 90 km/h, the behaviour of the catenary system is quasi-static as the train passes. However, numerical simulations indicate that as the velocity is increased, the dynamic behaviour also rapidly increases until an excessive vibration response is produced.

The primary goal of this study is to use the response of the catenary to quantify the dynamic parameters in an optimization of existing soft catenary systems. The study evaluates a dynamic coupled system, which consists of the catenary system and pantograph. This paper focuses on the interpretation of the dynamic behaviour of the catenary before the train passes, as the train passes and after it has passed. Although the pantograph-catenary interaction

contact force is an important part of the system, it does not fully explain how the catenary behaves before and after passage. Thus, it is not a focus of this study; however, the contact force is within reasonable magnitudes. Three-dimensional FE models of full-length sections of an existing soft Norwegian catenary system have been developed. The numerical model should consider the potential for nonlinear geometry, damping and material properties. A sufficiently long stretch is modelled to prevent the boundary conditions from becoming a decisive factor. The dynamic behaviour has been investigated by considering displacement time series from the numerical analyses and power spectral densities estimated using the Burg method.<sup>15</sup>

### Tension forces in catenary systems

The main existing catenary systems in Norway are called Tabell 54, System 35, System 20 and System 25. The last three systems are the only used in new railway sections in Norway.<sup>16</sup> The main difference between these systems is that they are designed for different train speeds. The maximum permissible speed and tension forces for the different systems are listed in Table 1, which illustrates the strong correlation between increasing tension forces and maximum allowed train speeds.

In the investigated Tabell 54 system, a small change in the tension in the messenger wire will produce a relatively large change in the geometry of the catenary. It also significantly affects the sag of the contact wire. A small increase in the force will cause a considerable lift of the contact wire and may produce negative sag. Positive pre-sag is initially determined to improve the performance of the current collection. However, Harada et al.<sup>17</sup> determined that no pre-sag is preferred at speeds higher than 300 km/h. No pre-sag or negative pre-sag is not optimal for the performance of the investigated catenary for the considered train velocities. Negative pre-sag has been detected on existing lines on systems with speed limits below 300 km/h.<sup>12</sup> Material failure restrictions regarding the maximum permissible tension force that is allowed in the contact wire are provided in EN 50119.<sup>18</sup> In addition to a safety factor, the parameters

included in this restriction are either climate or structure dependent. The maximum level has been calculated to be 17 kN.

## FE models

### The catenary

Several three-dimensional FE models of different railway section configurations have been created in the software Abaqus for this investigation. The contact wire, messenger wire and droppers were modelled with three-dimensional deformable beam elements. Timoshenko beam elements were used to ensure a stable numerical solution. Euler–Bernoulli beam elements could have been used; however, the use of either element has a negligible effect on the results.<sup>2</sup> The damping of the wire system was introduced by the use of Rayleigh damping,<sup>19</sup> which yielded a mass- and stiffness-proportional damping matrix. This type of damping has been used in several studies on catenary systems.<sup>20–22</sup> A damping coefficient of 2% was utilized. The frequencies used to calculate the Rayleigh coefficients were 0.86 Hz, the first natural frequency of Tabell 54, and 15 Hz. The effective damping ratio for each of the natural frequencies was identified in Abaqus to provide control of the actual damping that was introduced in the numerical model. The majority of the effective damping ratios originated from the mass-proportional part of the Rayleigh damping, as Abaqus includes Rayleigh damping coefficients only as a linear combination with the strain–stiffness matrix. Thus, damping contributions that originated from the geometric stiffness were not included. For slender structures, such as catenary systems, the geometric stiffness is a major portion of the total stiffness. The damping was accurately introduced for low frequencies, whereas the higher-frequency damping contributions were slightly underestimated. As the fundamental motions of the vertical vibrations in the catenary fall in the low-frequency range of 0–2 Hz, the damping of the dynamic response was accurately represented.

An easy and practical solution for varying the properties of the catenary system is to use different tension forces. Four models with different tension force settings were constructed for this reason, and one span from each of the models is presented in Figure 1 to illustrate the differences in their geometry. The first set, M1, includes the tension forces that the initial design (in 1956) of Tabell 54 recommended. The second set, M2, includes the tension forces that are currently used in an existing Tabell 54 catenary section at Soknedal in Norway. The tension forces in the final two sets, M3 and M4, are considered to illustrate how changes in tension forces, including different ratios between the contact wire and the messenger wire, affect the dynamic performance in an optimization of the catenary system. The goal of M3 was to

**Table 1.** Tension force distributions in Norwegian catenary systems, contact wire (CW) and messenger wire (MW).

Catenary system <sup>16</sup>	Tabell 54	System 35	System 20	System 25
Tension in the CW (kN)	10	7.1	10	15
Tension in the MW (kN)	5	7.1	10	15
Max. speed (km/h)	130	150	200	250

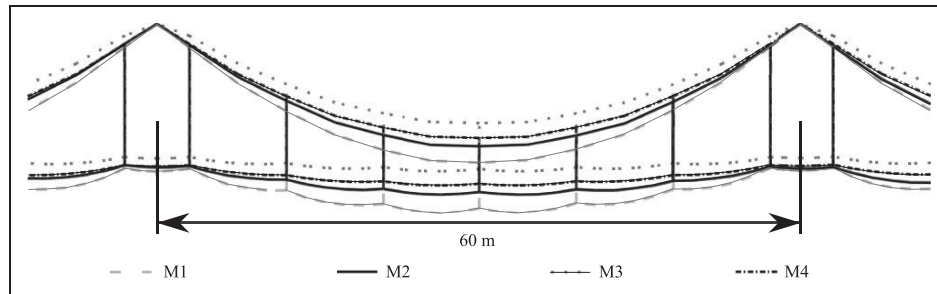


**Figure 1.** A scaled representation of the geometry of a catenary span for various tension forces. Tension levels for all models are included (contact wire/messenger wire).

**Table 2.** The geometric properties of the droppers and their positions along a span.

	Dropper number						
	1	2	3	4	5	6	7
Position along a span (m)	3	12	21	30	39	48	57
Length of the dropper (cm)	135	88	60	51	60	88	135

obtain a stiffer system with no pre-sag and an increase in both the contact wire and messenger wire tensions. The goal of M4 was to obtain some pre-sag (38 mm) and a stiffer system. All of the models had the same initial geometry, 25 consecutive 60-m long spans with seven droppers in each span and no stitch wires. The position along a span and the length of the dropper are listed in Table 2, and the system height is 1.6 m. The mechanical properties of the Tabell 54 catenary system are listed in Table 3. The possible influence of tension changes on the dynamic response is initially evident in the variation of the fundamental frequency. The corresponding natural frequencies in the vertical direction were estimated by the FE model for all tension force sets; the first five frequencies for each set are presented in Table 4. The estimated frequencies also correspond with the values calculated using the formulas suggested by Kiessling et al.<sup>3</sup>

**The pantograph**

Four different pantographs are currently used in Norway: Schunk WBL 85, Schunk WBL 88, Schunk WBL88 AT and RM374. The pantograph WBL 88 is used in this study, as it is a common pantograph in the investigated section. The aerodynamic contact force, which is presented in equation (1), contains a static contact force and an aerodynamic component that is

dependent on the speed of the train. The equation was obtained from the manufacturer of the pantograph

$$F_{uplift} = 55 + 0.0068v^2 \tag{1}$$

where  $F_{uplift}$  is the total uplift force and  $v$  is the velocity.

The pantograph was modelled as a spring–mass–damper model in accordance with a model obtained from the manufacturer Schunk Nordiska AB. This model, which is illustrated in Figure 2, includes mass  $m_1 = 6.6$  kg, which represents the pan head, and mass  $m_2 = 19.7$  kg, which represents the mass of the pantograph arm. Both of these components are modelled as rigid bodies. Spring  $k_1 = 4400$  N/m and dampers  $c_1 = 75.6$  Ns/m and  $c_2 = 63.5$  Ns/m represent the measured values for the stiffness and the damping between the respective components.  $F_2 = 17$  N is the constant friction,  $F_s = 55$  N is the static uplift force and  $F_a = 0.0068v^2$  is the aerodynamic uplift force. This simple model can only have one natural frequency, which was determined to be 4.78 Hz.

**Dynamic response estimation and evaluation of the system configuration for an increasing train velocity**

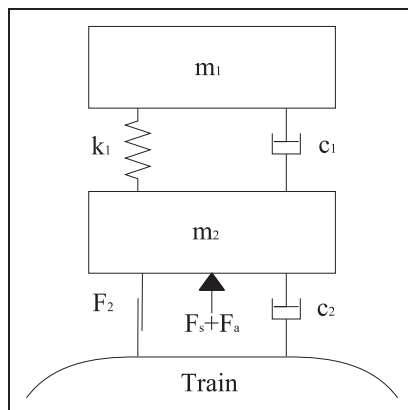
Dynamic analyses were performed at several train speeds for the four different models. The train speeds of 90, 130, 200 and 250 km/h are of particular interest. The first train speed of 90 km/h is the running velocity at the Soknedal section, and the second train speed of 130 km/h is the current maximum velocity of the Tabell 54 system. A general objective for the investigations on the Tabell 54 is to determine how close to 200 km/h a train can travel on straight sections. Newly built catenary sections around Oslo in Norway are designed for speeds up to 250 km/h. The analysis results were sampled from specific positions in specific spans. The results were sampled in spans A–F, as shown in Figure 3, and from positions 1 and 2, as shown in Figure 4. The reference selected

**Table 3.** The mechanical properties of the wires in the Tabell 54 catenary system.

Wire	Name	E-modulus (GPa)	Density (kg/m <sup>3</sup> )	Poisson's ratio	Cross-sectional area (mm <sup>2</sup> )
Contact wire	Ri 100 Cu	120	8890	0.34	100
Messenger wire	Bz II 50/19	120	8890	0.34	49.48
Dropper	Bz II 10/49	120	8890	0.34	9.6

**Table 4.** The different tension forces and their corresponding vertical natural frequencies.

Model	M1	M2	M3	M4
Tension in the contact wire (kN)	6.1	10	13	15
Tension in the messenger wire (kN)	4.9	5	5.4	5
First natural frequency (Hz)	0.73	0.86	0.95	0.99
Second natural frequency (Hz)	1.0	1.05	1.07	1.1
Third natural frequency (Hz)	1.5	1.7	1.9	2.0
Fourth natural frequency (Hz)	2.2	2.5	2.8	2.9
Fifth natural frequency (Hz)	2.9	3.0	3.3	3.4

**Figure 2.** The numerical model of the WBL 88 pantograph.

for the investigation was the current situation for Tabell 54: 130 km/h in model M2 (Table 4).

The thorough study of the dynamic response of the system was based on the displacement time series sampled in the 12 identified positions. As expected, the results depict the changes in the responses for increasing velocities and changes in tension forces. Typical plots of the vertical displacement time series at mid-span as the train passes for 90, 130 and 200 km/h on model M2 are shown on the left in Figure 5. These diagrams show the response range from the quasi-static response at 90 km/h via the transient and rapidly decaying response at 130 km/h, to the nearly stationary response after the uplift for 200 km/h. The influence of the dynamic behaviour at 90 km/h is independent of the tension forces applied in the four models and exhibit the same type of quasi-

static response as shown in Figure 5. As the original catenary system was designed for operation at 90 km/h and a quasi-static behaviour, the system exhibits a steady decreasing uplift for an increasing tension force, as shown in Figure 6. As the train speed is increased, the catenary response will vary depending on the selected tension forces, due to the increasing influence of the inertia and damping forces compared with the steady quasi-static increase. Thus, further investigation of these changes in the response is essential, as the dynamics will gradually dominate the response. The dynamic response demonstrated by the spectral densities gradually change from the low-banded and broad-banded descriptions of a quasi-static uplift to a few dominating structural response frequencies of the catenary vibration.

Analyses of the frequency content were performed to better evaluate the amount of dynamic content in the response. The power spectral densities were estimated using Burg's method.<sup>15</sup> To understand the significance of the dynamic response, it is quantified by the changes in the spectral peak of the dominating harmonic component. The amount of dynamic response can be correlated to the magnitude of the spectral density. The spectral densities that correspond to the displacement time series are shown on the right side of Figure 5. The figure illustrates how the dynamic content around the dominating harmonic component evolves with increasing speed; here, the frequency axis is limited to 2 Hz for clarity. The diagrams reveal that there is nearly no dynamic content for a train speed of 90 km/h, only the quasi-static peak uplift. The situation changes for a speed of 130 km/h. A distinct peak is observed at approximately 0.7 Hz, which is the frequency of the motion induced by the moving pantograph and it dominates the vibration



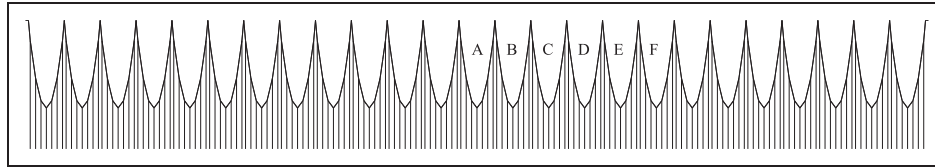


**Figure 3.** The spans that were used to sample the results from the analyses of model M2.

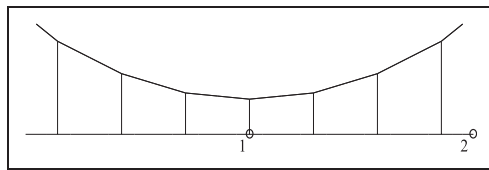


**Figure 4.** The points in the spans that were used to sample all results.

after the uplift. An increase in the peak magnitude at the same frequency is detected in the analyses performed for a speed of 200 km/h.

The time series of a passage is a time-variant process. However, if the time series is broken down into sufficiently small time segments, the segments will only exhibit a weak time variance, which enables the use of spectral densities to analyse the structural response. The minimum time length is given by the order size of the current Burg spectrum and the sampling frequency, maximum order 400 and 100 Hz in this study, respectively. This gives a maximum time length of 4 s. The dynamic displacements of the contact wires system will have its largest value at mid-span due to the elasticity distribution. Therefore, changes in the dynamic response will be easier to identify at mid-span than at the pole-position. The dynamic behaviour analyses were primarily evaluated at mid-span. The significance of the dynamic responses of catenary systems is particularly important when increasing speed on a soft catenary system, such as for the Norwegian Tabell 54. The passage reveals variable information about the different time stages. These vibrations are distinguished from the more common concerns of higher-speed rail, i.e. minimum velocities of 250 km/h. For these systems, a major concern is the effects of wave propagation in the contact wire. The reflection coefficient, the Doppler Effect and the possible increase in the response by dynamic magnification factors greater than unity should be evaluated. These effects do not comprise the main dynamic responses of concern for soft catenary systems, in which the wave propagation speed for the different configurations of Tabell 54 ranges between 300 and 470 km/h. The speed at which the dynamic magnification factor exceeds a value of one was calculated to be in the range 130–260 km/h, i.e. both velocities exceed realistic velocities for this system.

As a part of this study, the maximum vertical displacements at both the support and mid-span were obtained. The mean and standard deviation of the maximum displacements from six successive spans, at mid-span and at the support, were estimated for each analysis, as shown in Figure 6(a) and (b). The importance of considering dynamic properties for system optimization at velocities greater than 130 km/h is demonstrated by the peak uplifts in Figure 6. The initial mid-span response steadily increases for all higher tension settings (M2–M4) compared with the original design (M1). However, the latter exhibits a total steady increase from 130 km/h; the effect is even greater for the pole-support response. The change in the response between 90 and 150 km/h occurs where the response changes from quasi-static to harmonic. An interesting and distinct change occurs for the Tabell 54 system between 150 and 160 km/h. Here, the dynamic magnification becomes significant and changes the deflection shape. The catenary response changes from a decaying impulse response to a harmonic vibration. The response frequency and mode shape are subsequently determined by the passing pantograph before reaching the fundamental frequency of the given span. The initial vibrations also become sufficiently important and influence the peak uplift at mid-span and create a slight reduction of this peak uplift. This effect is controlled by the dynamic properties of the catenary system and the amount of kinetic energy that the pantograph introduces to the vertical motion due to the interaction of the coupled dynamic systems. This effect is greater for system setting M2 than the effect for M3 and M4, which renders a smaller reduction of the mid-span peak uplift, as shown in Figure 6. This change is also observed for the pole-support response, in which the peak uplift distinctly increases due to equivalent effects. The transition also occurs for the original setting M1; however, due to its early dominating harmonic response, the change is not as distinct as for the remaining three systems, M2–M4. The next change in the dominating harmonic component occurs between 190 and 200 km/h, it generates a substantial increase in the peak uplift at the pole position and a smaller decrease at mid-span. However, these velocities are not sufficiently realistic to use, as the permitted dynamic response is already exceeded; however, they are included for completeness and further understanding of the development of the system's response.

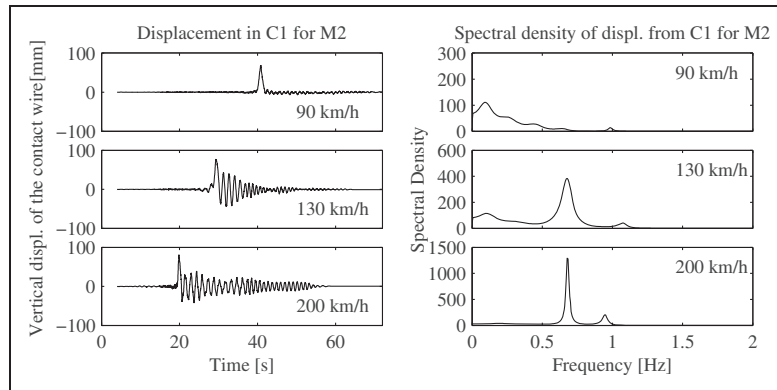


**Figure 5.** Left, the vertical displacement of the contact wire at mid-span, span C and model M2. Right, the spectral densities obtained from the vertical displacement at mid-span, span C and model M2, from 0 to 2 Hz.

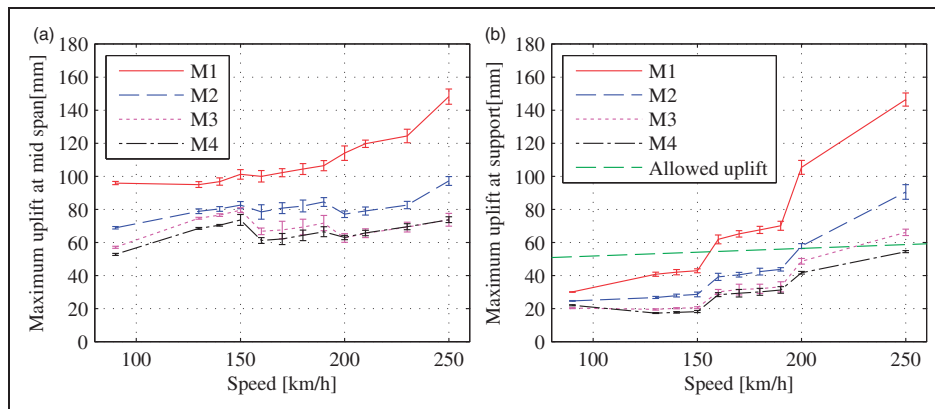


**Figure 6.** The mean maximum uplifts and one standard deviation obtained at (a) the mid-span and (b) the support for all four tension-force settings for each of the 12 velocities. The error bars show one positive and one negative standard deviation.

The vibration after passage at low velocities, such as 90 km/h, is nearly non-existent. As the post-passage vibration becomes significant, the initial harmonics are given by the fundamental frequencies and load span-pass frequency. The latter is dependent on the train velocity and span length. As the velocity increases, the catenary response also increases. As the train speed increases, the post-passage motions become dominated by the load-induced frequency and corresponding mode shape. These modes are created by a moving load and are also influenced by the velocity. As the catenary's vertical motion at the pole cantilever is only restricted by the attachment of the messenger wire, the load-induced motion lifts a longer span than the pole span and activates sections of the neighbouring spans. This creates a load response with correspondingly lower frequencies. Excitation of the fundamental mode will simultaneously place several

consecutive spans in motion; therefore, it is limited to the natural mode of a pole span length and is consequently higher.

The described effects are clearly shown in Figure 7. Diagrams of the three settings, M2–M4, for selected velocities between 90 and 190 km/h are included. The original setting, M1, already experiences problems at low velocities and exhibits limitations within the range of 90–130 km/h, which is equally defined by its quasi-static behaviour as its dynamic behaviour. The second setting, M2, which is the current setting for the Tabell 54 system, exhibits a strong increase in the dynamic response at its maximum allowed speed, which is a distinct indicator that this system is near its practical limit. The limiting velocities of this setting, which are defined by its dynamic behaviour, are within the range 130–140 km/h. The last two system settings, M3 and M4, are both distinctly controlled and limited by their

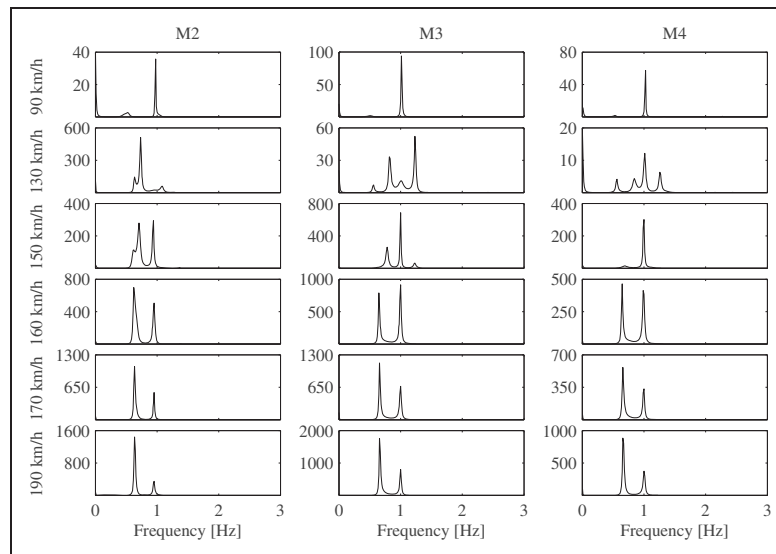


**Figure 7.** Spectral density plots (in  $\text{m}^2/\text{s}$ ) at varying tension configurations and train velocities.

dynamic behaviours. At low velocities, they both exhibit an initial high peak of the fundamental frequency, which originates from the decaying impulse response of the passage. As the velocity surpasses 150 km/h, a transition to a standing load response is observed by regarding the lower frequency peak, which dominates approximately half the post-passage duration. The higher frequency peak originates from the fundamental frequency-controlled response in the final decay. As the velocity continues to increase, the kinetic input increases, which renders longer duration of the load-induced vibrations, i.e. increases the lower frequency spectral peak, as shown in Figure 7. Here, excessive vibrations completely dominate the system's response. System settings M3 and M4 reach their limits within 150–160 and 160–170 km/h, respectively. This finding reflects the fact that a small pre-sag of the contact wire in M4 is preferable to no pre-sag in M3 at the investigated speeds, as expected.

## Conclusions

The use of dynamic response as a tool to evaluate and improve an optimization of existing soft catenary systems for higher speeds has been suggested. The evaluation and interpretation of spectral densities and peak values were used to quantify the changes in the dynamic response. This investigation was implemented on the dynamic behaviour of the Norwegian soft catenary system Tabell 54. The dynamic behaviour was evaluated at mid-span by focusing on the variation in the dynamic response at this point. The dynamic response is more significant at mid-span than at the pole position, especially at lower train speeds.

The transition from quasi-static to transient response typically falls within acceptable levels, whereas the transition to continuous oscillations creates a higher probability of excessive vibrations for these systems. The evaluation of the optimization was quantified by an evaluation of the changes in the peaks of spectral density plots and their corresponding frequencies. Spectral estimations post-passage were presented; these estimations demonstrated the importance of controlling the changing progression in these results. The importance of the underlying dynamic process confirmed the variation between the peak uplifts at mid-span and at the pole position and the peak uplift change gradient at given velocity segments. To retain the current pole uplift, it is an advantage to optimize for the dynamic response, as it provides more distinct indications compared with the actual uplift at either mid-span or the pole position. The combination of uplift and dynamic response creates a more complete result for the evaluation of soft systems. Thus, this study indicates that an investigation that only considers the uplift values is insufficient to fully understand and optimize the structural parameters. The results from this investigation imply that changing the properties of a catenary system is necessary to significantly increase the speed on that system. Although the current tension force setting has reached its speed limit, the setting M4 allows for a 23% increase in speed when only considering the uplift and dynamic response in the system. For the investigated catenary and train velocities, a small pre-sag, as shown in M4, is favourable to no pre-sag, as shown in M3. Several other limiting factors should be considered before an increase in speed can be fully verified.

### Declaration of Conflicting Interests

The author(s) declared no potential conflicts of interest with respect to the research, authorship, and/or publication of this article.

### Funding

The author(s) disclosed receipt of the following financial support for the research, authorship, and/or publication of this article: The authors are grateful to the Norwegian National Rail Administration for their funding of this research.

### References

1. Ambrósio J, Pombo J, Pereira M, et al. Recent developments in pantograph-catenary interaction modelling and analysis. *Int J Railway Technol* 2012; 1: 249–278.
2. Poetsch G, Evans J, Meisinger R, et al. Pantograph/catenary dynamics and control. *Veh Syst Dyn* 1997; 28: 159–195.
3. Kiessling F, Puschmann R, Schmieder A, et al. *Contact lines for electric railways?: planning, design, implementation, maintenance*. Munich, Germany: Publicis, 2009.
4. Gostling R and Hobbs A. The interaction of pantograph and overhead equipment: practical applications of a new theoretical method. *Proc IMechE, Part C: J Mech Engng Sci* 1983; 197: 61–69.
5. Bruni S, Ambrosio J, Carnicero A, et al. The results of the pantograph-catenary interaction benchmark. *Veh Syst Dyn* 2014; 53: 412–435.
6. Schaub M and Simeon B. Pantograph-catenary dynamics: an analysis of models and simulation techniques. *Math Comput Model Dyn Syst* 2001; 7: 225–238.
7. Ambrósio J, Pombo J, Rauter F, et al. A memory based communication in the co-simulation of multibody and finite element codes for pantograph-catenary interaction simulation multibody dynamics. In: CL Bottasso (ed.) *Multibody dynamics*. Amsterdam, The Netherlands: Springer, 2008, pp.231–252.
8. Scott GA and Cook M. Extending the limits of pantograph/overhead performance. In: *Better journey time - better business*. Bury St Edmunds, UK: Mechanical Engineering Publications Limited, 1996, pp.207–218.
9. Ikeda K. Optimization of overhead contact lines for Shinkansen speed increases. *JR EAST Tech Rev* 2008; 12: 64–69.
10. Zhou N and Zhang W. Investigation on dynamic performance and parameter optimization design of pantograph and catenary system. *Finite Elem Anal Design* 2011; 47: 288–295.
11. Bucca G and Collina A. A procedure for the wear prediction of collector strip and contact wire in pantograph-catenary system. *Wear* 2009; 266(1-2): 46–59.
12. Shing AWC and Wong PPL. Wear of pantograph collector strips. *Proc IMechE, Part F: J Rail Rapid Transit* 2008; 222: 169–176.
13. JD540 Teknisk regelverk, Kontaktledning/Projektering. <https://trv.jbv.no/PDF/Kontaktledning/542/vedlegg/T4205h00.pdf> (2012, accessed 2 October 2013).
14. Bucca G, Carnevale M, Collina A, et al. Adoption of different pantographs' preloads to improve multiple collection and speed up existing lines. *Int J Veh Mech Mob* 2012; 50(1): 403–418.
15. Burg JP. *Maximum entropy spectral analysis*. PhD thesis, Stanford University, USA, 1975.
16. Mekanisk systembeskrivelse av kontaktledningsanlegg. [http://www.jernbanekompetanse.no/wiki/Mekanisk\\_systembeskrivelse\\_av\\_kontaktledningsanlegg#Ledningsf.C3.B8ring](http://www.jernbanekompetanse.no/wiki/Mekanisk_systembeskrivelse_av_kontaktledningsanlegg#Ledningsf.C3.B8ring) (2011, accessed 2 October 2013).
17. Harada S, Shimizu M, Ikeda K, et al. Development of simple catenary equipment using PHC contact wire for Shinkansen. *Q Rep RTRI* 2008; 49: 96–102.
18. EN 50119: 2009. Railway applications - fixed installations - electric traction overhead contact lines.
19. Rayleigh JWS. *The theory of sound, vol. 1*. Second ed. London, UK: Macmillan, 1894.
20. Ambrósio J, Pombo J and Pereira M. Optimization of high-speed railway pantographs for improving pantograph-catenary contact. *Theor Appl Mech Lett* 2013; 3: 013006-1–013006-7.
21. Benet J, Alberto A, Arias E, et al. A mathematical model of the pantograph-catenary dynamic interaction with several contact wires. *Int J Appl Math* 2007; 37: 136–144.
22. Facchinetti A, Gasparetto L and Bruni S. Real-time catenary models for the hardware-in-the-loop simulation of the pantograph-catenary interaction. *Veh Syst Dyn* 2013; 51: 499–516.



## Paper II

Anders Rønnquist, Petter Nåvik

Dynamic assessment of existing soft catenary systems using modal analysis to explore higher train velocities: A case study of a Norwegian contact line system

Vehicle System Dynamics 2015;53(6):756-774

DOI:10.1080/00423114.2015.1013040

Is not included due to copyright



## Paper III

Petter Nåvik, Anders Rønnquist, Sebastian Stichel

Identification of system damping in railway catenary wire systems from  
full-scale measurements

Engineering Structures 2016;113:71-78

DOI:10.1016/j.engstruct.2016.01.031

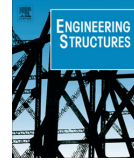






Contents lists available at ScienceDirect

Engineering Structures

journal homepage: [www.elsevier.com/locate/engstruct](http://www.elsevier.com/locate/engstruct)

## Identification of system damping in railway catenary wire systems from full-scale measurements



Petter N avik<sup>a,\*</sup>, Anders R onnquist<sup>a</sup>, Sebastian Stichel<sup>b</sup>

<sup>a</sup> Norwegian University of Science and Technology, Department of Structural Engineering, Rich. Birkelandsvei 1A, 7491 Trondheim, Norway

<sup>b</sup> KTH Royal Institute of Technology, Department of Aeronautical and Vehicle Engineering, SE-100 44 Stockholm, Sweden

### ARTICLE INFO

#### Article history:

Received 17 August 2015

Revised 18 January 2016

Accepted 20 January 2016

#### Keywords:

Structural damping

Railway catenary systems

Full-scale measurements

Pantograph–catenary interaction

Covariance-driven stochastic subspace

identification

Rayleigh damping

### ABSTRACT

Damping is an important property in predicting the response of any civil or mechanical engineering structure, including railway catenary systems. Numerical models describing the pantograph–catenary interaction are dependent on a proper description of the structural damping for both systems to obtain accurate results. A proper description of the damping in different pantographs can easily be found in the literature. However, few studies have considered the damping properties in railway catenary systems even though such systems are considered to be lightly damped. The aim of this study was to identify the system damping of catenary sections by thoroughly analyse several recorded acceleration time series. These time series were sampled in several points on three different existing railway catenary systems, rendering a good description of the system damping in the frequency range of 0–20 Hz. The covariance-driven stochastic subspace identification (Cov-SSI) method was used to analyse the time series, and Rayleigh coefficients were successfully identified for all three catenary sections.

  2016 Elsevier Ltd. All rights reserved.

### 1. Introduction

All civil engineering structures vibrate in operation to a certain degree, although some vibration responses can be regarded as quasi-static for practical purposes. Vibration is often not desirable in a structure and should thus be kept as low as possible. Thus, engineers often aim to reduce the response by mitigating the vibration energy through structural damping. It is essential to have a proper understanding of the damping in a structure to describe its dynamic behaviour.

The pantograph–catenary interaction is a coupled nonlinear dynamic system. Uninterrupted contact between the two components is essential for the power supply of the train [1]. The structural behaviour of the railway catenary sections as trains pass by is critical to achieve adequate contact between the pantograph and catenary. This contact initiates the vibration of the catenary system. The coupled dynamic system consists of one spatially stationary dynamic system, i.e., the catenary, and one moving dynamic system, i.e., the pantograph. The structural behaviour of the pantograph, including the damping, is well described in the literature, e.g., [2]. However, the system damping of catenary systems is not as well documented and published.

Railway catenary systems are considered to be lightly damped structures [1,3,4]. Thus, oscillations appear in a wide area in front of and behind the pantograph–catenary interaction contact point [1]. Hence, a leading pantograph will run into an already vibrating system excited by waves sent ahead of the contact point. Trailing pantographs will run into the wake of the leading pantograph as well as its own oscillations. The amount of damping in the catenary determines whether the pantographs will run into a highly vibrating wire [1]. Thus, the contact quality is directly dependent on the amount of structural damping in the catenary [4,5]. The damping in railway catenary systems is typically assumed to be on the order of 1% of the critical damping coefficient, and some frequency dependence has been observed [1].

A recent review paper stated that the estimation of damping in catenary systems is still recognised as a challenge [4]. It is difficult to estimate the damping ratio of catenary systems because of several closely spaced natural modes and because the estimations are easily corrupted by noise [5]. Another difficulty in estimating the damping lies in the fact that the coupled system's natural frequencies decrease due to changes in stiffness with increasing train speed. Thus, the damping ratio will also increase slightly with increasing speed [6]. Environmental disturbances, e.g. wind, snow and ice, may also affect the estimate of damping. However, few studies have been published on the estimation of damping from measurements sampled on existing catenary sections. Stickland

\* Corresponding author. Tel.: +47 480 30 379.

E-mail address: [petter.r.navik@ntnu.no](mailto:petter.r.navik@ntnu.no) (P. N avik).

**Table 1**

Damping coefficients found in the literature, where  $\alpha$  and  $\beta$  are the mass- and stiffness-proportional damping coefficients, respectively, and  $\zeta$  is the damping ratio (CW and MW are the contact wire and messenger wire, respectively).

Paper	$\alpha_{cw}$	$\alpha_{mw}$	$\beta_{cw}$	$\beta_{mw}$	$\zeta_{cw}$	$\zeta_{mw}$
Bruni et al. [3]	0.0125	0.0125	0.0001	0.0001		
Ambrósio et al. [4]	0	0	0.027	0.027		
Ambrósio et al. [20]	0	0	0.0027–0.027	0.0027–0.027		
Seo et al. [9]	0.01	0.05	0.0001	0.0001		
Cho [21]					0.01	0.05
Zhang et al. [22]					0.01	0.01
Jung et al. [23]					0.01	0.05

et al. [7] estimated the damping ratio of a railway catenary section of the UK East Coast Main Line by determining the logarithmic decrement of a displacement time series collected from drawstring potentiometers. The results were obtained by sampling at five different positions at which forced vibration tests were conducted. The damping ratio for the first mode, at 1.4 Hz, was in the range of 0.02–0.1, with an average of 0.05. According to Stickland et al., this result was likely a slight overestimate due to friction in the drawstring potentiometers. Cho et al. [5] extracted damping ratios from sampled accelerometer time series from one position on a railway contact wire by using a continuous wavelet transform and found values between 0.01 and 0.04 for the frequency range of 1.7–4.1 Hz for a conventional railway line in Korea. These damping estimates were obtained from analyses of the free decay response of the given system, where the ratios were estimated by the logarithmic decay of a band-passed filtered time series by continuous wavelet transforms. The sampling rate was 50 Hz, and the time series was 20 s long.

One important reason for estimating the damping in a structure is its use in numerical modelling. The damping must be estimated to describe the structural behaviour as accurately as possible. The energy of the vibrating structure is dissipated by many mechanisms that are impossible to identify individually in actual structures. Thus, the damping of structures is often described in an idealised manner. Popular methods used to describe damping in numerical models for pantograph–catenary interaction studies are proportional, Rayleigh or modal damping [3]. The most common method used is a combined mass and stiffness proportional damping matrix, as introduced by Lord Rayleigh [8–19] and shown in Eq. (1).

$$C = \alpha \cdot M + \beta \cdot K \quad (1)$$

where  $C$  is the damping matrix,  $\alpha$  is the mass-proportional damping coefficient,  $M$  is the mass matrix,  $\beta$  is the stiffness-proportional damping coefficient and  $K$  is the stiffness matrix. Some different coefficients used in the literature are shown in Table 1.

A recent benchmark regarding the simulation of the pantograph–catenary interaction by Bruni et al. [3] stated that damping is critical in the numerical models and that small differences in its description may significantly affect the simulation results. This report and the fact that few studies have considered damping in existing railway catenary systems highlight the importance of studying damping in railway catenary systems more closely.

The current paper aimed to identify the system damping in existing railway catenary systems via an output-only modal analysis of the acceleration time series sampled directly on several locations on the catenary system during normal rail traffic. This work was performed on three different catenary sections with both time series from ambient vibration (wind) and vibration just after the train has passed the sampling positions. The damping ratios were estimated using the covariance-driven stochastic subspace identification (Cov-SSI) method [24]. The modal damping and frequency parameters estimated by the Cov-SSI were successfully



Fig. 1. Sensor mounted on the contact wire. Photo: Petter Nàvik/NTNU.

used to estimate the Rayleigh damping coefficients for the three railway catenary sections.

## 2. Measurement setup

A newly developed wireless sensor system was used in this study. The system was developed in collaboration between the Norwegian University of Science and Technology, Norway, and Elektromotus, Lithuania. The system consists of up to ten sensors (Fig. 1) with motion-processing units (MPUs) and one master unit. The MPUs are a combination of a microelectromechanical system (MEMS) based tri-axis gyroscope and a tri-axial accelerometer. The weight of each sensor is 390 g. These units also feature in-built analogue-to-digital converters (ADCs). The accelerometers have a programmable full-scale range of  $\pm 2$  g,  $\pm 4$  g,  $\pm 8$  g and  $\pm 16$  g, and the gyroscopes have a full-scale range of  $\pm 250$ ,  $\pm 500$ ,  $\pm 1000$  and  $\pm 2000$  deg/s. The measurement width is 16 bits. The sensors transfer sampled data to the master unit using a custom designed low-power 2.4 GHz radio network. The system can sample data up to 500 Hz for 4 min. The system can either be triggered by exceeding a boundary value, which can be chosen separately for each degree of freedom (DOF) in both the positive and negative directions, or manually through a Wi-Fi or GSM-connection. The entire system can be managed from a website through a GSM-connection in the master unit. Thus, all of the parameters can be set remotely whenever the user desires, and all sampled data can be downloaded from wherever one desires.

## 3. Railway catenary systems

The railway catenary system is a cable system that supplies electrical power to trains on electrical railways. The main



Fig. 2. Main structural components of a railway catenary system. Photo: Petter Návik/NTNU.

**Table 2**  
General information regarding the investigated railway catenary sections.

Section	Soknedal	Melhus	Vålåsjø
Length (m)	1451	528	1265
Catenary system	Table 54	System 35	System 20 C1
Tension force in the contact wire (kN)	10	7.06	13
Tension force in the messenger wire (kN)	5	7.06	13
Cross-sectional area of the contact wire (mm <sup>2</sup> )	100	100	120
Cross-sectional area of the messenger wire (mm <sup>2</sup> )	50	50	70
Density of the wire material (kg/m <sup>3</sup> )	8890	8890	8890
Wave propagation speed (km/h)	382	321	435
Stitch wire (Yes/No)	No	Yes	Yes
Number of spans in contact with the pantograph	27	7	23
Number of different span lengths	4	2	18

structural parts of the system are a contact wire, a messenger wire, and droppers (and occasionally stitch wires), as shown in Fig. 2. Cantilevers support this wire system both vertically and horizontally, as shown in Fig. 2. The contact wire is fastened to light steady arms, whereas the messenger wire is fastened to brackets. The contact wire is the main conductive part, which transfers the electricity to the train through a pantograph. The messenger wire carries the contact wire via the droppers and enables the desired geometry, stiffness, and elasticity to be obtained. The catenary is also divided into suitable lengths along the railway line, with one length called a section. The length of different sections varies, but they can be up to 1600 m long for some catenary systems in Norway. Each section is divided into spans, which is the distance between two poles. One section can consist of up to 25 spans of different lengths in Norway. Axial tension forces are introduced in both the contact wire and messenger wire to obtain the desired geometry, stiffness of the catenary system and wave propagation speed.

A pantograph is the device mounted on top of the train. The only purpose of the pantograph is to ensure an uninterrupted and reliable energy transfer to the train. Two bow strips of coal at the top of the pantograph are the components that transfer the electricity from the contact wire to the train. Simeon and Arnold [25] describe this contact as the most critical part of the

transmission of the electricity to the trains of today. The contact is mainly ensured by an uplift force in the pantograph, static and aerodynamic, and a proper catenary design.

#### 4. Instrumentation and full-scale monitoring of three catenary sections

The sensor system was employed on three existing railway catenary sections, one at Soknedal, “wire 152”, one at Melhus, “wire 191”, and one at Vålåsjø, “wire 12”. All locations are in Norway on the Dovre railway line. General facts about these systems are presented in Table 2.

The vertical geometry of the railway catenary sections as well as the placement of all the sensors are shown for Soknedal, Melhus and Vålåsjø in Figs. 3, 4 and 5, respectively. A detailed description of the spans in each section and the expected first non-symmetric and symmetric frequencies, according to Kiessling et al. [26], are presented for Soknedal, Melhus and Vålåsjø in Tables 3, 4, 5.1 and 5.2, respectively.

#### 5. Methodology

Two approaches were used to estimate the damping in railway catenary systems. The first was to study the system parameters of

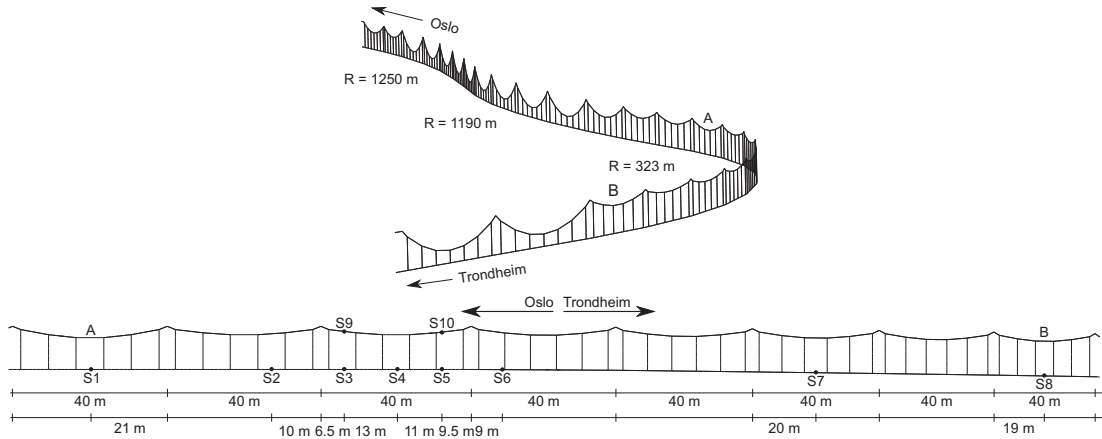


Fig. 3. Instrumentation of "Wire 152" at Soknedal in Norway.

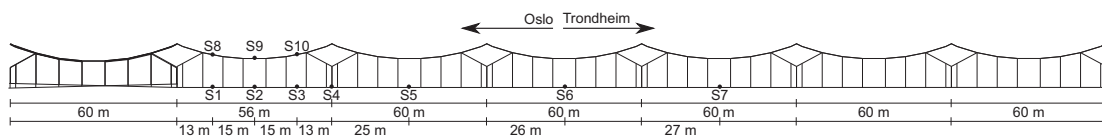


Fig. 4. Instrumentation of "Wire 191" at Melhus in Norway (a straight section).

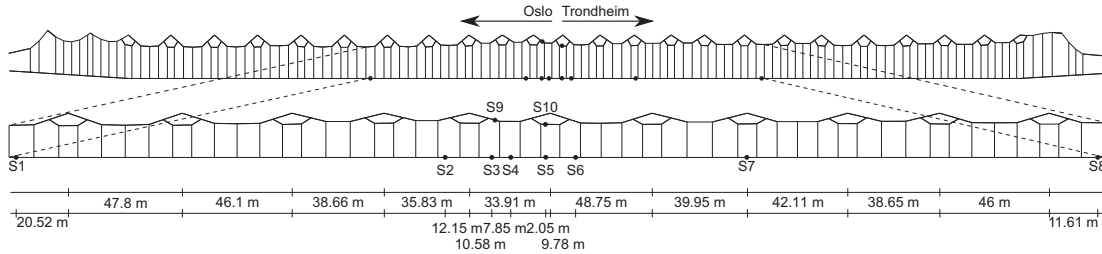


Fig. 5. Instrumentation of "Wire 12" at Vålåsjø in Norway.

Table 3

Detailed description of the spans and their expected frequencies in the Soknedal section.

Span length	40 m	45 m	50 m	60 m
Number of spans	11	2	2	12
Length to the outside dropper	2.1 m	1.9 m	2.3 m	3 m
Freq. of the first expected symmetric mode	1.263 Hz	1.133 Hz	1.016 Hz	0.844 Hz
Freq. of the first expected non-symmetric mode	1.329 Hz	1.181 Hz	1.063 Hz	0.886 Hz

Table 4

Detailed description of the spans and their expected frequencies in the Melhus section.

Span length	56 m	60 m
Number of spans	1	6
Length to the outside dropper	2 m	2 m
Freq. of the first expected symmetric mode	0.905 Hz	0.846 Hz
Freq. of the first expected non-symmetric mode	0.921 Hz	0.86 Hz

only the catenary system by investigating time series sampled when the train is not present within the studied catenary section, i.e., the ambient response due to wind excitation. The second was

to study the system parameters just after the train/pantograph has passed the investigated points on the catenary; the result of this approach is called the post-passage time series. The post-passage time series mainly contains information about motion-induced harmonic components and the structural damping as well as some information about the fundamental system frequencies [27]. Numerous samplings were performed for both cases at all investigated sections. The only response that was measured was the accelerations of the catenary system, i.e., all analyses are based on output-only measurements. The original sampling rate was 200 Hz, which was low-pass filtered at 80% of the Nyquist frequency [28], i.e., 80 Hz, to account for the roll-off rate of the filter.

**Table 5.1**  
Detailed description of the spans and their expected frequencies in the Vålåsjo section.

Span length	33.91	35.83	38.65	39.95	40.5	42.11	42.75	43	44
Number of spans	1	1	2	1	1	1	1	1	1
Length to the outside dropper	4	4	4	4	4	4	4	4	4
Freq. of the first expected symmetric mode	1.739	1.651	1.537	1.489	1.470	1.416	1.396	1.388	1.358
Freq. of the first expected non-symmetric mode	1.842	1.743	1.616	1.564	1.542	1.483	1.461	1.453	1.420

**Table 5.2**  
Continuation, detailed description of the spans and their expected frequencies in the Vålåsjo section.

Span length	46	46.1	47.8	49	49.56	49.7	49.75	49.84	50.4
Number of spans	3	1	1	3	1	1	1	1	1
Length to the outside dropper	4	4	4	4	4	4	4	4	4
Freq. of the first expected symmetric mode	1.301	1.299	1.254	1.225	1.211	1.208	1.207	1.205	1.192
Freq. of the first expected non-symmetric mode	1.358	1.355	1.307	1.275	1.260	1.257	1.256	1.253	1.239

The power spectral densities (PSDs) were estimated using the Burg method [29] separately for each time series as an initial investigation to identify which frequencies are of interest. The PSDs were then added together for each of the approaches to establish which frequencies are the most important for the entire catenary section. This process was performed separately for each section and for each approach. This investigation was then used as a guide for the more detailed analyses that follow to improve the quality of their results.

The covariance-driven stochastic subspace identification (Cov-SSI) method [24] was used to obtain a successful identification of the modal frequency and damping parameters. The Cov-SSI method was used on the data sets from all sensors at once to identify the system damping.

The Cov-SSI method uses output-only data to identify a stochastic state-space model. Assuming white noise, the discrete-time stochastic state space model can be represented by the following equation, as given in Rainieri and Fabbrocino [30]:

$$\begin{aligned} S_{k+1} &= A \cdot S_k + w_k \\ y_k &= \Gamma \cdot S_k + v_k \end{aligned} \quad (2)$$

where  $s$  is the discrete-time state vector,  $A$  is the discrete state matrix,  $w$  is the process noise,  $y$  is the sampled output,  $\Gamma$  is the discrete output matrix,  $v$  is the measurement noise, and  $k$  is the discrete time step. The modal parameters can be extracted from matrices  $A$  and  $\Gamma$  in the identified state space model. This method requires that the order of the model is defined; however, this is unknown for practical applications. The solution to overcome this problem is to estimate the modal parameters for all orders within a conservative interval and then show the results in a stabilisation diagram [30]. The Cov-SSI method is able to identify the frequencies and damping of closely spaced modes, which is crucial for highly flexible structures. It can also be used when there are limited amounts of data [31]. The method has been successfully used on civil engineering structures [32–36]. Brownjohn et al. [34] tested several operational modal analysis techniques on sampled acceleration time series from the Humber Bridge, and when comparing these methods, the Cov-SSI method was found to perform the best. A similar finding was reported by Giraldo et al. [35] for an acceleration time series from a scaled-down four-storey building.

The damping ratio for the  $n$ th mode when Rayleigh damping is chosen is given by

$$\zeta_n = \frac{\alpha}{2} \frac{1}{\omega_n} + \frac{\beta}{2} \omega_n \quad (3)$$

where  $\zeta$  is the damping ratio,  $\alpha$  and  $\beta$  are the Rayleigh coefficients and  $\omega$  the frequency in rad/s. Collecting the modal parameters

estimated from different time series in matrices, the Rayleigh coefficients can be obtained by solving this over-determined matrix system as follows:

$$\begin{Bmatrix} \zeta_1 \\ \zeta_2 \\ \vdots \\ \zeta_i \\ \vdots \\ \zeta_n \end{Bmatrix} = \frac{1}{2} \begin{bmatrix} 1/\omega_1 & \omega_1 \\ 1/\omega_2 & \omega_2 \\ \vdots & \vdots \\ 1/\omega_i & \omega_i \\ \vdots & \vdots \\ 1/\omega_n & \omega_n \end{bmatrix} \begin{Bmatrix} \alpha \\ \beta \end{Bmatrix} \quad (4)$$

The backslash operator was used in Matlab R2014a [37] on this matrix system to obtain the least-squares solution and an estimate of the Rayleigh coefficients.

## 6. Identification of the damping ratio estimates and Rayleigh coefficients

All of the results are based on the sampled acceleration time series from the railway catenary sections at Soknedal, Melhus and Vålåsjo. The trains that passed the investigated section under the sampling period were scheduled passenger and freight trains. Thus, variations in the input force for each passage are expected and depend mainly on the train speed, the wear of the individual pantograph and the amount of wind during each passage. A typical acceleration time series for ambient, post-passage and an entire train passage are shown in Fig. 6.

The variation in damping estimates is dependent on the section geometry, catenary tension forces, and applied loading. There are several difficulties with estimating the system damping of the catenary sections. One, as presented earlier, is the presence of closely spaced modes [5]. This difficulty is particularly evident for railway sections in which there are many different span lengths and thus many different natural frequencies. Small geometric differences between spans lead to small differences in the natural frequencies, which have been observed for all investigated sections. These variations in frequencies and damping were thoroughly investigated through the gathering of a large database and then examining trends, rendering the Rayleigh curves that fit the sampled data.

Several damping ratio estimations were extracted through the Cov-SSI analyses for stable poles up to 20 Hz from the acceleration time series. Rayleigh damping coefficients were estimated from the resulting damping ratios distributed over the investigated frequency range for all three railway catenary sections. The estimates of the coefficients, the corresponding Rayleigh curves and the

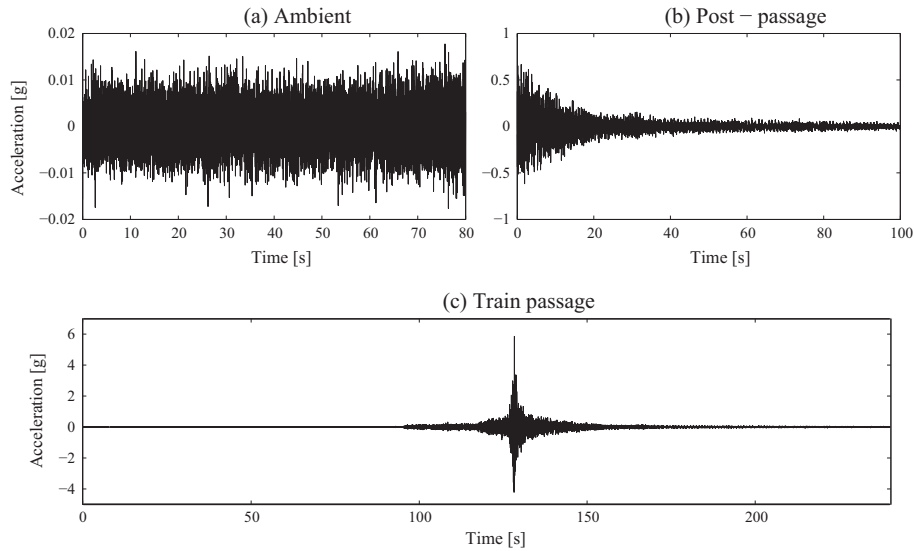


Fig. 6. Example of acceleration time series of (a) ambient, (b) post-passage and (c) the entire train passage low-pass filtered to 80 Hz.

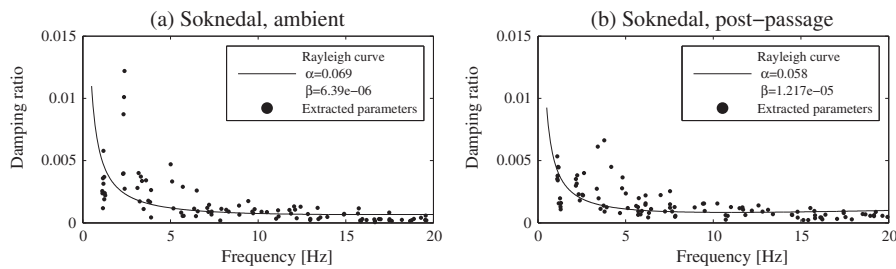


Fig. 7. Damping extraction and Rayleigh damping curve fitting from ambient vibration tests (a) and post-passage (b) at Soknedal.

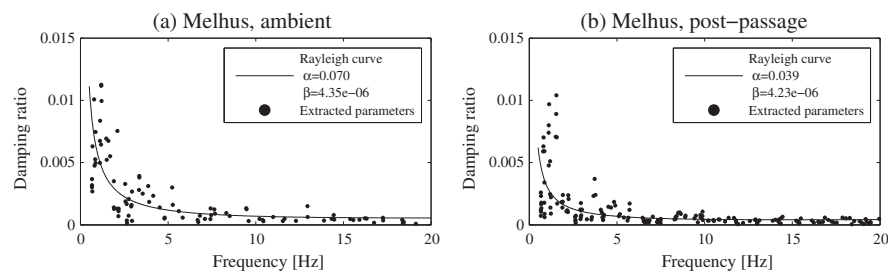


Fig. 8. Damping extraction and Rayleigh damping curve fitting from ambient vibration tests (a) and post-passage (b) at Melhus.

modal parameters extracted from the Cov-SSI analyses are shown in Figs. 7, 8 and 9 for Soknedal, Melhus and Vålåsjø, respectively.

The amount of damping for all the investigated sections is highest at the lower frequencies and decreases quite rapidly for higher frequencies, as shown in Figs. 7–9. This trend demonstrates that the Rayleigh damping matrix for the sections is dominated by the mass-proportional part and only slightly affected by the stiffness-proportional part. This damping is also commonly used in current numerical models, as shown in Table 1. Furthermore,

the damping ratio associated with the first natural frequencies is less than that of the second natural frequencies for all three investigated sections. That is, a Rayleigh description of the damping will either slightly overestimate the former or underestimate the latter.

Differences between the damping ratio estimates are found between ambient and post-passage as well as between the different sections. The ambient results from Soknedal, as shown in Fig. 7, indicate a slightly higher damping at lower frequencies than the post-passage results and reduced damping at higher

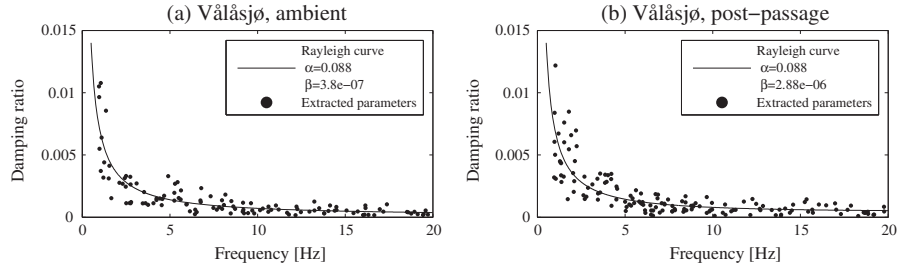


Fig. 9. Damping extraction and Rayleigh damping curve fitting from ambient vibration tests (a) and post-passage (b) at Vålåsjø.

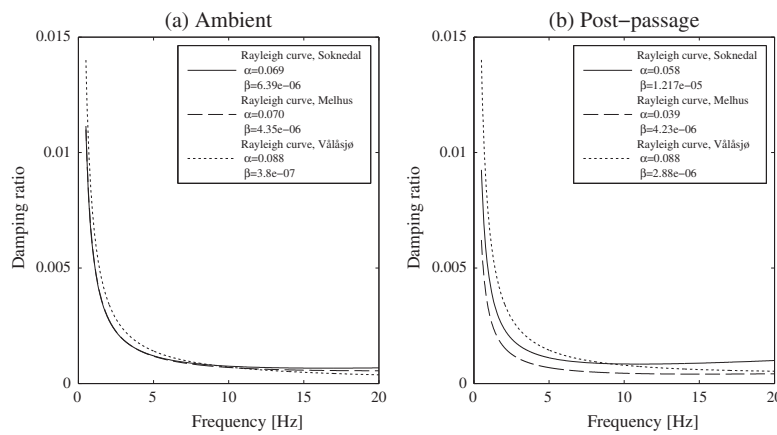


Fig. 10. Rayleigh curve fits for all investigated cases, ambient (a) and post-passage (b).

Table 6  
Rayleigh damping coefficients from Soknedal, Melhus and Vålåsjo.

	Soknedal		Melhus		Vålåsjo		Mean
	Ambient	Post-passage	Ambient	Post-passage	Ambient	Post-passage	
$\alpha$	0.069	0.058	0.070	0.039	0.088	0.088	0.062
$\beta$	6.39e-06	11.27e-06	4.35e-06	4.23e-06	0.38e-06	2.88e-06	6.13e-06

frequencies. The Melhus section exhibits the greatest differences in damping ratios between the ambient and post-passage results, as shown in Fig. 8. The post-passage data indicate considerably lower damping ratios at the first frequencies than for the ambient. This difference is likely due to the type of excitation, wind or train, because the type of excitation is the only difference between the measurements. A higher amount of excitation was observed for the post-passage time series around these particular frequencies. The damping amount in the remainder of the frequency range is highly similar between the two methods. Both results from the Vålåsjo section are largely equal and describe the extracted data well, as shown in Fig. 9. Furthermore, when considering the geometry of the different sections and the difference in tension forces, the softer and more geometrically varying Soknedal section is found to exhibit the largest variation. This observation is expected because such a section is difficult to structurally optimise and will vary more over the spans. This behaviour is reflected in all modal property estimations. For the other two sections, the scatter is less, and the trend is clearer.

Comparing the damping of the different sections, the Rayleigh damping estimates from the ambient responses are highly similar, as shown in Fig. 10, particularly for the Soknedal and Melhus sections. However, the Vålåsjo section has slightly more damping at the lower frequencies. Greater differences are observed in the post-passage results, again at the lower frequencies, whereas the damping at higher frequencies is more similar among the sections. Although the Vålåsjo section exhibits higher damping ratios, damping in the sections are within the same magnitude. The variation in Rayleigh damping estimates between the different sections is typically less than the variation of the individual estimates.

Based on the results from the three sections, the mean value of the post-passage coefficients presented in Table 6 are recommended when modelling the structural damping of a catenary section because the coefficients are well within the accepted damping description of the three studied sections. The results from the investigation as well as the mean values are presented in Table 6.



## 7. Conclusions

This paper presented an investigation of system damping in existing railway catenary systems using full-scale measurements. The data used for the analyses were the acceleration time series sampled directly on the catenary systems via a newly developed wireless sensors system. The system damping was studied due to the need to better describe and quantify damping parameters for use in numerical models. Furthermore, both ambient and post-passage time series were analysed to investigate the differences within frequencies as well as the damping content from measurements performed with and without trains passing the catenary system. These results are critical for any numerical model. Because the estimated values differ slightly between the ambient and post-passage situations, the latter are recommended when evaluating the catenaries regarding possible arching problems via the numerical modelling of train passage analyses. The post-passage coefficients better describe the coupled dynamic system of the pantograph–catenary interaction. The Rayleigh damping coefficients were successfully identified; however, some differences between the investigated railway catenary sections were observed. Although the sections follow nearly the same trends and the amount of damping is of the same order, different Rayleigh coefficients were obtained for the different railway catenary sections. If the Rayleigh coefficients are unknown for a catenary section, the mean values found in this paper are recommended:  $\alpha = 0.062$  and  $\beta = 6.13e-06$ .

## Acknowledgements

The authors are grateful to the Norwegian National Rail Administration for their assistance and funding of this research and to Elektromotus for the development of the sensor system.

## References

- Poetsch G, Evans J, Meisinger R, Kortüm W, Baldauf W, Veitl A, et al. Pantograph/catenary dynamics and control. *Vehicle Syst Dyn* 1997;28(2–3):159–95.
- Liu Z, Jönsson PA, Stichel S, Rönquist A. Implications of the operation of multiple pantographs on the soft catenary systems in Sweden. *Proc Inst Mech Eng Part F–J Rail Rapid Transit* 2014. <http://dx.doi.org/10.1177/0954409714559317>.
- Bruni S, Ambrosio J, Carnicero A, Cho YH, Finner L, Ikeda M, et al. The results of the pantograph–catenary interaction benchmark. *Vehicle Syst Dyn* 2015;53(3):412–35.
- Ambrósio J, Pombo J, Pereira M, Antunes P, Mósca A. Recent developments in pantograph–catenary interaction modelling and analysis. *Int J Railw Technol* 2012;1(1):249–78.
- Cho YH, Lee JM, Park SY, Lee ES. Robust measurement of damping ratios of a railway contact wire using wavelet transforms. *Key Eng Mater* 2006;321–323:1629–35.
- Wu TX, Brennan MJ. Dynamic stiffness of a railway overhead wire system and its effect on pantograph–catenary system dynamics. *J Sound Vib* 1999;219(3):483–502.
- Stickland MT, Scanlon TJ, Craighead IA, Fernandez J. An investigation into the mechanical damping characteristics of catenary contact wires and their effect on aerodynamic galloping instability. *Proc Inst Mech Eng Part F–J Rail Rapid Transit* 2003;217(2):63–71.
- Rayleigh JWSB, Nachtrieb NH. *The theory of sound*, 2nd ed., vol. 1. London: Macmillan; 1894.
- Seo J, Kim S, Jung I, Park IH, Mok J, Kim Y, et al. Dynamic analysis of a pantograph–catenary system using absolute nodal coordinates. *Vehicle Syst Dyn* 2006;44(8):615–30.
- Alberto A, Benet J, Arias E, Cebrian D, Rojo T, Cuartero F. A high performance tool for the simulation of the dynamic pantograph–catenary interaction. *Math Comput Simul* 2008;79(3):652–67.
- Benet J, Alberto A, Arias E, Rojo T. A mathematical model of the pantograph–catenary dynamic interaction with several contact wires. *Int J Appl Math* 2007;37(2):136–44.
- Facchinetti A, Bruni S. Hardware-in-the-loop hybrid simulation of pantograph–catenary interaction. *J Sound Vib* 2012;331(12):2783–97.
- Ambrósio J, Pombo J, Pereira M. Optimization of high-speed railway pantographs for improving pantograph–catenary contact. *Theor Appl Mech Lett* 2013;3(1) 013006.
- Ambrósio J, Pombo J, Antunes P, Pereira M. PantoCat statement of method. *Vehicle Syst Dyn* 2014;53(3):314–28.
- Cho YH. SPOPS statement of methods. *Vehicle Syst Dyn* 2015;53(3):329–40.
- Jönsson P, Stichel S, Nilsson C. CaPaSIM statement of methods. *Vehicle Syst Dyn* 2015;53(3):341–6.
- Zhou N, Lv Q, Yang Y, Zhang W. <TPL-PCRUN> statement of methods. *Vehicle Syst Dyn* 2014;53(3):380–91.
- Sánchez-Rebollo C, Carnicero A, Jiménez-Octavio JR. CANDY statement of methods. *Vehicle Syst Dyn* 2014;53(3):392–401.
- Tur M, Baeza L, Fuenmayor FJ, García E. PACDIN statement of methods. *Vehicle Syst Dyn* 2015;53(3):402–11.
- Ambrósio J, Pombo J, Pereira M, Antunes P, Mósca A. A computational procedure for the dynamic analysis of the catenary–pantograph interaction in high-speed trains. *J Theor Appl Mech* 2012;50(3):681–99.
- Cho YH. Numerical simulation of the dynamic responses of railway overhead contact lines to a moving pantograph, considering a nonlinear dropper. *J Sound Vib* 2008;315(3):433–54.
- Zhang W, Liu Y, Mei G. Evaluation of the coupled dynamical response of a pantograph–catenary system: contact force and stresses. *Vehicle Syst Dyn* 2006;44(8):645–58.
- Jung S, Kim Y, Paik J, Park T. Estimation of dynamic contact force between a pantograph and catenary using the finite element method. *J Comput Nonlinear Dynam* 2012;7(4) 041006.
- Van Overschee P, De Moor BL. *Subspace identification for linear systems: theory—implementation—applications*. Dordrecht, Netherlands: Kluwer Academic Publishers; 1996.
- Simeon B, Arnold M. Coupling DAEs and PDEs for simulating the interaction of pantograph and catenary. *Math Comput Model Dyn Syst* 2000;6(2):129–44.
- Kiessling F, Puschmann R, Schmieder A, Schneider E. *Contact lines for electric railways: planning, design, implementation, maintenance*. 2nd ed. Munich: Publicis; 2009.
- Rönquist A, Nàvik P. Dynamic assessment of existing soft catenary systems using modal analysis to explore higher train velocities: a case study of a Norwegian contact line system. *Vehicle Syst Dyn* 2015;53(6):756–74.
- Nyquist H. *Certain topics in telegraph transmission theory*. *Trans Am Inst Electr Eng* 1928;47(2):617–44.
- Burg JP. *Maximum entropy spectral analysis*. PhD diss, Stanford University; 1975.
- Rainieri C, Fabbrocino G. *Operational modal analysis of civil engineering structures*. New York: Springer Verlag; 2014.
- Rainieri C, Fabbrocino G, Cosenza E. Some remarks on experimental estimation of damping for seismic design of civil constructions. *Shock Vib* 2010;17(4–5):383–95.
- Magalhães F, Caetano E, Cunha Á. Operational modal analysis and finite element model correlation of the Braga stadium suspended roof. *Eng Struct* 2008;30(6):1688–98.
- Liu Y, Loh C, Ni Y. Stochastic subspace identification for output-only modal analysis: application to super high-rise tower under abnormal loading condition. *Earthquake Eng Struct Dyn* 2013;42(4):477–98.
- Brownjohn JMW, Magalhães F, Caetano E, Cunha A. Ambient vibration re-testing and operational modal analysis of the Humber bridge. *Eng Struct* 2010;32(8):2003–18.
- Giraldo DF, Song W, Dyke SJ, Caicedo JM. Modal identification through ambient vibration: comparative study. *J Eng Mech* 2009;135(8):759–70.
- Magalhães F, Cunha Á, Caetano E, Brincker R. Damping estimation using free decays and ambient vibration tests. *Mech Syst Signal Process* 2010;24(5):1274–90.
- MATLAB R2014a. Natick (MA): The MathWorks Inc.





## Paper IV

Petter Nåvik, Anders Rønnquist, Sebastian Stichel

**A wireless railway catenary structural monitoring system: Full-scale case study**

Case Studies in Structural Engineering 2016;6:22-30

DOI:10.1016/j.csse.2016.05.003





Contents lists available at ScienceDirect

## Case Studies in Structural Engineering

journal homepage: [www.elsevier.com/locate/csse](http://www.elsevier.com/locate/csse)

## A wireless railway catenary structural monitoring system: Full-scale case study



Petter Nàvik<sup>a,\*</sup>, Anders Rønquist<sup>a</sup>, Sebastian Stichel<sup>b</sup>

<sup>a</sup> Norwegian University of Science and Technology, Department of Structural Engineering, Rich. Birkelandsvei 1A, 7491 Trondheim, Norway

<sup>b</sup> KTH Royal Institute of Technology, Department of Aeronautical and Vehicle Engineering, SE-100 44 Stockholm, Sweden

### ARTICLE INFO

#### Article history:

Received 3 March 2016

Received in revised form 13 April 2016

Accepted 5 May 2016

Available online 6 May 2016

#### Keywords:

Full-scale measurements

Wireless monitoring

Soft railway catenary systems

Operational modal analysis

Pantograph-catenary interaction

Structural dynamics

### ABSTRACT

Full-scale structural measurements of new and existing railway catenary systems are becoming increasingly important due to continually increasing train speeds and the resulting consequences. Higher speeds lead to increased loads and greater structural dynamic responses, necessitating that both static and dynamic regulations be fulfilled. Sampling directly on railway catenary sections is necessary to assess their structural behaviour. The results can both be analysed directly and be used for validating and/or improving numerical models, which in turn can be used to explore the structural response at higher speeds. This case study presents and explores a newly developed wireless sensor system that includes multiple sensors that can be mounted arbitrarily on any of the wires in a catenary system. All sensors synchronously sample accelerations and rotational velocities over a range of up to 1400 m. This paper shows the results of mounting the developed sensor system and sampling the data of an existing railway catenary section at the Hovin station in Norway. Sampling was performed from both self-excited tests and 140 scheduled train passages. The outputs have been analysed to show that the data can be used to successfully assess railway catenary structural response components.

© 2016 The Authors. Published by Elsevier Ltd. This is an open access article under the CC BY-NC-ND license (<http://creativecommons.org/licenses/by-nc-nd/4.0/>).

### 1. Introduction

Full-scale measurements can significantly contribute to understanding the dynamic behaviour of a structure. The nature of the structure determines which types of measurements are best suited for analysing its behaviour. In addition, the environment (e.g., location, usage) of the structure may also favour or exclude certain types of measurements. It is therefore necessary for a monitoring system to be designed specifically for each type of structure. In the case of railway catenary sections, it is important to assess their behaviour as trains pass through the sections. In addition, the system that is assessed while the trains pass through the sections is a coupled dynamic system consisting of two dynamic systems: the moving pantograph and the spatially stationary catenary section. Uninterrupted contact between the pantograph and the catenary system is essential for maintaining electrical power to the train [1]. The complexity of this interaction and the dynamic responses increase with increasing train speed [2], and speeds above the design speed make the dynamic response even more critical [3]. In general, railway catenary systems are considered lightly damped [1,4,5], so oscillations are present in a substantial time around the actual contact point on a catenary system [1]. Thus, the quality of contact is directly dependent

\* Corresponding author.

E-mail addresses: [petter.r.navik@ntnu.no](mailto:petter.r.navik@ntnu.no), [petter.naavik@gmail.com](mailto:petter.naavik@gmail.com) (P. Nàvik).

<http://dx.doi.org/10.1016/j.csse.2016.05.003>

2214-3998/© 2016 The Authors. Published by Elsevier Ltd. This is an open access article under the CC BY-NC-ND license (<http://creativecommons.org/licenses/by-nc-nd/4.0/>).

on a desired structural behaviour and to the amount of wear. This is of even greater importance on lines where multiple pantographs is used.

Measurements sampled directly on a catenary system are needed to investigate the dynamic behaviour of the catenaries during a complete train passage. Drugge [6] directly sampled displacement time series from a catenary at five points in one span by mounting measuring equipment at both adjacent supports and at three additional poles within the span. Stickland et al. [7] obtained sampled displacement series from the UK East Coast Main Line by using a drawstring potentiometer. Cho et al. [8] and Cho [9] sampled acceleration time series by using a strain-gauge type of accelerometer mounted on the contact line. Multiple wireless sensors were used for full-scale railway catenary damping estimations in a study by Návík et al. [10].

This paper explores the development of a new wireless sensor system for examining the structural behaviour of existing railway catenary sections while in operation. The purpose is to develop a monitoring system that can be used both to monitor the structural response of railway catenary systems for a brief period as scheduled trains pass and for sampling responses from the experiments. A short mounting time is critical to be allowed access to the track, so it is necessary to develop a monitoring system that is easy to mount and unmount. Thus, a wireless system was developed that included multiple sensors that are easily fastened to the wires in the catenary system. The sensors measure acceleration and rotational velocity in and around three axes and simultaneously sample data. The data are at once made accessible online through a wireless router connection after the transfer of data to the master unit is complete. Nine sensors are mounted on one railway catenary section at the Hovin station in Norway, all in close vicinity to one pole span. This sensor set-up is used to predict different parameters and responses in one span and create a base line for future monitoring.

It is important to control maximum uplift on soft contact lines, particularly at the pole support, whereas oscillations are a major concern within the span. It is therefore important to assess several points at and between the pole supports. There are a variety of operational modal analysis (OMA) methods that can be used on the output-only data, i.e., the acceleration or rotational velocity time series, for modal parameter estimation [11]. The analysis methods used in this investigation of monitoring system performance are power spectral densities (PSDs) estimated by the Burg method [12], histograms resulting from peak picking from the PSDs, and continuous short-time Fourier transforms [13]. The results include an assessment of the dynamic response measurements sampled by the new monitoring system, identification of the important system frequencies and the energy transfer between frequencies from the pre- to the post-passage part of the time series. The assessment is executed by analysing measurements from simple hand excitations and the more complex train passages at the Hovin station catenary section. A very important result of sampling and analysing measurements from full-scale existing structures is that numerical models can be validated and/or improved so that they describe the reality as close as possible. These models can only then be used to explore properties outside of what is built, such as higher train speeds, more pantographs, bigger uplift force, changes in wear, and if these changes leads to excessive structural vibrations. Many of these structures have a life span longer than 50 years, so a change in wear or point wear would be crucial for the maintenance costs.

## 2. Monitoring system

The developed monitoring system consists of up to ten wireless sensors and one master unit. The sensors consist of a commercial motion-processing unit (MPU) [14], a battery pack and a radio antenna. The MPU units (MPU-6000) combine a microelectromechanical system (MEMS) tri-axis gyroscope, a MEMS tri-axial accelerometer and a Digital Motion Processor™. The units feature six 16-bit analogue-to-digital converters (ADCs) to digitize the accelerometer and gyroscope outputs. They also feature a user-programmable full-scale range of  $\pm 250$ ,  $\pm 500$ ,  $\pm 1000$  and  $\pm 2000^\circ/\text{s}$  for the gyroscope, along with a range of  $\pm 2\text{ g}$ ,  $\pm 4\text{ g}$ ,  $\pm 8\text{ g}$  and  $\pm 16\text{ g}$  for the accelerometer [14]. The rechargeable battery in the sensors, a Boston Power Sonata® 5300, was chosen so that the monitoring system could run for at least one week without charging. Each sensor weighs 390 g; an example is shown in Fig. 1.

The sampled data are transferred from the sensors to the master unit through a custom-designed low-power 2.4 GHz radio network. The master unit antenna is an Alfa AOA-2049TM, the antenna on the sensors is a Pulse Electronics W1030, the radio chip is a Nordic nRF24L01 and the microprocessor is a STM32L152. In the current configuration, sampling can be performed at a rate of up to 500 Hz and a time duration of up to 8 min. Data are continuously sampled to flash memory, but data are only transferred when the system is triggered. The system is primarily self-triggered by train passages, i.e., when a threshold value is exceeded, but it can also be manually triggered through the master unit. Thus, data can also be selected for transfer from up to 8 min before triggering. The threshold value can be chosen separately for each degree of freedom. When the value is exceeded in any one sensor, the master unit triggers all sensors at the same time stamp to ensure synchronized data. An internal clock is used in the sensors and is synchronized to the internal clock of the master unit to ensure that the time is correct. The master unit's internal clock is updated to the correct time using internet time. Synchronization is not performed continuously due to possible problems from strong electrical currents that occur as the train passes each sensor. Thus, a time stamp is sent at selected time intervals to all sensors from the master unit. The master unit can either be accessed directly by connecting through a local Wi-Fi or remotely on a website using a wireless wide area network. Data can be downloaded, measuring parameters can be changed and the system can be triggered through both connections. The transferring setup is shown in Fig. 2.

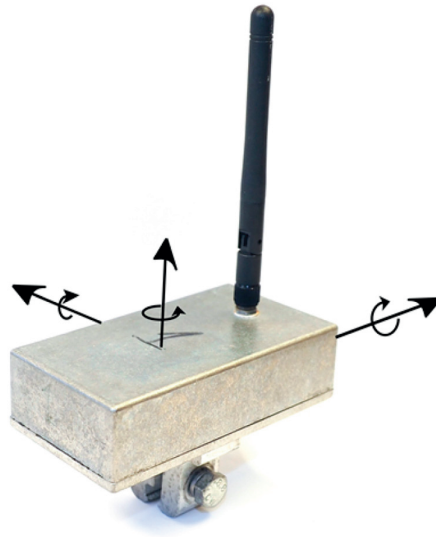


Fig. 1. A sensor with axes directions. Photo: NTNU/Petter N avik.

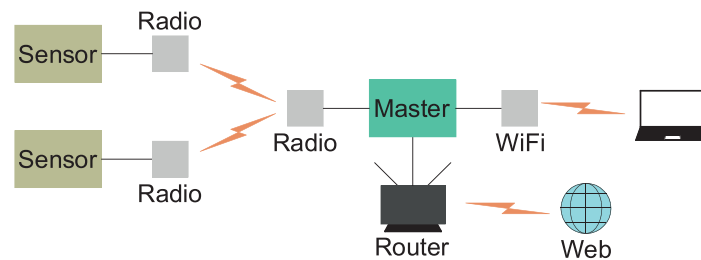


Fig. 2. Setup for the communication and transfer of data.

### 3. Railway catenary systems and pantograph

Railway catenary systems are wire systems that supply power to electrical trains. The major structural components are a contact wire, a messenger wire, droppers, registration arms and brackets, as shown in Fig. 3. The contact wire is the conductive part that transfers the electricity to the train through the pantograph. The primary role of the messenger wire is to carry the contact wire via the droppers, which also enables the desired geometry, stiffness and elasticity of the system. The cantilevered brackets that carry the messenger wire are fastened to the poles along the line. The contact wire is connected to these brackets through the light steady arm. The main function of the light steady arm, aside from being a fastener to the contact wire at the supports, is to obtain the desired horizontal geometry of the contact wire. The contact and messenger wires stretch over many pole spans and are pre-tensioned to obtain the desired vertical geometry. The tension forces are obtained by using a tensioning device consisting of weights and a transmission system. The length of the droppers is also important for the vertical geometry. It is often desirable for the quality of the pantograph–catenary interaction to include a small sag in the vertical height of the contact wire in the middle of each span. For more details on railway catenary systems, see Kiessling et al. [2].

The pantograph is mounted on the roof of the train with the sole purpose of supplying an uninterrupted and reliable energy transfer to the passing train. The contact between the pantograph and contact wire initiates the dynamic response in the catenary system. In this case study, the electricity is transmitted by two bow strips of carbon at the top of the pantograph. This contact is the most critical part of the energy transfer to modern trains [15]. A static and aerodynamic uplift force in the pantograph and a proper catenary design primarily ensures continuous contact.

The major existing catenary systems used in Norway are Tabell 54, System 35, System 20 and System 25. The three latter systems can be used in new railway catenary sections [16]. The type of catenary systems that should be used for new railway sections is thoroughly specified in technical regulations [17]. The criteria that decide which system is to be used are train velocity, allowed type and number of pantographs, train density, and open vs. tunnelled lines [16,17].





Fig. 3. Presentation of important structural components of railway catenary systems. Photo: NTNU/Petter Návík [10].

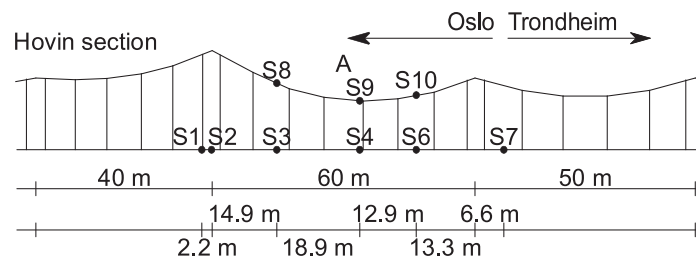


Fig. 4. Vertical geometry of Hovin station railway catenary section “wire 1”.

**Table 1**  
Description of the Hovin section spans and their theoretical natural frequencies [2].

Span length	40 m	45 m	50 m	55 m	60 m
Number of spans	5	2	5	4	9
Length to the outside dropper	2 m	2 m	2 m	2 m	2 m
First symmetric frequency [2]	1.26 Hz	1.12 Hz	1.01 Hz	0.92 Hz	0.85 Hz
First non-symmetric frequency [2]	1.29 Hz	1.15 Hz	1.03 Hz	0.94 Hz	0.86 Hz

#### 4. Case study: railway catenary section at the hovin station

The monitoring system is evaluated through this case study, which is performed on a railway catenary section located at the Hovin station and numbered “wire 1”. The section is part of the Dovre railway line in Norway, the major line between Oslo and Trondheim. It is a 1411-m-long section that utilizes a “System 35” catenary system. The vertical geometry of the section is presented in Fig. 4.

The investigated section is divided in 27 spans with lengths between 40 and 60 m. The first and last spans are not in contact with the pantograph at any time. A more detailed description of the spans of the Hovin section and their theoretical natural frequencies are presented in Table 1. The theoretical natural frequencies are computed in accordance with Kiessling et al. [2]. The horizontal geometry contains four curves from south to north with radii of 4000, 1000, 526 and 1670 m. The speed limit at the section is 100 km/h, except that it is 130 km/h at the largest curve running south.

The instrumentation of the section consists of nine sensors mounted in close vicinity to one span. The sensors are fastened to the wire by tightening a single screw, and in this case study it took approximately 5 min to mount the 9 sensors. Running the service train to the different mounting locations was the most time-consuming process. The distances between the poles and sensors are measured with a laser. A detailed description of where the sensors are mounted is presented in Fig. 5. The mounted monitoring system, as presented in Fig. 6, shows some of the sensors, how they are mounted, the master unit and the wireless wide-area network antenna.

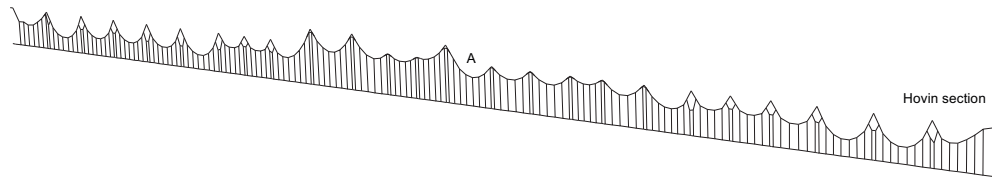


Fig. 5. Instrumentation of Hovin station railway catenary section “wire 1”.



Fig. 6. Mounted monitoring system at the Hovin station: left—sensors; middle—mounting of a sensor; right—master unit and wireless wide-area network antenna. Photo: NTNU/Petter N avik.

#### 4.1. Dynamic assessment

In evaluating the monitoring system, the sensor performance can be assessed in the frequency domain; this is common for evaluating any dynamic system. The evaluation of the time series will depend on the actual occurrences. It has previously been shown in numerical investigations of catenary systems that different information can be extracted from the different parts of a train passage time series [18,19]. The pre-passage data typically include information about the load frequencies relevant to the section that originate from the pantograph frequencies and the different span-pass frequencies. However, the post-passage data reveal more information on the fundamental system frequencies and damping properties [18].

The test results from the Hovin Station section originate from two different types of excitation: simple hand excitations intended to yield the expected behaviour through harmonic excitation and free vibration, and the responses from train passages during operational loading that render a greater complexity in the time series. The data of interest for train passages are not in the single passage but in the catenary system response to the general traffic loading from which it is exposed at any given location. Thus, the train passage data are analysed as the total collection of data. Furthermore, the response from the train passage may also be divided into pre- and post-passage segments. The variation near the peak uplift is evaluated by combining the pre- and post-passage segments with different operational modal analysis tools, such as the power spectral density, the power spectral peak histogram and the spectrograms from the short-time Fourier transform. The combined effort of these different analyses facilitates possibilities for a good validation of the operational performance of the monitoring system for assessing the energy input and transfer between frequencies originating from the train’s passage.

##### 4.1.1. Power spectral density (PSD) estimation

There are several methods available for estimating PSDs in structural dynamics. The method chosen to be used for estimating the PSD of pantograph passages depend largely on the passage duration. It is important to be aware that if the frequency distribution and energy transfer in the frequency domain are to be investigated in detail, the current time series will quickly become very short; therefore, it is important to choose the method accordingly [11]. The Burg method is used for PSD estimation in the investigation of the train passage [12]. The Burg PSD estimate is a parametric method based on a pre-chosen order for the employed autoregressive (AR) prediction model. In parametric methods, the signal is assumed to be an output of a linear system driven by white noise, i.e., parametric methods estimate the PSD by initially estimating the parameters of the linear system assumed to generate the signal. The Burg method does not apply a window function to the dataset, as is common in non-parametric methods. The Burg method may be considered better than non-parametric methods when applied to short parts of a recorded time series, such as a train passage. However, it is important to be aware of some of its disadvantages; for example, the Burg method exhibits spectral line splitting, particularly at high signal-to-noise

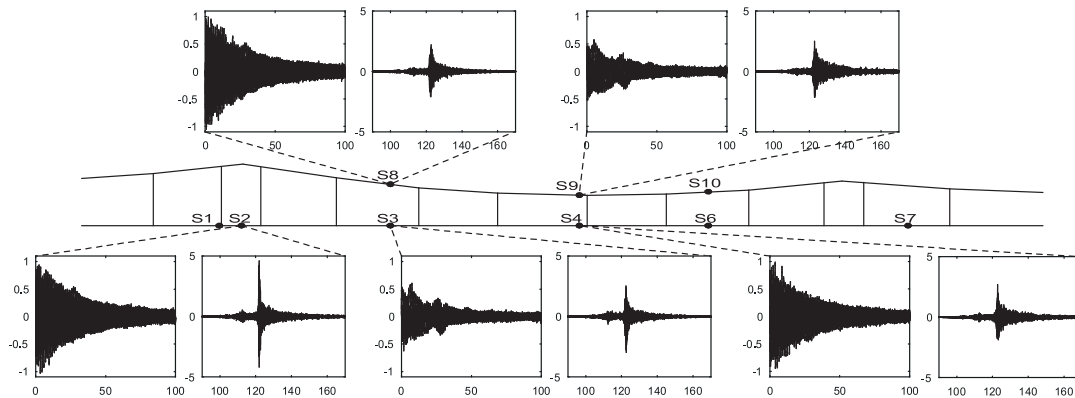


Fig. 7. Sampled acceleration time series from a hand excitation and a train passage for S2, S3, S4, S8 and S9.

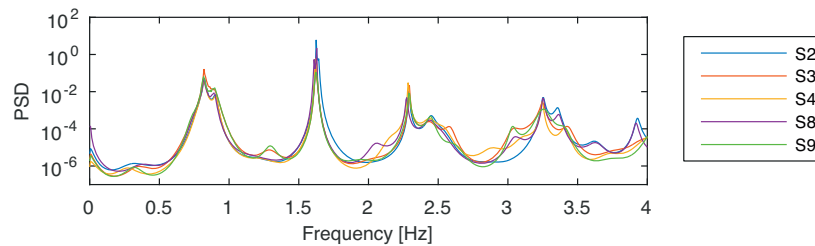


Fig. 8. Power spectral density of the response from S2, S3, S4, S8 and S9 hand excitation.

ratios. In addition, the Burg method can also introduce spurious spectral peaks in high-order systems, and when estimating sinusoids in noise, it can exhibit a bias that is dependent on the initial phase [20].

#### 4.1.2. Short-time Fourier transform (STFT) and spectrogram analysis

Strictly speaking, the recorded time series during a train passage will be non-stationary and possess time-varying spectral characteristics. An STFT is a helpful tool when analysing the changing characteristics of the process. More complete and precise information about the uplift process can be provided by using an STFT in the analysis of the time series [18]. The calculated spectrogram provides a visual representation of the motion, thus providing a useful time-frequency representation. In the STFT, time series are segmented into time intervals that are sufficiently narrow to be considered stationary [13]. It is important to recognize that the time resolution, i.e., how well two peaks in time can be separated from each other, and the frequency resolution, i.e., how well two spectral components can be separated from each other, cannot be determined arbitrarily because they are both directly related to the time window size used to segment the original time series. It is equally important to consider the amount of overlap between the chosen windows. Avoiding overlap will result in more distinct differences between windows, whereas in overlapping windows, the results will be averaged to reduce random errors. By conducting an analysis for each incremental shift using overlapping windows, the STFT can also be used as a sliding discrete Fourier transform [21]. Finally, the spectrogram from the STFT analysis is achieved by squaring the magnitude. The Burg spectrum method is used to evaluate the frequencies in the short-windowed time series.

#### 4.2. Analysis and results

Data have been collected at the Hovin Station to evaluate and validate the full-scale functionality of the developed monitoring system. The analysed data originate from two different types of excitation. Examples of the time series from several sensors for both the simple hand-excited response (left) and train-passage response (right) are presented in Fig. 7. The hand excitation was performed between the second and the third sensors, which can be seen in the time series magnitude mirroring the excited second fundamental frequency of the given span. This is further enhanced by the PSD estimates in Fig. 8, where a large response at the second mode is present, as expected. The PSD estimate also verifies the expected harmonic behaviour of the structure shown by including estimates for all five time series shown in Fig. 7. In this case, all five PSD estimates clearly coincide, showing up to 4 Hz for clarity in Fig. 8. The recorded time series show that the synchronized measurements in the monitoring system work as intended, whereas the harmonic hand excitation shows the correct frequency representation between sensors.

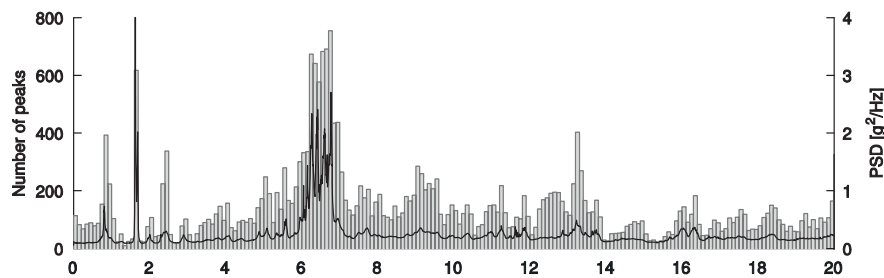


Fig. 9. Total PSD from 140 train passages and 9 sensors and histogram with all peaks picked from individual PSDs.

To test the functionality of the monitoring system in operational conditions, all sensors were left on the catenary for an anticipated monitoring duration to collect a sufficient number of train passages. The loading from the train passages varies due to variations in train type, train speed, the given pantograph and its individual setting, and environmental parameters, such as wind and temperature. All pantographs are assumed to have settings based on the Norwegian design rules but may also contain aleatoric and epistemic uncertainties of any system; in other words, both the train and train speed, as well as the pantograph settings, can cause considerable variation in the catenary dynamic response. Numerical models of catenary systems [18] have shown that the catenary is a slender and flexible system with many similar frequency components that can include small variations. This gives similar frequency components from an eigenvalue analysis, which can be seen to accumulate around given frequencies.

All sampled time series are used to find relevant frequencies that dominate the system response at the current catenary section. The entire time series is included, i.e., the pre-, peri- and post-passage, to show the total frequency content. Due to the variations in train passages, the result can be further clarified by picking the estimated PSD peaks from each passage and presenting their distribution as a frequency function in a histogram. The estimated PSD from all passages and the peak distribution histogram are included in Fig. 9. This represents both the peak and the energy distribution. The importance of the histogram representation becomes evident when remembering that the response data are collected from an in-space stationary system excited by a secondary system (pantograph) in motion. Both the motion in itself and the internal dynamic response of the secondary system will influence the result of the catenary. Thus, the pre-passage data will have a lower response level than the post-passage data. This implies that the PSD estimate will show a low energy content for frequencies dominated by pre-passage responses compared with the post-passage response components. In other words, when a sufficient time duration is used, the monitoring system can provide sufficient data to analyse and identify the frequency components of concern. The frequencies will be location dependent and not merely dependent on the chosen catenary system, i.e., the importance of collecting sufficient data at any trouble span or section. This will enable the possibility of considering either direct actions or actions via numerical modelling and model updating when examining necessary changes.

The oncoming train will create a broad-banded load frequency distribution as it passes the initial spans. Thus, the pre-passage response includes responses from propagating waves and reflections that are one limiting factor for the allowed train speed of a catenary system. The post-passage is different because it reflects the motion introduced by the pantograph uplift, i.e., the sudden impulse and the following free decaying response will be dominated by the fundamental frequencies.

To identify the major frequencies and the frequency transfer zone of the passage, corresponding spectrograms are introduced in Fig. 10b–d showing their characteristics. The important uplift influence zone can be determined based on the time series of the passages and the results from the spectrograms. This provides a good estimation of the part that should be included in the division into the pre- and post-passage analysis. According to the train passage shown in Fig. 10b–d, the monitoring system is triggered by the peak passage and the time series is saved for a given period both before and after passage. The passage occurs at 120 s, with small variations depending on sensor positions and running direction. An influence zone of approximately 5 s is clearly observed, remembering that the time window used in the STFT will also affect the width of the displayed zone. The properties of the remaining part of the time series are then less time variant and correspond better to the conditions of a detailed operational modal analysis, i.e., determining the modal properties and executing the necessary model updating of finite element models. As a result, the previously mentioned techniques included in this investigation also become more distinct. For instance, the lines in the spectrograms in Fig. 10 show that frequency peaks of 1.63 and 2.4 Hz found in Figs. 8 and 9 are typical components in a post-passage segment along with frequencies of approximately 6.7 Hz in Fig. 9, which indicates the frequency band of the pantograph-catenary interaction. The pre-passage does not have as clear lines as the post-passage segment, but some of the dominating frequencies are the components around 0.81 Hz, the pantograph-catenary interaction band, and frequencies between 8 to 14 Hz. The strength of the histogram is clearly present in the latter frequency band, where the lower energy level in the pre-passage becomes weighted such that it render equal importance as the post-passage frequencies. Note that the fundamental modes have a considerably longer duration; several frequency components are excited, but the energy converges toward fundamental modes, rendering the other mode shapes with high damping, whereas the lasting fundamental modes typically have a low damping characteristic. The latter is further

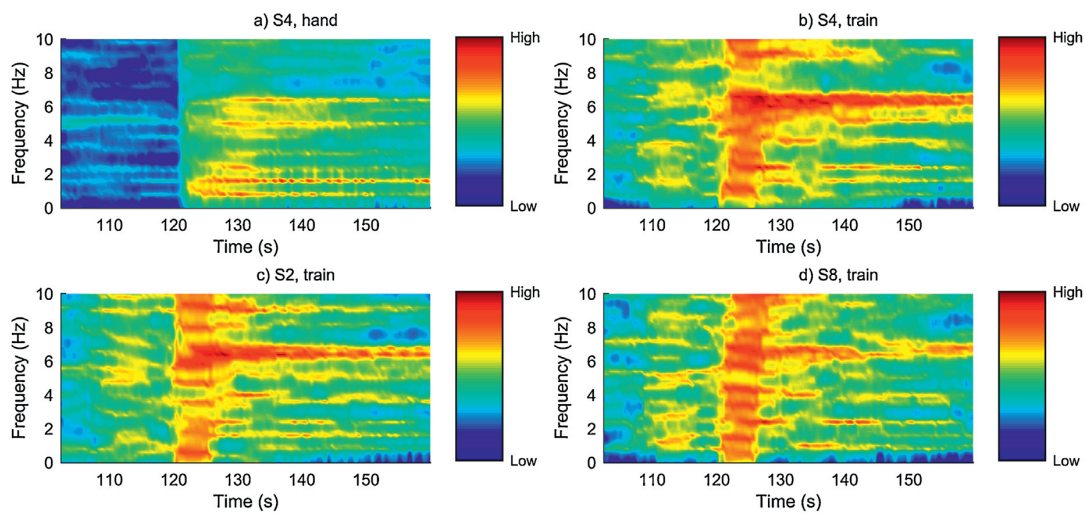


Fig. 10. Spectrograms of the frequency response from hand excitation (a) S4 and train passages (b) S4, (c) S2 and (d) S8.

shown by the spectrogram of the simple hand excitation in Fig. 10a, which shows the fundamental frequency components and their energy mitigation after the initial excitation.

## 5. Conclusions

A new monitoring system was described and applied to an assessment of the dynamic behaviour of railway catenary systems. The investigation also provided possible analyses of sampled full-scale measurements using operational modal analysis. A railway catenary section located at the Hovin station in Norway was used as a case study for the monitoring system evaluation. The monitoring system was successfully mounted within a limited time; mounting all sensors took 5 min, which demonstrated the ability to mount the system rapidly in arbitrary locations. The system automatically sampled all train passages for a week—a total of 140 passages, which was more than sufficient to assess and demonstrate that the monitoring system was energy efficient. The results showed that the developed system was capable of monitoring relevant oscillations occurring in the catenary system regardless of the initiation source (e.g., wind, train). To ensure relevant sampling, the monitoring system could be controlled either manually through a wireless wide-area network or by appropriate trigger values. Finally, an operational modal analysis applied to the collected data showed that relevant information could be extracted and dynamic properties could be identified based on the sampled data, thus making it possible to use the modal results in a numerical model updating procedure.

## Acknowledgements

The authors are grateful to the Norwegian National Rail Administration for their assistance and funding of this research and to Elektromotus for the development of the sensor system.

## References

- [1] G. Poetsch, J. Evans, R. Meisinger, W. Kortüm, W. Baldauf, A. Veitl, J. Wallaschek, Pantograph/catenary dynamics and control, *Veh. Syst. Dyn.* 28 (1997) 159–195, <http://dx.doi.org/10.1080/00423119708969353>.
- [2] F. Kiessling, R. Puschmann, A. Schmieder, E. Schneider, *Contact Lines for Electric Railways: Planning, Design, Implementation, Maintenance, Publicis, Munich, 2009*.
- [3] G.A. Scott, M. Cook, Extending the limits of pantograph/overhead performance, in: *Better Journey Time—Better Business*. IMECH Conference Transactions, Mechanical Engineering Publications Limited, Bury St Edmunds, UK (1996), pp. 207–218.
- [4] S. Bruni, J. Ambrosio, A. Carnicero, Y.H. Cho, L. Finner, M. Ikeda, S.Y. Kwon, J.P. Massat, S. Stichel, M. Tur, W. Zhang, The results of the pantograph-catenary interaction benchmark, *Veh. Syst. Dyn.* (2014) 1–24, <http://dx.doi.org/10.1080/00423114.2014.953183>.
- [5] J. Ambrósio, J. Pombo, M. Pereira, P. Antunes, A. Móscas, Recent developments in pantograph-catenary interaction modelling and analysis, *Int. J. Railw. Technol.* 1 (2012) 249–278, <http://dx.doi.org/10.4203/ijrt.1.1.12>.
- [6] L. Drugge, *Modelling and Simulation of Pantograph-Catenary Dynamics*, Doctoral Thesis, Luleå University of Technology, Luleå, Sweden, 2000.
- [7] M.T. Stickland, T.J. Scanlon, I.A. Craighead, J. Fernandez, An investigation into the mechanical damping characteristics of catenary contact wires and their effect on aerodynamic galloping instability, *Proc. Inst. Mech. Eng. Part F J. Rail Rapid Trans.* 217 (2003) 63–71, <http://dx.doi.org/10.1243/095440903765762814>.
- [8] Y.H. Cho, J.M. Lee, S.Y. Park, E.S. Lee, Robust measurement of damping ratios of a railway contact wire using wavelet transforms, *Key Eng. Mater.* 321–323 (2006) 1629–1635, <http://dx.doi.org/10.4028/www.scientific.net/KEM.321-323.1629>.

- [9] Y.H. Cho, Numerical simulation of the dynamic responses of railway overhead contact lines to a moving pantograph, considering a nonlinear dropper, *J. Sound Vib.* 315 (2008) 433–454, <http://dx.doi.org/10.1016/j.jsv.2008.02.024>.
- [10] P. Nàvik, A. Rønquist, S. Stichel, Identification of system damping in railway catenary wire systems from full-scale measurements, *Eng. Struct.* 113 (2016) 71–78, <http://dx.doi.org/10.1016/j.engstruct.2016.01.031>.
- [11] C. Rainieri, G. Fabbrocino, *Operational Modal Analysis of Civil Engineering Structures*, Springer Verlag, New York, 2014.
- [12] J.P. Burg, *Maximum Entropy Spectral Analysis*, Stanford University, Stanford, CA, 1975.
- [13] L. Rabiner, J. Allen, On the implementation of a short-time spectral analysis method for system identification, *IEEE Trans. Acoust.* 28 (1980) 69–78.
- [14] InvenSense Inc., MPU-6000 and MPU-6050 Product Specification, third revision, InvenSense, Sunnyvale, CA (2013), p. 4.
- [15] B. Simeon, M. Arnold, Coupling DAEs and PDEs for simulating the interaction of pantograph and catenary, *Comput. Model. Dyn. Syst.* 6 (2000) 129–144, [http://dx.doi.org/10.1076/1387-3954\(200006\)6:2;1-M;FT129](http://dx.doi.org/10.1076/1387-3954(200006)6:2;1-M;FT129).
- [16] Mechanical system description of catenary, (n.d.), [http://www.jernbanekompetanse.no/wiki/Mekanisk\\_systembeskrivelse\\_av\\_kontaktledningsanlegg](http://www.jernbanekompetanse.no/wiki/Mekanisk_systembeskrivelse_av_kontaktledningsanlegg) (accessed 02.10.13).
- [17] JD540 Teknisk regelverk, Kontaktledning, <https://trv.jbv.no/wiki/Kontaktledning/Prosjektering/Kontaktledningssystemer> (undated) (accessed 08.02.16).
- [18] A. Rønquist, P. Nàvik, Dynamic assessment of existing soft catenary systems using modal analysis to explore higher train velocities: a case study of a Norwegian contact line system, *Veh. Syst. Dyn.* 53 (2015) 756–774, <http://dx.doi.org/10.1080/00423114.2015.1013040>.
- [19] P. Nàvik, A. Rønquist, S. Stichel, The use of dynamic response to evaluate and improve the optimization of existing soft railway catenary systems for higher speeds, *Proc. Inst. Mech. Eng. Part F J. Rail Rapid Trans.* (2015), <http://dx.doi.org/10.1177/0954409715605140>.
- [20] L. Ljung, *System Identification: Theory for the User*, second edition, Prentice Hall, Upper Saddle River, NJ, 1999, <http://dx.doi.org/10.1002/047134608X.W1046>.
- [21] R. Lyons, DSP tips & tricks—the sliding DFT, *IEEE Signal Process. Mag.* 20 (2003) 74–80, <http://dx.doi.org/10.1109/MSP.2003.1184347>.



## Paper V

Gunnstein Thomas Frøseth, Petter Nåvik, Anders Rønnquist

Operational displacement estimations of railway catenary systems by  
photogrammetry and the integration of acceleration time series

Submitted for journal publication, 2016





# Operational displacement estimations of railway catenary systems by photogrammetry and the integration of acceleration time series

G.T. Frøseth<sup>1</sup>, P. Nåvik<sup>1</sup> and A. Rønnquist<sup>1</sup>

<sup>1</sup>Department of Structural Engineering, NTNU, Norwegian University of Science and Technology, Trondheim, Norway

## Abstract

The dynamic behaviour of railway catenary systems is critical for the quality of the power supply as well as for the amount of wear on both the wires and pantograph. To date, the assessment of the dynamic behaviour of railway catenary systems has focused mainly on the contact force measured from the pantograph. Some examples of using displacement and acceleration measurements sampled at specific locations on the catenary can be found in the literature. Recent work has used wireless accelerometers, which are able to sample accelerations at any location of interest on the catenary system to assess the dynamic behaviour with success. Although accelerations give valuable information about the dynamic behaviour of the systems, it is also desirable to know the displacements. Accelerations have proven easy to sample, so it is natural to integrate these into displacements to obtain the desired displacements. A more direct method to measure the displacement is photogrammetry. This paper describes and uses photogrammetry for operational estimations of the displacement and uses it to successfully validate a procedure for integrating the accelerations into displacements for railway catenary systems. Finally, one week of train passages is recorded, integrated and statistically evaluated to analyse the validated integration procedure used in daily operation monitoring. The evaluation shows single-passage and extreme value distributions with up-crossing frequencies of up to 1/10,000. The 95-percentile threshold value for the yearly probability of exceedance is also included and compared to the maximum allowed uplift at the cantilever. Finally, the yearly probability of failure is estimated at Fokstua.

**Keywords:** displacement estimations, contact wire uplift, railway catenary system, close-range photogrammetry, wireless monitoring, field measurements, pantograph-catenary interaction, structural dynamics.

# 1 Introduction

Full-scale measurements of the response of structures are essential for understanding their structural behaviour and for making proper numerical models. The behaviour of the structure investigated, a railway catenary section, is particularly important when trains are passing through the section. The contact between the train and catenary system is essential for the electrical power supply to the train [1]. The pantograph-catenary interaction is a coupled nonlinear dynamic system consisting of two different dynamic systems, the moving pantograph and the spatially stationary catenary section. An increase in the train speed will lead to an increased complexity of the interaction as well as a larger dynamic response [2]. The dynamic response becomes an even more important property to investigate when the running speed is increased above the design speed [3]. Railway catenary systems are generally considered lightly damped [1,4,5], as confirmed by measurements, e.g., [6]. Oscillations are therefore present in a wide area around the actual contact point [1]. The dynamic behaviour of the pantograph-catenary interaction is typically assessed by the evaluation of a contact force time series sampled on the pantograph and hence essentially describes the dynamic behaviour at the contact point while the train runs along the rail line. Measurements sampled on the catenary systems while in daily operation are necessary to investigate the behaviour of this part of the coupled system more closely. Numerical studies have demonstrated this need by finding differences between the values before and after the passage of a train for a point on the catenary [7] as well as different responses according to the position in the span [7,8]. Drugge [9] sampled displacement time series at five points in one span by mounting measuring equipment on three additional poles within the span as well as on the supports at both ends. Stickland et al. [10] used a drawstring potentiometer to sample a displacement time series on the UK East Coast Main Line. Cho et al. [11] sampled an acceleration time series by mounting a sensor on the contact line. Cho [12] measured the acceleration using a strain-gage type of accelerometer. Nåvik et al. [6,13] used a wireless sensor system consisting of 10 triaxial accelerometers to measure the accelerations under operation. All of these types of measurement require access to the catenary system and the mounting of equipment on the system itself.

Close-range photogrammetry is a non-contact method based on image processing and camera technology for measuring the displacements in a wide range of applications, e.g., [14,15]. The method is attractive in relation to measurements of the catenary system because 1) it is potentially non-intrusive to traffic conditions at the site, 2) it is non-contact and does not interfere with the dynamic properties of the system, and 3) accurate measurements may be obtained at low cost due to recent developments in camera technology. Zhou et al. [16,17] used photogrammetry to measure the displacement in an experimental set-up of a railway catenary part in a laboratory with success.

This paper presents and uses two measurement techniques for the estimation of the displacement of the wires in a railway catenary system during operation. The first method is using close-range photogrammetry, and the second is using

accelerometers. For the photogrammetry in this work, a calibrated stereo camera setup is used together with image processing techniques to track a well-defined target, and triangulation is employed to infer the position of the target. The target is attached to a wireless accelerometer, and the integrated acceleration from this sensor is compared to the displacement obtained by photogrammetry. There are some major differences between the methods. First, photogrammetry does not need access to the track to conduct the measurements, whereas the wireless accelerometers must be mounted onto the system. Second, photogrammetric measurements are sensitive to changing field conditions, such as lighting, rain and snow, whereas measurements from accelerometers are largely unaffected in the normal operating range. Third, more resources in terms of preparation, hardware requirements and post-processing is needed per measurement point for photogrammetry compared to measurements obtained by accelerometers. In addition, the accelerations themselves are critical measurements for assessing the dynamic performance of railway catenary systems. This study shows that both methods yield good estimations of the displacement time series of the catenary wires. The photogrammetry method estimates the displacements in a more direct manner than the integration of the accelerometer measurements and has been used to validate this method. Finally, to demonstrate that the results can advantageously be used to evaluate the daily operational response by statistical means even though there are uncertainties tied to the integration procedure. Passages are treated as statistically independent events to estimate the maximum probability distribution of different up-crossing frequencies. This allows for the control of the probability of exceeding the allowed maximum uplift, e.g., as defined at the cantilever of a given section. Here, these results are shown as threshold values for the 95<sup>th</sup> percentile of non-exceedance. The result is beneficial in evaluating the daily operational uplift as well as estimating the yearly up-crossing values or maxima with a return period equal to the design life of the catenary system. This paper is based on Frøseth et al. [18], but all of the results regarding the in-field daily operation are new, including fitting the displacement and acceleration time series in daily operation, applying them to several train passages, and performing the statistical evaluation of the uplift estimates.

## **2 Methods**

### **2.1 Displacements by photogrammetry**

#### **2.1.1 Data acquisition**

Two Basler Ace acA2000-165  $\mu\text{m}$  cameras [19] with fixed focal length lenses from Edmund Optics with a nominal focal length of 25 mm [20] were used to acquire the images. The cameras have a sensor with a  $2,048 \times 1,088$  pixel array and quadratic pixels of size  $s = 5.5 \mu\text{m}/\text{px}$ . The cameras were synchronized by hardware triggering from the IO pins of an Arduino UNO. The entire imaging system was mounted on a rig with a nominal baseline of 3,000 mm, as shown in Figure 1.



Figure 1. Camera set up for photogrammetry at Hovin. Photograph: NTNU/Petter N avik.

### 2.1.1 Camera model

The projective camera model is used to model the imaging system, and it is represented by the pinhole camera model [21]. It is established by tracing rays from the world coordinates,  $\mathbf{X} = [X Y Z]^T$ , through a pinhole and onto image sensor coordinates,  $\mathbf{x}_s = [x_s y_s]^T$ , yielding

$$\lambda \tilde{\mathbf{x}}_s = \mathbf{P} \tilde{\mathbf{X}} \quad (1)$$

where  $\lambda$  is a scale factor,  $\mathbf{P}$  is the projective matrix and  $\tilde{(\cdot)}$  denotes homogenous coordinates, i.e.,  $\tilde{\mathbf{X}} = [X^T 1]^T$ . The projective matrix is a  $3 \times 4$  matrix and can be written as

$$\mathbf{P} = \mathbf{K} [\mathbf{R} \quad \mathbf{t}] \quad (2)$$

$$\mathbf{K} = \begin{bmatrix} f_x & 0 & c_x \\ 0 & f_y & c_y \\ 0 & 0 & 1 \end{bmatrix} \quad (3)$$

where  $\mathbf{K}$  is the camera calibration matrix and  $[\mathbf{R} \quad \mathbf{t}]$  is the rotation and translation of the centre of projection relative to the chosen coordinate system. The camera calibration matrix consists of the focal length ( $f_x, f_y$ ) and the offset of the sensor coordinate system relative to the optical centre ( $c_x, c_y$ ), and they define the transformation from the centre of the projection to the sensor coordinates. Thus, the camera calibration matrix is governed by the internal geometry of the camera and lens system.

The projective camera is a linear transformation from world coordinates to image coordinates and is an idealization of the imaging system. Distortion is a non-linear effect that is introduced by the imperfect geometry of the lens and inaccuracies in the manufacture and assembly of the overall system. Distortion may be classified into several types [22], but the two that are typically the most prominent in modern imaging systems are radial and tangential distortion [23]. Tangential distortion, introduced by misalignment between the sensor and imaging plane, was found to be

negligible for the present camera system and is therefore not included in the camera model. Radial distortion was considered in the camera model using a two-parameter model:

$$\begin{aligned} x'_c &= x_c \left( 1 + \kappa_1 r_c^2 + \kappa_2 r_c^4 \right) \\ y'_c &= y_c \left( 1 + \kappa_1 r_c^2 + \kappa_2 r_c^4 \right) \end{aligned} \quad (4)$$

where  $r_c^2 = x_c^2 + y_c^2$  is the radial distance and  $(x_c, y_c)$  are the camera coordinates before scaling with the focal length  $(f_x, f_y)$  and shifting the optical centre  $(c_x, c_y)$  and  $\kappa_i$  are the distortion coefficients to be determined.

### 2.1.3 Stereo geometry

A stereo configuration is two cameras capturing the same scene from different viewpoints. This setup features an important constraint known as the epipolar constraint. The epipolar constraint may be exploited to find matching points in two images from the stereo rig. The epipolar plane is defined by a point in the world coordinates  $\mathbf{X}$  and the centres of projection of the first and second cameras  $\mathbf{C}_1$  and  $\mathbf{C}_2$ , as shown in Figure 2.

Through the calibration process, the relative pose between the two cameras is determined, i.e., the centre of projection  $\mathbf{C}$  of both cameras is known. A point in the world coordinates  $\mathbf{X}$ , is found to have sensor coordinates  $\mathbf{x}_{s1}$  in the first camera. The intersection between the epipolar plane and the sensor plane of the second camera defines an epipolar line  $\mathbf{l}_2$ . The epipolar constraint then states that point  $\mathbf{x}_{s2}$  must lie on epipolar line  $\mathbf{l}_2$ . The fundamental matrix  $\mathbf{F}$  expresses the constraint imposed by the epipolar plane and relates the sensor coordinates in one camera with the epipolar line of the other camera, as shown by the equation below.

$$\begin{aligned} \mathbf{l}_2 &= \mathbf{F} \tilde{\mathbf{x}}_1 \\ \mathbf{l}_1 &= \mathbf{F}^T \tilde{\mathbf{x}}_2 \end{aligned} \quad (5)$$

The fundamental matrix is established from feature points matched within an image pair in the calibration step described below.

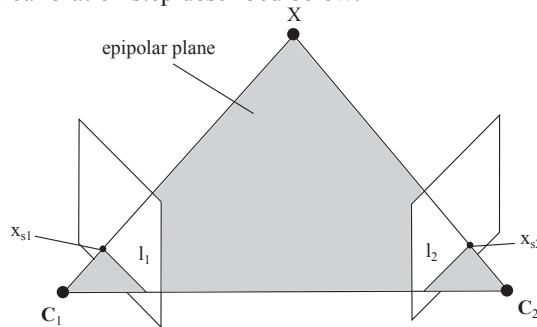


Figure 2. Epipolar plane defined by world coordinates  $\mathbf{X}$ , and the centre of projection for two cameras  $\mathbf{C}_1$  and  $\mathbf{C}_2$ .

#### 2.1.4 Calibration

The purpose of the calibration step is to identify the intrinsic parameters of each camera model and the stereo geometry, i.e., the camera calibration matrix, distortion coefficients, relative pose between cameras and fundamental matrix.

The intrinsic parameters of the imaging system are determined by taking images of an object with easily identifiable feature points and a known geometry. The calibration object was a planar  $6 \times 9$  chessboard pattern with 42-mm squares. Twenty image pairs of the calibration object were used to extract the intrinsic parameters. The calibration procedure was carried out using parts of the open source computer vision library (OpenCV) [24]. The overall root mean square (RMS) error of the calibrated stereo system was 0.107 pixels.

#### 2.1.5 Triangulation

Triangulation is used to extract depth information from an image pair. In this paper, the images are rectified to obtain a standard rectified geometry [25] that involves rotating and scaling the images such that the optical axis and rows of the corresponding cameras are aligned. The depth  $D$  is then found by

$$D = \frac{f_x b}{x_{s1} - x_{s2}} \quad (6)$$

where  $b$  is the baseline, i.e., the distance between the camera centres in the stereo setup,  $f_x$  is the focal length and  $x_{s1}$ ,  $x_{s2}$  are the column coordinates of corresponding points in the first and second images. The point correspondence algorithm is described further in the section below.

#### 2.1.6 Point correspondence

A simple yet effective method is used to track the well-defined target. The tracking process is divided into two stages. In the initial stage, only the first image pair in the series is considered. The method by Shi and Tomasi [26] is used to detect features in the image pair. The feature corresponding to the target centre is then chosen manually for both frames in the image pair. A *reference* subimage around the chosen feature is then extracted to be used for tracking purposes. Due to the relatively high framerate, the target is not expected to move considerably between each frame, and a mask is also created that limits the search for the corner in the subsequent image pairs.

The second stage of the processing involves the subsequent image pairs. First, the features in the image pair are extracted under the restriction of the mask found in the initial stage. A *target* subimage for each feature is then extracted, and the zero mean normalized sum of squared differences (ZNSSD) is calculated between the target  $G$  and reference subimage  $F$ , as expressed below.

$$\epsilon = \sum_i \left( \frac{\sum_j \bar{F}_j \bar{G}_j}{\sum_j \bar{G}_j^2} (G_i - \bar{G}) - (F_i - \bar{F}) \right)^2$$

$$\bar{F} = \frac{1}{n} \sum_{i=1}^n F_i, \quad \bar{G} = \frac{1}{n} \sum_{i=1}^n G_i \quad (7)$$

$$\bar{F}_j = F_j - \bar{F}, \quad \bar{G}_j = G_j - \bar{G}$$

ZNSSD is chosen because it is robust to changes in light conditions [22], an essential property in field measurements and environments where control of the lighting is difficult. The feature point with the lowest ZNSSD is chosen for further processing. If the epipolar constraint is not satisfied for the feature points with the lowest ZNSSD in the image pair, there is a mismatch, and the next feature point in the list is matched with the one with the overall lowest ZNSSD in the image pair. This provides additional robustness to the tracking algorithm.

When the matching feature points in the image pair are found, the subpixel locations of the corners are found by using the iterative algorithm implemented in [24] to increase the accuracy of the point localization.

### 2.1.7 Resolution

The resolution in world coordinates is dependent on the intrinsic camera parameters. The resolution  $\delta$  in a plane, parallel to and a distance  $D$  from the image plane, is determined by

$$\delta = \eta \frac{sD}{f} \quad (8)$$

where  $\eta$  is the capability of the subpixel localization algorithm. The depth resolution can be approximated by the following relation [27]:

$$\Delta \approx \eta \frac{sD^2}{bf} = \delta \frac{D}{b} \quad (9)$$

Thus, the resolution in stereo vision systems that operate on depths greater than the baseline is governed by the depth resolution. Equation (9) illustrates that the depth to the target should be kept low to maximize the resolution. From a practical perspective, the camera rig cannot be placed too close to the track due to safety restrictions. What constitutes an adequate resolution is dependent on the magnitude of the displacement to be measured. The uplift of the catenary system is dependent on both the catenary system design and the operational parameters of the train. Assuming an uplift of 20 mm, a resolution of 1 mm would provide measurements within 5% of the expected displacement. Figure 3 shows the resolution of the presented imaging system at various depths and the efficiency of the subpixel localization algorithm.

The literature reports various efficiencies of subpixel localization algorithms, e.g., Sutton et al. [28] reports  $\eta=1/10$  px in a laboratory experiment. The lighting conditions affect the efficiency. Ribeiro et al. [29] investigated the precision of a close-range photogrammetry setup and found that the performance of the subpixel localization



algorithm deteriorated in field conditions due to suboptimal brightness and contrast in the images. This again suggests that that the distance to the target should be kept as small as possible. Thus, the tests carried out in this study were based on the desire to maximize the resolution under the constraint of maintaining a safe distance from the track.

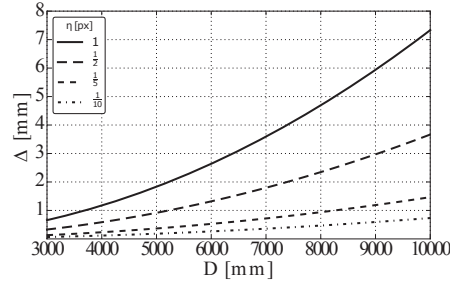


Figure 3. Theoretical resolution of an imaging system with  $s = 5.5 \mu\text{m}$ ,  $f = 25 \text{ mm}$ , and  $b = 3,000 \text{ mm}$  as a function of the depth to the target

## 2.2 Integration of acceleration time series into displacements

The procedure for integrating the acceleration time series into displacement time series for measurements sampled at railway catenary systems using the Newmark-beta method [30],

$$\begin{aligned} \dot{u}_{i+1} &= \dot{u}_i + ((1-\gamma)\Delta t)\ddot{u}_i + (\gamma\Delta t)\ddot{u}_{i+1} \\ u_{i+1} &= u_i + \Delta t\dot{u}_i + ((0.5-\beta)(\Delta t)^2)\ddot{u}_i + (\beta(\Delta t)^2)\ddot{u}_{i+1} \end{aligned} \quad (10)$$

with  $\beta$  and  $\gamma$  equal to 0.25 and 0.5, respectively, where  $\Delta t$  is the time step and  $u$ ,  $\dot{u}$  and  $\ddot{u}$  are the displacement, velocity and acceleration, respectively, is as follows. First, the drift in the acceleration time series is removed by a constant detrending of the data. Second, the acceleration time series is band pass filtered to remove erroneous sensor data close to 0 Hz and aliasing above the Nyquist frequency [31]. This was achieved using a digital Chebyshev Type II filter. Third, the detrended and filtered acceleration time series is first integrated into a velocity time series and then to a displacement time series. The drift in the time series is removed after each step. The velocity time series was high pass filtered, whereas the displacement time series was detrended linearly.

The Type II Chebyshev filter is one of the four classical infinite impulse response (IIR) filter types. The magnitude response of the filter is monotonic in the passband and equiripple in the stopband. The magnitude-squared function is [32]

$$|H_a(j\omega)|^2 = \frac{1}{1 + (\epsilon^2 T_n^2(\omega_0 / \omega))^{-1}} \quad (11)$$

where  $T_n$  is a Chebyshev polynomial of the  $n^{\text{th}}$  order,  $\omega$  is the frequency,  $j$  is the imaginary unit,  $\omega_0$  is the cut-off frequency, and  $\epsilon$  is related to the stopband ripple,  $\delta_s$ , which is given as [32]

$$\frac{\epsilon^2}{1+\epsilon^2} = (1-\delta_s)^2 \quad (12)$$

This study used an order of  $n=5$  and a stopband ripple of  $\delta_s = 40$  dB.

### 2.3 Statistical assessment of train passages in ordinary operation

To evaluate the operational safety of catenary systems, it is important to perform an extreme value analysis of data collected from daily operations. Excessive uplift is one of several design criteria and is one of the main reasons for the unsatisfactory behaviour or failure of the catenary systems. Starting with an ensemble of single passages renders the statistical properties for single events. First, let the maximum uplift of a passage be defined by the random variable  $X_{\text{uplift}}$ . The probability of failure is defined as the exceedance of the uplift threshold value  $x_{\text{uplift}}$ . The up-crossings in the series system are evaluated by the survival of all elements. The survival probability is defined by the cumulative distribution function (cdf). That is, the failure probability is  $p_f^o = P(X_{\text{uplift}} > x_{\text{uplift}})$ , and the survival probability is given by  $p_s^o = P(X_{\text{uplift}} \leq x_{\text{uplift}})$ . This functions under the assumption that the maximum uplift for each passage is independent and identically distributed  $p_s^k = P(X_{\text{uplift}} \leq x_{\text{uplift}})^k$ , where  $k$  is the number of passages analysed, i.e., a weakest link series system [33].

A new data ensemble consisting of  $k$  single samples is introduced into a series system. The cumulative distribution function (cdf) of the maximum values of the new ensemble describes the probability of failure of the assumed statistically independent single samples of the series system. By differentiating the cdf of the new random variable, the corresponding probability density distribution function (pdf) can be estimated. Once the pdf is established, the first two moments of the random variable, the mean and variance, can be calculated by the expected values [34,35]:

$$E(X) = \mu_X = \int_{-\infty}^{\infty} x \cdot f_X(x) dx = \sum_i x_i p_x(x_i) \quad (13)$$

$$E(X - \mu_X)^2 = \text{var}(X) = \int_{-\infty}^{\infty} (x - \mu_X)^2 f_X(x) dx = \sum_i (x - \mu_X)^2 p_x(x_i)$$

Here, the continuous probability density function is given by  $f_X$ , and the random variable  $X$  takes the value  $x$ . Analogous definitions apply for the discrete random variable  $x_i$  and the corresponding probability  $p_x$ . For the investigation of the uplift, it will be shown that the new random variable follows a Weibull distribution, and the two corresponding parameters,  $\alpha$  and  $\beta$ , define the density function, given by

$$f(x; \alpha, \beta) = \begin{cases} \frac{\alpha}{\beta} \left(\frac{x}{\alpha}\right)^{\beta-1} e^{-(x/\alpha)^\beta} & x > 0 \\ 0 & \text{elsewhere} \end{cases} \quad (14)$$

For an ensemble of  $N$  samples, the maximum likelihood estimator can be used to find the two parameters. That is, the  $\beta$  parameter is given by

$$\hat{\beta}^{-1} = \frac{\sum_{i=1}^N x_i^\beta \ln x_i}{\sum_{i=1}^N x_i^\beta} - \frac{1}{N} \sum_{i=1}^N \ln x_i \quad (15)$$

where  $\beta$  must be solved using numerical solutions. The maximum likelihood estimator for  $\alpha$  when  $\beta$  is given is expressed by

$$\hat{\alpha}^\beta = \frac{1}{N} \sum_{i=1}^N x_i^\beta \quad (16)$$

Furthermore, the first two statistical moments are given by

$$\mu_{x_{\text{uplift}}} = \alpha \left[ \Gamma(1 + \beta^{-1}) \right] \quad \text{and} \quad \sigma_{x_{\text{uplift}}}^2 = \alpha^2 \left[ \Gamma(1 + 2\beta^{-1}) - \Gamma(1 + \beta^{-1})^2 \right] \quad (17)$$

where  $\Gamma$  is the gamma function.

### 3 Field measurements

The field measurements used in this paper are from two different railway catenary systems. Both are along the Dovre railway line in Norway. The first one, Hovin station wire 1, was primarily used for the experiments with photogrammetry, whereas the second, Fokstua wire 21, was used to measure the displacements and accelerations during the train passages. The exact same position along the catenary was used for both the photogrammetry and accelerometers.

Hovin station wire 1 is a Norwegian System 35 catenary section, which is a system using 7.06 kN in both the contact and messenger wires. Fokstua wire 21 is a Norwegian System 20 C1 catenary section, which uses 13 kN in both the contact and messenger wires.

#### 3.1 Displacements

The displacements were obtained through photogrammetry, as described in section 2. At Hovin station wire 1, the camera set-up was placed by the support, whereas it was placed around the mid-span at Fokstua wire 21. The camera rig was placed at a nominal distance of approximately 6 m for both cases. The focus point of the camera was a target mounted on an accelerometer. The location of this sensor at Fokstua can be seen in Figure 6, denoted S1. It is important that the camera rig has open sight to the focus point, as too low position will result in the train containers blocking the sight during passage. The camera rig aiming at a sensor at Fokstua is shown in Figure 4, and a single taken image is shown in Figure 5.



Figure 4. Camera rig aiming at a sensor, S1, at Fokstua. Photograph: NTNU/Petter N avik.

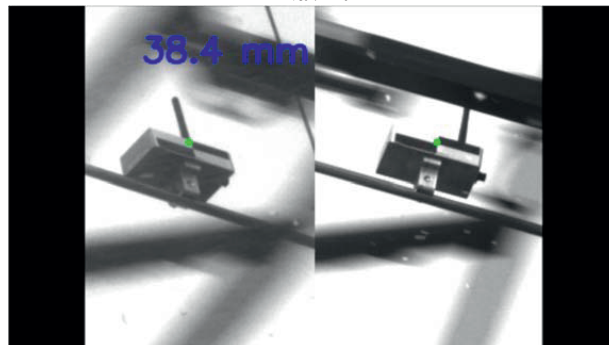


Figure 5. Snapshot from the photogrammetry picture series at Fokstua as the pantograph is at the sampling position.

### 3.2 Accelerations

The accelerations were sampled from the Fokstua wire 21 section using the wireless sensor system described in N avik et al. [13]. Ten tri-axial accelerometers were mounted on the catenary, as shown in Figure 6. All accelerations were sampled at 200 Hz but low-pass filtered at 80 Hz and high-pass filtered at 0.2 Hz.

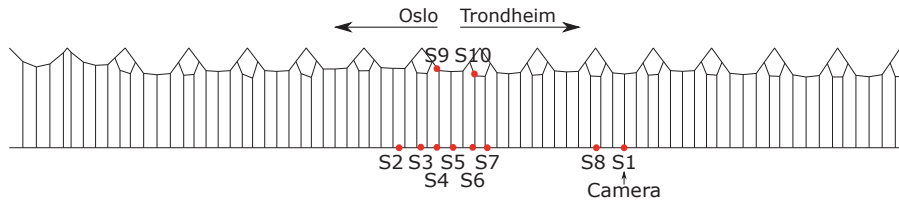


Figure 6. Instrumentation of Fokstua wire 21. The red dots are sensors.

## 4 Results and discussion

This section is divided into three parts. The first part is the estimation of the displacements from manual testing close to the first natural frequency of the system using both photogrammetry and integrated accelerations. The second part uses the same procedures as the first but on measurements sampled during daily train operation. The third and final part is a statistical analysis of the maximum uplift and its corresponding extreme value distribution. The assembled data are integrated acceleration uplift displacements estimated from daily operations. The statistical analysis of the maximum uplift evaluates the variation effects in the recorded data set and the threshold values for the catenary design.

### 4.1 Manual testing

The manual test was a forced vibration test performed by exciting the contact wire at the first natural frequency by an isolator rod in the middle of a span. The test was performed at Hovin station wire 1, and both the displacements, by photogrammetry, and accelerations were sampled at the same position at a support. The displacement estimations are shown in Figure 7. The integration method is found to work very well. High-pass cut-off frequencies of 0.1 and 0.1 Hz were used on the acceleration time series and velocity time series, respectively.

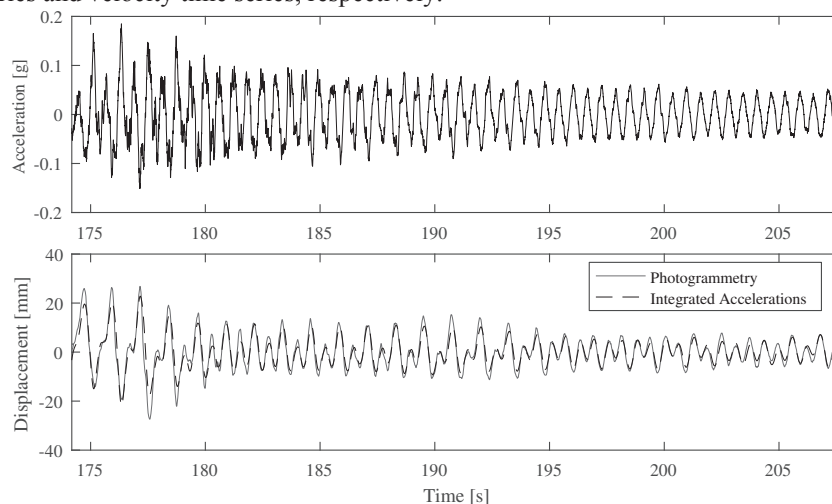


Figure 7. Displacements of contact wire at support under experimental tests using photogrammetry and integrated acceleration time series.

## 4.2 Daily train operation

### 4.2.1 Validation of the integration procedure

The same integration procedure as for the manual test was used on a single train passage. The speed of this train was approximately 130 km/h. The resulting displacements are compared with the photogrammetry measurements in Figure 8. The results obtained by photogrammetry and the accelerations correspond well. The dip in the displacement just before the uplift is due to filtering. Some of the response close to 0 Hz is removed due to the accuracy of the sensors in that range, and thus, this dip occurs. That is, all of the effects with longer periods than 3.33 s are filtered when using a high-pass filter with a cut-off frequency of 0.3 Hz.

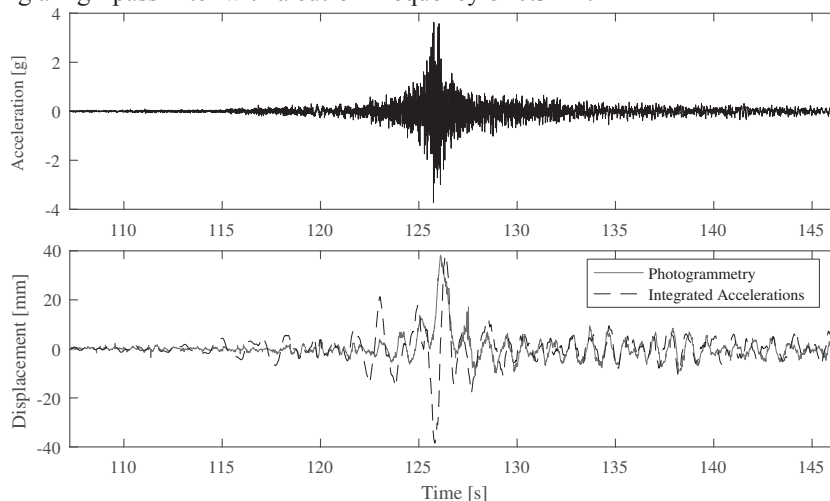


Figure 8. A single train passage. Top: acceleration time series. Bottom: estimated displacement time series using photogrammetry and integration of accelerations.

The peak values of the estimated displacement are quite sensitive to the high-pass filter cut-off limit, so information from the power spectral density of the series, Figure 9, was used to determine it. One can see a clear reduction of the amplitude of the PSD at approximately 0.3 Hz, indicating that 0.2 Hz is a good cut-off frequency to describe the effects above 0.3 Hz. Thus, 0.2 Hz has been used as the high-pass cut-off frequency for the acceleration time series in this paper. High-pass filtering the velocity time series at 0.3 Hz has also shown good results and has therefore been used. It is important to set the cut-off frequency according to the time series at hand. Thus, the cut-off frequencies have been set differently from the manual testing, as expected, due to the different loadings of the system. Although the manual testing looks much smoother than that of a train passage, it is more sensitive to the high-pass cut-off due to the greater response energy at lower frequencies. The estimated maximum uplift for a particular train passage is identical when determined using photogrammetry and accelerations. The acceleration-derived displacement estimate dependency on the high-pass filter limit is shown by adding results, displacement series and PSDs, from

integration with acceleration cut-off frequencies of 0.2, 0.3, 0.4, and 0.5 Hz, together with the photogrammetry series in Figure 9.

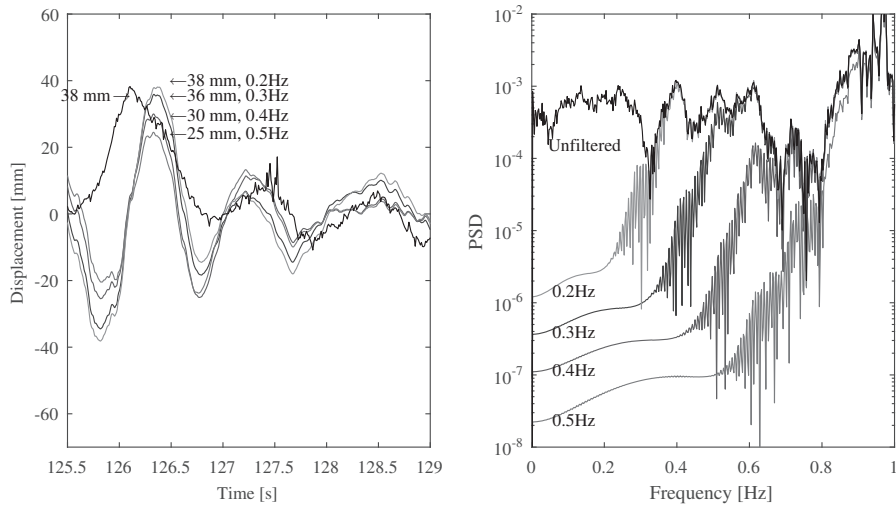


Figure 9. High-pass filter cut-off frequency dependency of displacement estimations using integrated accelerations.

#### 4.2.2 Statistical assessment of train passages in ordinary operation

In any analysis where future predictions are made, there will always be uncertainties. For the case of catenary systems, it is important to investigate the variations in the acquired data set. Some of the collected information may, in itself, have inherent uncertainties or may simply be far from complete. Uncertainties in investigations, as in the current paper, will of course come from several sources. The aleatory uncertainties, i.e., natural or inherent variability, cannot be reduced without changing the phenomenon under consideration. Epistemic uncertainties, i.e., a lack of knowledge, can be reduced by gathering more data. The statistical uncertainties can be addressed by updating the information on our statistical parameters by including additional data or improving the model through obtaining increasing experience.

One week of passages was sampled at Fokstua to evaluate the integration procedure and the variations in the derived displacement uplift from the acceleration integration-based procedure. The data ensemble is shown in Figure 10 and is a slightly skewed distribution. The statistical distribution fitting procedure shows a good fit when using the Weibull distribution, as given in 2.3, and the pdf is expressed by Equation (14). The Weibull distribution is well suited for the maximum peak data set of the uplift, as shown in Figure 10, right.

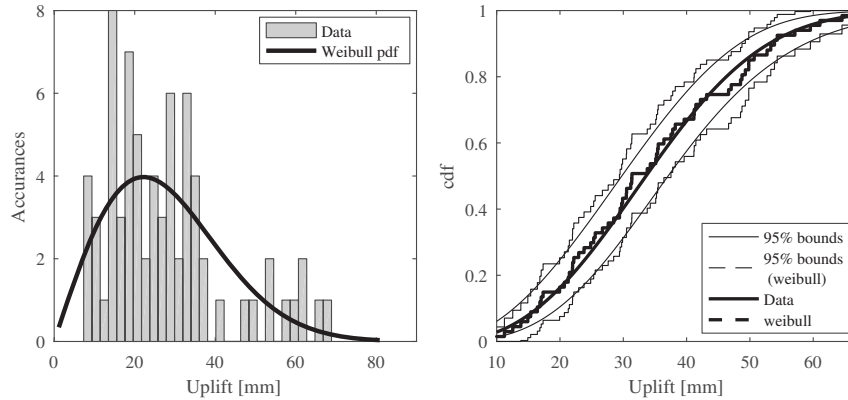


Figure 10. Left, maximum uplift displacement from sampled integrated acceleration time series and corresponding estimated Weibull pdf. Right, cdf fitting plot of the sampled data: rugged broken lines are sampled data including the 95% confidence bounds, whereas the solid lines are the fitted Weibull distribution with the corresponding bounds.

Consider a sample of max uplift due to single passages. If several passages are to be evaluated and they are assumed to be statistically independent, then they can be treated as a series system predicting the extreme value distribution. Thus, if the probability distribution for a single-passage uplift is known, the probability distribution for a larger amount of passages can be predicted. The statistical parameters of the Weibull distribution are obtained for the single-passage ensemble as well as for series systems, for  $k$  passages, as described in 2.3. The single-passage ensemble ( $k=1$ ) is shown as broken lines in Figure 11, which shows both the cdf (see also Figure 10, right) and the pdf (see also Figure 10, left). The series system calculations were performed for  $k = 5, 10, 100, 1,000$  and  $10,000$ .

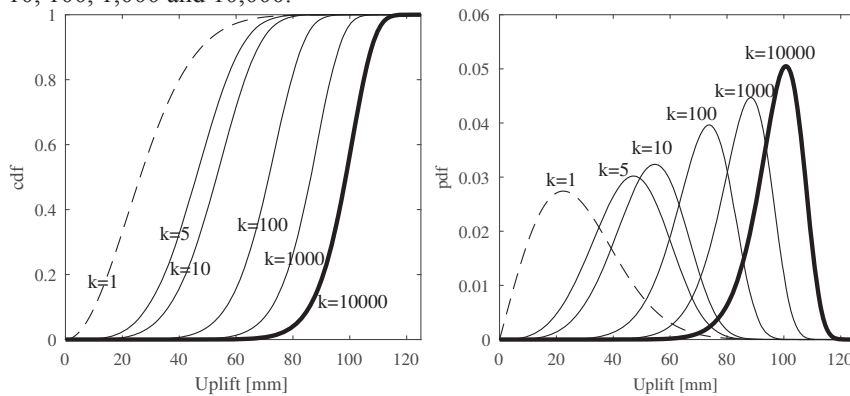


Figure 11. Estimated cdf and pdf of the maximum uplift extreme value predictions from statistical independent passages in a series system, from one up to ten thousand passages.



The number  $k$  will naturally depend heavily on the expected traffic on any given section. For example, at Fokstua, the expected yearly number of passages is approximately 5,100. Thus, the single-passage ensemble is first fitted and gives the Weibull parameters  $(\alpha, \beta) = (31.2449, 1.9981)$ . The data set has a mean value and standard deviation of 28 mm and 14 mm, respectively. For completeness, the Weibull parameters for  $k = 10,000$  are also presented, given as  $(\alpha, \beta) = (101.1607, 13.7345)$ , which corresponds to a mean of 97 mm and a standard deviation of 9 mm.

For the current section, the maximum allowed uplift of the contact wire at the cantilever is 120 mm [36]. The maximum expected uplift at the cantilever can be estimated using the 95<sup>th</sup> percentile value using the data set from Fokstua, with the estimated distribution and parameters corresponding to the chosen  $k$ -values. For  $k = 1, 1,000, 5,100$  (yearly no. of passages at Fokstua) and 10,000, the uplift is found to be 54, 99, 107 and 110 mm, respectively. That is, the yearly characteristic value defined by the 95<sup>th</sup> percentile of maximum up-crossing is 107 mm and thus lower than the maximum allowed, 120 mm. The corresponding probability of failure for the yearly up-crossing event is given as  $p_f^{1yr.} = 2.1 \cdot 10^{-5}$ .

## 5 Conclusions

In this paper, two different techniques are presented and used to estimate the displacement of contact wires in railway catenary systems in daily operation. The first method uses close-range photogrammetry, and the second uses an acceleration integration procedure. For the latter, wireless sensors designed for use on railway catenary systems are used to record acceleration time series. For the photogrammetry, the tracking target is attached to one of the wireless sensors.

In the present paper, both methods are thoroughly described and tested, and the implications for their use on catenary systems are investigated. Because there are major differences between the two methods, the current paper focuses on the prediction and validation of the time series. That is, the displacement series from integrated accelerations are compared to those obtained by photogrammetry. Both methods have their advantages and disadvantages, as although photogrammetry does not need track access, its measurements are sensitive to changing field conditions, whereas the measurements by accelerometers are largely unaffected by normal operation. However, there are always uncertainties attached to any integration scheme of the acceleration time series into displacements. This uncertainty comes from the sensor sensitivity and frequency range as well as undetermined integration constants. Both uncertainties demand the implementation of a data processing and integration procedure, which is described, implemented and tested in the present paper. This study shows that both photogrammetry and acceleration integration provide good estimates of the displacement of the catenary wires.

Finally, it is shown that although there are uncertainties tied to the integration procedure, the data are easily collected, and the results can be used to evaluate the safety of daily operations by statistical means. For this, the train passages are treated as statistically independent events to estimate the maximum probability distribution of different up-crossings. This allows for the control of the probability of the

exceedance of the maximum allowed uplift, e.g., as defined at the cantilever of the given section at Fokstua. Here, the results are used to estimate threshold values for the 95<sup>th</sup> percentile of non-exceedance. This result is beneficial in evaluating the safety of the daily operational uplift as well as estimating yearly up-crossing values or maxima with a return period equal to the design life of the catenary system. Comparisons can easily be made between different sections by using a common number of train passages for the extreme value up-crossing, say, 10,000 passages.

## Acknowledgements

The funding for the research was provided by Jernbaneverket (The Norwegian National Rail Administration) and is gratefully acknowledged by the authors.

## References

- [1] G. Poetsch, J. Evans, R. Meisinger, W. Kortüm, W. Baldauf, A. Veitl, J. Wallaschek, “Pantograph/catenary dynamics and control”, *Vehicle System Dynamics*, 28, 159–195, 1997.
- [2] F. Kiessling, R. Puschmann, A. Schmieder, E. Schneider, “Contact Lines for Electric Railways: Planning, Design, Implementation, Maintenance”, Publicis, Munich, Germany, 2009.
- [3] G. A. Scott, M. Cook, “Extending the limits of pantograph/overhead performance”, in “IMEch. E. Conference Transactions 1996”, vol. 8, Mechanical Engineering Publications, 207–218, 1996.
- [4] S. Bruni, J. Ambrosio, A. Carnicero, Y. H. Cho, L. Finner, M. Ikeda, S. Y. Kwon, J.-P. Massat, S. Stichel, M. Tur, W. Zhang, “The results of the pantograph–catenary interaction benchmark”, *Vehicle System Dynamics*, 53, 412-435, 2014.
- [5] J. Ambrósio, J. Pombo, M. Pereira, P. Antunes, A. Mósca, “Recent developments in pantograph-catenary interaction modelling and analysis”, *International Journal of Railway Technology*, 1, 249–278, 2012.
- [6] P. Nåvik, A. Rønquist, S. Stichel, “Identification of system damping in railway catenary wire systems from full-scale measurements”, *Engineering Structures*, 113, 71–78, 2016.
- [7] A. Rønquist, P. Nåvik, “Dynamic assessment of existing soft catenary systems using modal analysis to explore higher train velocities: a case study of a Norwegian contact line system”, *Vehicle System Dynamics*, 53, 756–774, 2015.
- [8] P. Nåvik, A. Rønquist, S. Stichel, “The use of dynamic response to evaluate and improve the optimization of existing soft railway catenary systems for higher speeds”, *Proceedings of the Institution of Mechanical Engineers, Part F: Journal of Rail and Rapid Transit*, 230, 1388-1396, 2015.
- [9] L. Drugge, “Modelling and Simulation of Pantograph-Catenary Dynamics”, Doctoral thesis, Luleå, Sweden, Luleå University of Technology, 2000.

- [10] M. T. Stickland, T. J. Scanlon, I. A. Craighead, J. Fernandez, “An investigation into the mechanical damping characteristics of catenary contact wires and their effect on aerodynamic galloping instability”, *Proceedings of the Institution of Mechanical Engineers, Part F: Journal of Rail and Rapid Transit*, 217, 63–71, 2003.
- [11] Y. H. Cho, J. M. Lee, S. Y. Park, E. S. Lee, “Robust measurement of damping ratios of a railway contact wire using wavelet transforms”, *Key Engineering Materials*, 321, 1629–1635, 2006.
- [12] Y. H. Cho, “Numerical simulation of the dynamic responses of railway overhead contact lines to a moving pantograph, considering a nonlinear dropper”, *Journal of Sound and Vibration*, 315, 433–454, 2008.
- [13] P. Nāvik, A. Rønnquist, S. Stichel, “A wireless railway catenary structural monitoring system: full-scale case study”, *Case Studies in Structural Engineering*, 6, 22–30, 2016.
- [14] M. Ozbek, D. J. Rixen, O. Erne, G. Sanow, “Feasibility of monitoring large wind turbines using photogrammetry”, *Energy*, 35, 4802–4811, 2010.
- [15] R. Jiang, D. V. Jáuregui, K. R. White, “Close-range photogrammetry applications in bridge measurement: literature review”, *Measurement*, 41, 823–834, 2008.
- [16] D. Zou, W. H. Zhang, R. P. Li, N. Zhou, G. M. Mei, “Determining damping characteristics of railway-overhead-wire system for finite-element analysis”, *Vehicle System Dynamics*, 54, 902-917. doi: 10.1080/00423114.2016.1172715, 2016.
- [17] D. Zou, N. Zhou, L. Ping, G. M. Mei, W. H. Zhang, “Experimental and simulation study of wave motion upon railway overhead wire systems”, *Proceedings of the Institution of Mechanical Engineers, Part F: Journal of Rail and Rapid Transit*. doi: 10.1177/0954409716648718, 2016.
- [18] G. T. Frøseth, P. Nāvik, A. Rønnquist, “Close range photogrammetry for measuring the response of a railway catenary system”, in “The Third International Conference on Railway Technology: Research, Development and Maintenance”, Cagliari, Sardinia, Italy. doi: 10.4203/ccp.110.102, 2016.
- [19] “Ace acA2000-15um product specification” [Online]. Basler AG, Ahrenburg. Available: <http://www.baslerweb.com/en/products/cameras/area-scan-cameras/ace/aca2000-165um>. [Accessed: 21-Jun-2016].
- [20] “EO 25 mm C Series Fixed Focal length Lens product specification” [Online]. Available: <http://www.edmundoptics.com/imaging-lenses/fixed-focal-length-lenses/compact-fixed-focal-length-lenses/59871/>. Edmund Optics Inc., Barrington, NJ, USA. [Accessed: 21-Jun-2016].
- [21] R. Hartley, A. Zisserman. “Multiple View Geometry in Computer Vision”, 2nd ed., Cambridge University Press, Cambridge, United Kingdom, 2004.
- [22] M. A. Sutton, J.-J. Orteu, H. Schreier, “Image Correlation for Shape, Motion and Deformation Measurements: Basic Concepts, Theory and Applications”, Springer, New York, United States, 2009.
- [23] Z. Zhang, “A flexible new technique for camera calibration”, *IEEE Transactions on Pattern Analysis and Machine Intelligence*, 22, 1330–1334, 2000.

- [24] G. Bradski, "OpenCV, open source computer vision", Dr. Dobb's Journal of Software Tools, 2000.
- [25] R. Szeliski. "Computer Vision: Algorithms and Applications", Springer-Verlag, London, United Kingdom, 2011.
- [26] J. Shi, C. Tomasi, "Good features to track", in "1994 IEEE Computer Society Conference on Computer Vision and Pattern Recognition", IEEE, 593–600, 1994.
- [27] C. Chang, S. Chatterjee, "Quantization error analysis in stereo vision", in "1992 Conference Record of The Twenty-Sixth Asilomar Conference on Signals, Systems and Computers, 1992", IEEE, 1037–1041, 1992.
- [28] M. Sutton, W. Wolters, W. Peters, W. Ranson, S. McNeill, "Determination of displacements using an improved digital correlation method", Image and Vision Computing, 1, 133–139, 1983.
- [29] D. Ribeiro, R. Calçada, J. Ferreira, T. Martins, "Non-contact measurement of the dynamic displacement of railway bridges using an advanced video-based system", Engineering Structures, 75, 164–180, 2014.
- [30] N. M. Newmark, "A method of computation for structural dynamics", Journal of the Engineering Mechanics Division, 85, 67–94, 1959.
- [31] H. Nyquist, "Certain topics in telegraph transmission theory", Transactions of the American Institute of Electrical Engineers, 47, 617–644, 1928.
- [32] L. J. Karam, J. H. McClellan, I. W. Selesnick, C. S. Burrus, "Digital filtering", in "Digital Signal Processing Handbook", V. K. Madisetti, D. B. Williams (Editors), CRC Press, Boca Raton, FL, United States, 1999.
- [33] A. Naess, T. Moan. "Stochastic Dynamics of Marine Structures", Cambridge, University Press Cambridge, 2012.
- [34] R. E. Melchers. "Structural Reliability Analysis and Prediction", 2nd ed., John Wiley & Sons, Chichester, United Kingdom, 1999.
- [35] R. E. Walpole, R. H. Myers, S. L. Myers, K. Ye. "Probability & Statistics for Engineers & Scientists", 8th ed., Pearson Education Ltd., London, United Kingdom, 2007.
- [36] "Dynamisk systembeskrivelse av kontaktledningsanlegg" [Online]. Available: [http://www.jernbanekompetanse.no/wiki/Dynamisk\\_systembeskrivelse\\_av\\_kontaktledningsanlegg](http://www.jernbanekompetanse.no/wiki/Dynamisk_systembeskrivelse_av_kontaktledningsanlegg). [Accessed: 30-Jun-2016].



## Paper VI

Anders Rønnquist, Petter Nåvik

Vertical vs. lateral dynamic behaviour of soft catenaries subject to regular loading using field measurements

Submitted for journal publication, 2016



# Vertical vs. lateral dynamic behaviour of soft catenaries subject to regular loading using field measurements

A. Rønnquist<sup>1</sup> and P. Nåvik<sup>1</sup>

<sup>1</sup>Department of Structural Engineering, NTNU, Norwegian University of Science and Technology, Trondheim, Norway

## Abstract

During the last couple of decades, there has been a steady increase in the development of higher-speed railways. Higher speeds increase the demands on existing railway infrastructure designed for older and different scenarios. This increase in demand is also true for the power supply of electric railways in which a two-level catenary system is commonly used. Current soft catenary systems are characterized by their design for optimal quasi-static behaviour. To modify and further develop catenary systems, it is important to have a solid overview of the dynamic characteristics. This paper further investigates the implications of using lateral response compared with the previous vertical response [1]. It is clear that there are dynamic processes that both directions have in common; equally, the two also show quite substantial differences. This effect is explored to improve the dynamic identification scheme. Data are collected by wireless sensors specifically designed for railway catenary systems. The sensors can be mounted arbitrarily to satisfy a beneficial description of the motion. In this investigation, up to ten sensors are used to measure the response within one span. The structural behaviour is examined in the vertical and lateral directions by collecting a significant amount of passage data. These data are analysed for both directions in terms of power spectra, peak histograms and spectrograms. Individual passages are analysed as well as all passages at once. Two catenary sections are included to determine system similarities and differences and to evaluate the combined effort of the two directions, one old and one new, both situated in Norway.

**Keywords:** soft catenary system, operational modal analysis, short-time Fourier analysis, pantograph–catenary interaction, dynamic monitoring, wireless monitoring, field measurements, dynamic assessment.



## 1 Introduction

In Norway, there is growing interest to explore increased speed on the existing railway infrastructure. This requires a thorough investigation into limiting factors. This paper will focus on the practical use of the lateral dynamic response to clarify sought information in the vertical response in two very different existing Norwegian catenary systems, Tabell 54 and System 20 C1. The passing trains typically use the pantographs WBL 88 and WBL 85 by Schunk Nordiska AB.

Currently, there is a large volume of older infrastructure, all designed for completely different scenarios than those scenarios to which they are currently exposed. The soft catenary systems designed for the old existing electric railway lines are characterized by their design for optimal quasi-static behaviour. Thus, to increase the allowable train speed, it is important to explore limiting factors—i.e., to identify dynamic consequences and limitations. Any significant increase in train speed must be verified regarding the effect on the catenary–pantograph interactive response [2].

The investigated dynamic system consists of the interaction between two nonlinear dynamic systems, the pantograph and catenary systems. The contact interaction will give both static and dynamic loads of the combined system and will vary with the train speed. The complexity of this interaction and the dynamic response of the system progressively increase with increasing train speed [3]. That is, the dynamic response of the catenary becomes more important to address as the speed of the train is increased above the design speed [4]. This may also become a problem when trains travel with multiple pantographs because the trailing pantographs will experience oscillations made by the first [5]–[8]. It is known that to estimate the structural modal properties such as fundamental frequencies, modal mass and damping in the catenaries is challenging [2]. Thus, the estimated structural properties may be evaluated only from validated numerical models used to evaluate the dynamic response of different catenary systems. In addition, for the validation process, measurements are needed to evaluate the behaviour of the catenary. Continuously sampling, before the train passes, as the train passes and after it passes is equally important as shown in a recent study [9]. A validation investigation by sampling displacement time series in [10] was conducted at five points within a pole span to validate the displacements in their numerical model. This was accomplished by placing three additional poles within a span for mounting the measuring equipment. However, acceleration measurements of the catenary as the train passes the section can also be used to assess the behaviour. Several different properties can be estimated if the sensors are well positioned, as shown in [11], [1].

When monitoring railway catenary systems, it is common to focus solely on vertical motions [10], [12]–[14]. However, in civil engineering, when examining large cable-supported systems, it is expected to see coupled cross-sectional motions. Because the railway catenary system has geometrical variations in both the lateral and vertical directions, it is natural to assume coupling in this dynamic system as well. Thus, to increase the understanding of catenary system behaviour, the lateral motion is also added to the operational modal analysis. To enable this investigation, a newly developed sensor system [1] for railway catenaries is employed. The sensor system is currently based on up to ten sensors placed over more than 700 m on either side of the

main unit. A wireless system in which the sensors can easily be clipped on and off the wires in the system has been very important in the development of the system. This gives a necessary short mounting and demounting time. To capture the dynamic behaviour, the sensors measure accelerations in three main axes with simultaneous sampling. The sensors then transfer the data to the main logging unit and transmit it to a server accessible online. The stiffness of the system changes between poles, and along the section, depending on the track geometry. With these changes, it is important to assess several points between pole supports. A range of different operational modal analysis (OMA) methods can be used on the output-only data for modal parameter estimation [15].

The results are presented in terms of power spectral densities (PSD) estimated by the Burg method [16], peak picking histograms of the PSDs and spectrograms. This constitutes the base for the present investigation into properties of a railway catenary system as a train pantograph passes underneath. A special focus through all investigations is on the lateral and vertical motions. Here, it is also shown how the properties vary between pre-passage and post-passage as well as two different types of catenary sections. This paper is based upon Rønnquist et al. [17] but includes the additional assessment of the dynamic behaviour in the lateral direction and especially the comparison between vertical and lateral responses in railway catenary systems.

## **2 Norwegian railway catenary systems**

The main existing catenary systems used in Norway are Tabell 54, System 35, System 20 and System 25. However, only the latter three can be used in any new design according to [18]. The choice of catenary system for the contact wire of new railway sections is thoroughly specified in the technical regulations [19]. The primary criteria that decide which system to be used are: train velocity, allowed type of pantographs, train density and type of tracks used [19].

The first system, Tabell 54, is an old catenary system commonly used on the existing railway sections. The maximum train speed allowed on this system is 130 km/h, but was originally designed for 90 km/h. The original tension forces were 7.6 kN in both the contact wire and the messenger wire. Later, to manage with higher speed both were changed to 10 kN and 5 kN, respectively. The main difference between system 35, 20 and 25 is the different train speeds they are designed for. The two modern systems used in Norway are System 20 and System 25. The latter is the Norwegian system designed for the highest train speed; a speed of 250 km/h and the minimum radii of the curvatures are 800 metres. The tension forces used in this system are 15 kN in both the contact wire and the messenger wire. System 20 is split into four different groups; A, B, C1 and C2, where the latter two are catenary systems primarily used for tunnels. System 20 A and C1 are developed for one pantograph with speeds up to 200 km/h where the radii of the curves should be larger than 800 metres. System 20 B and C2 are designed for train speeds only up to 160 km/h with one pantograph. Normally System 20 A and B have 10 kN in both wires while System 20 C1 and C2 have 13 kN in both wires. However, the system can also be used with curvature radii below 800 metres [19]. Finally, System 35, which has 7.1 kN tension in both wires, allows for a maximum speed of 130 km/h [18].

### 3 Wireless sensors, data acquisition and operational modal analysis

A newly developed wireless sensor system is used in this study. The sensor system at present consists of up to ten wireless sensors with motion processing units (MPU) and one master unit. A thorough description can be found in N avik et al.[1]. A sampling rate of 200 Hz was used for all time series, and they were low-pass filtered at 80% of the Nyquist frequency [20] to avoid aliasing and account for the roll-off rate of the filter [15].

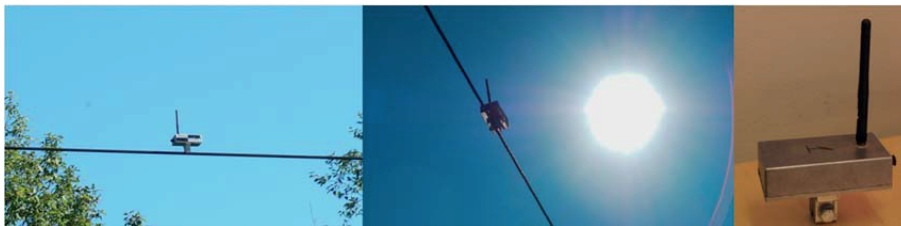


Figure 1. The catenary sensor consists of up to ten tri-axial accelerometers and gyroscopes.

Conducting frequency analysis of time series is vital for understanding the dynamic response. Previously, it was shown that different information can be extracted from the different parts of a train passage time series; see [9], [21]. That is, the pre-passage data include more information about the load frequencies relevant to the section, such as the pantograph frequency and the different span-pass frequencies and fundamental frequencies. The post-passage data on the other side typically reveal the fundamental system frequencies. The advantage of dividing the signal into parts with possible various information contents is also supported by the findings in [22]. The sensitivity to time variation near the peak uplift makes it important to consider the separation of the time series in pre- and post-passage segments before applying different operational modal analysis tools. Here, power spectral density estimations, also represented by picked peak histograms, are used. Finally, spectrograms are used in evaluating the frequency content of single passages. The combined effort of different analyses facilitates a good understanding of the energy input and transfer between frequencies originating from the train's passage.

#### 3.1 Power spectral density (PSD) estimation and histogram representation

In operational modal analysis, there are several methods available for estimating a PSD in structural dynamics. The selected method used to estimate the PSD of pantograph passages depends largely on the passage duration. It is also important to be aware that if the frequency distribution and energy transfer in the frequency domain are to be investigated in detail, the current time series will quickly become very short. Therefore, it is important to choose the method accordingly [15].

For the estimation of the PSD, two common types of estimators are frequently used: parametric and nonparametric methods [23]. In the present investigation, a parametric method is selected. That is, the signal is assumed to be the output of a linear system driven by white noise; i.e., the parametric method estimates the PSD by first estimating the parameters of the linear system assumed to generate the signal. Generally, the parametric methods produce smoother estimates of the PSD than do the nonparametric methods. Commonly, parametric PSD estimation methods use an autoregressive (AR) prediction model for the signal.

In the investigation of the train passage, the Burg method is used for PSD estimation [16]. The Burg method estimates the PSD of the sampled time signal based on a pre-selected order for the AR prediction model. The method does not apply a window function to the dataset, as is common in nonparametric methods. The Burg method may be considered better than nonparametric methods for the application to short parts of the recorded time series such as a train passage. However, it is important to be aware of some of its disadvantages. For example, the Burg method exhibits spectral line splitting, especially at high signal-to-noise ratios. In high-order systems, the Burg method can also introduce spurious spectral peaks, and when estimating sinusoids in noise, this method shows a bias that is initial-phase dependent [24].

To further clarify and identify general trends and how the PSD peak distribution converges, it is natural to introduce histograms. Here, the histograms are used to represent the peak distribution by analysing continuous data collected over a large number of observations. Thus, the histogram represents all collected time series and the individual frequency distribution. That is, the histogram will represent the probability distribution of the observations, which represents the probability of the spectral peak distribution corresponding to the response energy distribution as all observations are included. The expected histogram of the spectral peaks over the given frequency range is clearly multimodal. The skewness of the histograms is equally important to observe, paying attention to the general trends as they produce a clustered result with a few outliers.

### **3.2 The short-time Fourier transform (STFT) and spectrogram analysis**

During a train's passage, the recorded time series will be, strictly speaking, non-stationary with time-varying spectral characteristics. To analyse the changing characteristics of the process, the STFT is essential. Using the STFT in the analysis of the time series provides more complete and precise information about the uplift process [9]. Spectrograms render a visual representation of the acceleration, thereby providing a useful time–frequency representation. In the STFT, time series are segmented into time intervals that are sufficiently narrow to be considered stationary [24]. It is of course important to recognize that the time resolution and the frequency resolution cannot be arbitrarily determined because of their direct relation to the time window size. That is, short windows give a better time resolution but will result in a lower frequency resolution. The spectrogram from the STFT analysis is achieved by squaring the magnitude. In the following investigations, the STFT is used as a sliding discrete Fourier transform in which the STFT is evaluated for each shift of the window

function. To evaluate the frequencies in the short-windowed time series, the Burg spectrum method is used.

## 4 Full-scale measurements of soft Norwegian catenaries

Two railway catenary sections were selected for monitoring. One section is close to Soknedal station, and one section is situated at Vålåsjø. Both sections are part of the same major railway line between Oslo and Trondheim, Dovrebanen. The Soknedal section is a 1301 m long Tabell 54 catenary, whereas the catenary System 20 C1 used at Vålåsjø is 1265 m long; both systems were introduced in chapter 2. The geometries of both sections are presented in Figure 2. The damping of both sections has been identified and is presented in [11].

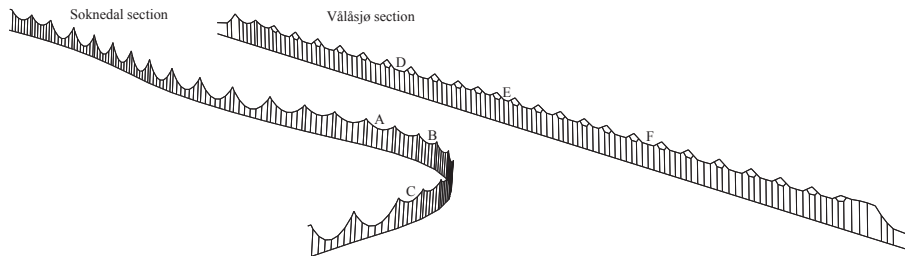


Figure 2. The two investigated railway catenary sections, Soknedal and Vålåsjø.

### 4.1 Soknedal section, description and instrumentation

The Soknedal section is divided into twenty-nine spans whose lengths vary between 40 and 60 m, twenty-seven of which are in contact with the pantograph; see also Table 1. In the selected railway section, there is an initial curve with a radius of  $R = 1250$  m and a part with very sharp curvature,  $R = 350$  m. Thus, a substantial variation in the lateral direction is present owing to the catenary design practice in sharp curves. The spans in the sharp curvature have a length of 40 m, whereas the straight section and the larger radius both have a length of 60 m. These lengths and curves are irregularities that currently significantly reduce the allowed running speed on the section to 90 km/h. The section has previously also been part of a numerical investigation with varying train speed, vertically only, and the results are presented in [9]. The sensor system geometrical configurations at Soknedal are presented in Figure 3.

Span length	40 m	45 m	50 m	60 m
Number of spans	11	2	2	12
Length to outside dropper	2.1 m	1.9 m	2.3 m	3 m
First symmetric frequency	1.263 Hz	1.133 Hz	1.016 Hz	0.844 Hz
First non-symmetric frequency	1.329 Hz	1.181 Hz	1.063 Hz	0.886 Hz

Table 1. Soknedal: detailed description of spans and theoretical frequencies.

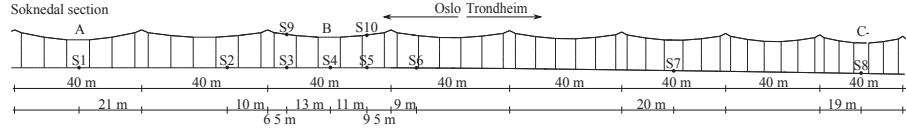


Figure 3. Sensor positioning and geometry of the Soknedal station catenary section.

## 4.2 Vålåsjø section, description and instrumentation

The Vålåsjø section consists of twenty-eight spans with lengths between 33.91 and 50.4 m. Twenty-six of them are in contact with the pantograph under passage. A description of the spans and their theoretical natural frequencies for the Vålåsjø section is given in Table 2.

<b>Span length</b>	<b>33.91</b>	<b>35.83</b>	<b>38.65</b>	<b>39.95</b>	<b>40.5</b>	<b>42.11</b>	<b>42.75</b>	<b>43</b>	<b>44</b>
Number of spans	1	1	2	1	1	1	1	1	1
Length to the outside dropper (m)	4	4	4	4	4	4	4	4	4
First expected symmetric frequency (Hz)	1.739	1.651	1.537	1.489	1.470	1.416	1.396	1.388	1.358
First expected non-symmetric frequency (Hz)	1.842	1.743	1.616	1.564	1.542	1.483	1.461	1.453	1.420
<b>Span length</b>	<b>46</b>	<b>46.1</b>	<b>47.8</b>	<b>49</b>	<b>49.56</b>	<b>49.7</b>	<b>49.75</b>	<b>49.84</b>	<b>50.4</b>
Number of spans	3	1	1	3	1	1	1	1	1
Length to the outside dropper (m)	4	4	4	4	4	4	4	4	4
First expected symmetric frequency (Hz)	1.301	1.299	1.254	1.225	1.211	1.208	1.207	1.205	1.192
First expected non-symmetric frequency (Hz)	1.358	1.355	1.307	1.275	1.260	1.257	1.256	1.253	1.239

Table 2. Vålåsjø: detailed description of spans and theoretical frequencies.

The horizontal geometry from south to north contains one straight section and one curve,  $R=1000$  m. The allowed train speed for the section is 130 km/h. The geometrical configuration of the sensor system at Vålåsjø is presented in Figure 4.

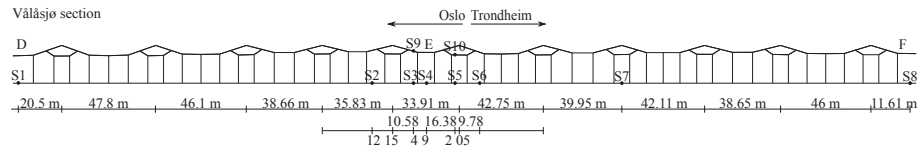


Figure 4. Sensor positioning and geometry of the Vålåsjø catenary section.

## 5 Results and discussion

To investigate the dynamic behaviour of the presented railway catenary sections and evaluate the importance of including an additional direction, recorded train passages are analysed via several different approaches. One approach includes an overall data analysis, which includes data from all sensors and all passages. This analysis is vital for a system, such as the soft catenary system, to observe the distribution towards which the system response converges. This study gives an overview of the energy distribution over frequencies up to 20 Hz. Further clarification of the dynamic content is achieved by dividing the analysis into pre- and post-passage as shown to be necessary in [9]. Parts of the analyses are performed for both the vertical and lateral responses to show the advantage of including the lateral direction in a complete

assessment of the dynamic behaviour. It is of course equally interesting and important to study the variation over the different sensors as well as the differences over a single time series; thus, such analyses are also introduced. The analysed data are collected during roughly one week of measurements, including every train passage and data from all sensors.

### 5.1 Full sensor system analyses by PSDs and histograms

It is important to understand that this is response data from an in-space stationary system excited by an in-motion secondary system, the pantograph. That is, both the motion in itself and the internal dynamic response of the secondary system will influence the catenary behaviour. This means that the pre-passage data will have lower response than the post-passage data. This implies that the PSD will show low energy content for frequencies dominated by the pre-passage response compared with the post-passage response components. In general, to weigh the different passage contributions fairly, representation of the PSD peaks by a histogram is introduced. Here, the emphasis is on the number of peaks in each passage. In Figure 5 and Figure 6, this is shown by the inclusion of the two, the PSD representation (right axis) and the peak histogram representation (left axis). Both result from analysing data from all sensors and passages during the measurements. Figure 5 includes only the pre-passage accelerations, whereas Figure 6 includes results from both the vertical (upper) and lateral (lower) accelerations from the post-passage.

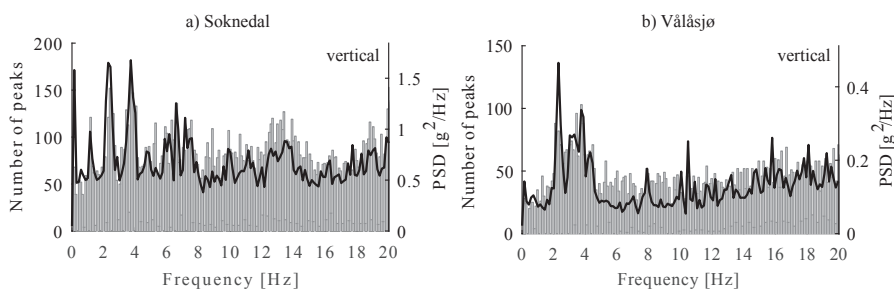


Figure 5. Pre-passage results a) Soknedal, vertical, b) Vålåsjo, vertical. Left axis: histogram representation of PSD peaks for all passages and all sensors; Right axis: PSD of all passages and all sensors.

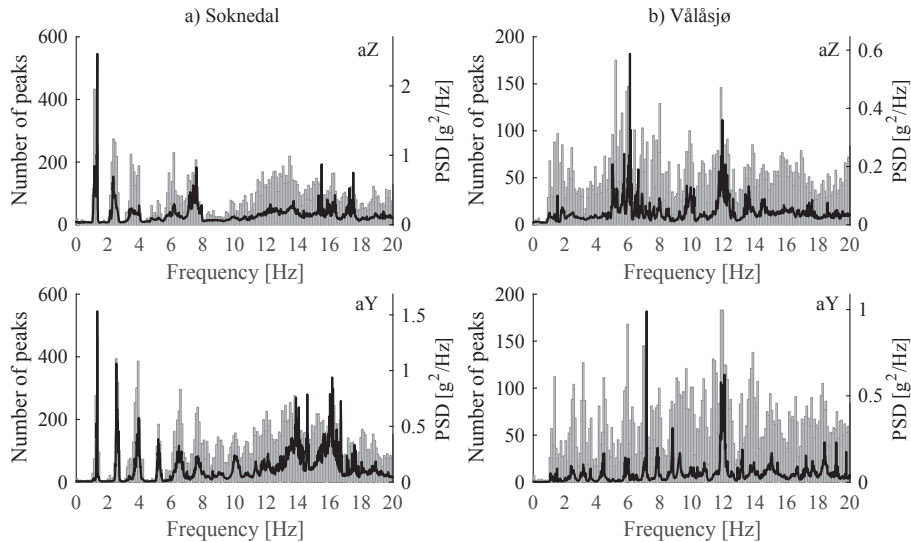


Figure 6. Post-passage results a) Soknedal: vertical, upper left, and lateral, lower left. b) Vålåsjø: vertical, upper right, and lateral, lower right. Left axis: histogram of PSD peaks for all passages and all sensors; Right axis: PSD of all passages and all sensors.

The Soknedal section measurements are shown in Figure 5 a) and Figure 6 a). In the pre-passage results, Figure 5 a), the energy levels, PSDs, are similar in shape to the histogram distribution when scaled as shown in the figure. That is, the number of peaks collected in each passage are correlated with the response energy distribution. This result is to be expected because the oncoming train will create a broadband load frequency distribution as it passes initial spans. In addition, included in the pre-passage response are effects from the propagating waves, reflections known to limit the train speed on a catenary system.

The post-passage is somewhat different, reflecting the motion introduced by the pantograph uplift. Thus, the sudden impulse and the following stationary response will be dominated by fundamental frequencies of the catenary. Figure 6 a) shows histograms that emphasize the dominant frequency peaks. However, the PSD of all passages show that although these frequencies are indeed affected, they do not all attract the same amount of energy. This is a direct consequence of the initial impulse loading of the system. Thus, in the lower 5 Hz band, there are three dominating frequencies, as shown by the histogram, in which the first have the majority of the response energy as shown by the PSD. To further investigate the frequency distribution and determine the central peak frequency of interest, both vertical and lateral results are introduced in Figure 6. It is clear that there are several motions that are spatial but, at the same time, more centred in the lateral results than the vertical. The first frequency peak closely above 1 Hz appears clear and valid for both directions in the figure, but looking more closely at the PSDs, the peak is split into two peaks for the vertical direction, one at 1.14 Hz and one at 1.33 Hz, whereas the lateral peak includes only the one at 1.33 Hz. This result shows that the lateral response includes



only the non-symmetrical first natural frequency, whereas the vertical response includes both the symmetrical and non-symmetrical first natural frequency; the non-symmetric and symmetric frequencies are defined in Kiessling et al. [3]. The next two peaks approximately 2.4 Hz and 3.9 Hz are clearly more distinct in the lateral direction, which simplifies the determination of true poles for the mode. Especially, the latter at 3.9 Hz is narrower in the lateral direction and is seemingly a combined motion of lateral and vertical accelerations. This result can be compared with the frequency peak at 5.2 Hz, which from the two diagrams is clearly only a lateral motion.

The variety of the two sections is clearly observed in the histograms and PSD diagrams of the Vålåsjø section introduced in Figure 6 b). Owing to the large variation of span lengths, the initiated response will be much more broadband than at Soknedal. This variation in span lengths is demonstrated in Table 1 and Table 2 for both sections. That is, the Soknedal have many more span repetitions, as shown. Another interesting observation is the much larger energy variation between pre- and post-passage at Vålåsjø. In the pre-passage, Figure 5 b), the lower frequency band, less than 5 Hz, clearly dominates the response again, as shown by both the histogram and PSD. The post-passage, Figure 6 b), has the response transferred higher up in the frequency band. Here, the first few fundamental frequencies are clear, and the PSD shows a response concentration at approximately 6 Hz and then again at approximately the multiple 12 Hz. Again, the lateral and vertical directions have similar results, showing spatial motions as expected. It is interesting to see that both the PSD and histogram in the lateral direction show more distinct peaks than the vertical direction, which is helpful in further frequency analysis. This result is also prominent in the frequency range 6–8 Hz, where the peaks are more distinguished in the lateral direction. Finally, this is true also when looking at frequencies of approximately 10 Hz; here, the vertical direction is clearly dominating the motion, with only small lateral contributions. Thus, the use of comparing lateral and vertical accelerations to assess the complex catenary motion helps identify important frequency components, as intended.

## 5.2 Single sensor analysis by histograms

To further explore the dynamic behaviour, histograms based on data from single sensors are established. These histograms consist of the ten highest PSD peaks from each individual passage. The results from the Soknedal section are shown in Figure 7, vertical, and Figure 8, lateral, where sensors S3 to S5 are on the contact wire, and sensors S9 and S10 are on the messenger wire, also shown in Figure 3. It should be noted that the fundamental frequency is represented in all sensor responses as expected, but the skewness of the different histograms clearly shows the energy variation in the catenary system. These effects are not easily detected using single passages but are more distinct in an assembly of collected data from all train passages.

In the Soknedal section, the span length repetition within the section is mirrored to an extent, and all major components are represented in all sensors as shown in Figure 7 and Figure 8. However, the differences between the responses at different positions in a span is apparent in the skewness of the distributions. The difference between sensors is easy to observe when comparing S3 and S5 with S4 around the second natural frequency, the mode shape with the inflection point in the mid-span. As

expected, S4, which is located in the middle span, does not have a response at that frequency, but S3 and S5 both have significant responses. Finally, it is important to recognize that parts without peak contributions are as important as those parts with contributions. Their importance will depend on whether their nonexistence in the histograms is due to a lack of load in these ranges or if this is a structural characteristic. This knowledge is important for an optimization situation.

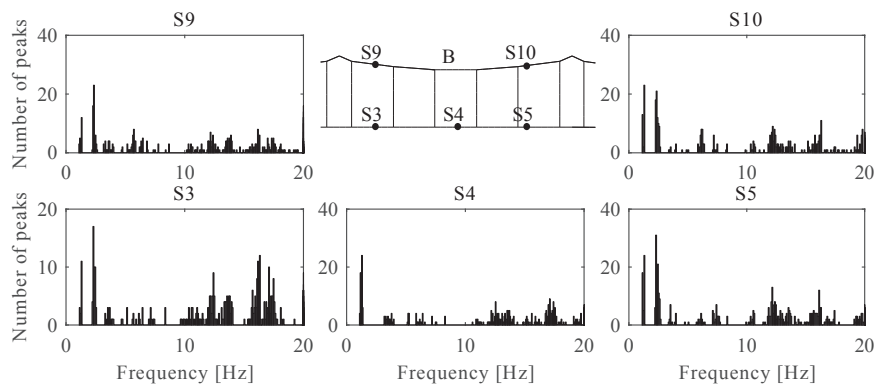


Figure 7. Histogram representation of the ten highest peaks at each passage for the relevant sensors (S3, S4, S5, S9 and S10 Figure 3) for all passages recorded at the Soknedal station, vertical response.

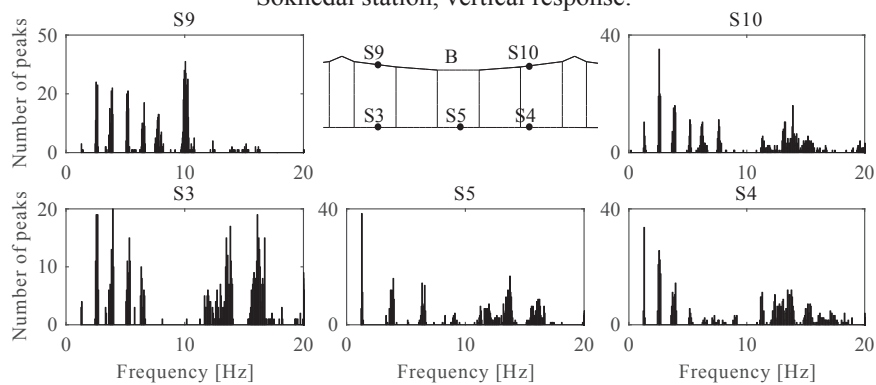


Figure 8. Histogram representation of the ten highest peaks at each passage for the relevant sensors (S3, S4, S5, S9 and S10 Figure 3) for all passages recorded at the Soknedal station, lateral response.

The Vålåsjø section response has some similarities and some deviations with the Soknedal section response. It is therefore important to note the differences between the two sections. The properties are quite different, as presented in chapter 4, but the sensor placements are only slightly different. The Vålåsjø section has a stitched wire, in contrast to the Soknedal section, and the sensors are placed differently relative to the stitched wire support to capture the similarities and differences. This applies to sensors S3 and S5, which are seemingly mirrored, but with S3 outside and S5 within

the stitched wire part of the contact wire. This applies equally to sensors S9 and S10, where S9 is placed outside and S10 is placed within and on the stitch wire.

The response distribution of all passages show how fundamental modes are captured and that the system modes are concentrated at higher frequencies than the Soknedal section. It should be noted that the train speed is higher at the Vålåsjø section, so the load distribution will be different between the two sections. The skewness between different sensor placements is interesting. Here, the skewness between S3 and S5 is apparent. To a large extent, the two positions are triggered by similar frequencies, but they are clearly differently weighted in the structural response. The same trend is also observed between sensors S9 and S10. However, the change is equal for both sensors, where the sensor outside the stitched part is skewed to the lower frequencies. Because this is a single track train line, the train travelling direction is not part of the answer to the skewness. The mid-span sensor, although containing several frequency components from both previous pairs, is not a collection of all components. That is, the sensor has similar features as those sensors outside the stitched part but also shows characteristics of the symmetry features of the catenary, as expected. The differences between sensors are presented in Figure 9 and Figure 10.

Regarding the lateral and vertical responses, it is interesting to see that there are more distinct frequency peaks in the lateral direction than in the vertical direction at the sensor level as well as overall, shown earlier. This result is especially prominent for the messenger wire. Here, several contributing frequency components from the contact wire are filtered out by the system, as clearly observed in the results from S10 on the stich wire. This is clearly confirmed by the combined lateral and vertical results. Thus, the analysis in two directions also shows the importance of different system components to the overall response. For example, the damping contributions at different frequencies are expected to be different from the messenger wire and stich wire compared with the contact wire. However, this should be used with care in any numerical simulations because the common Rayleigh damping contribution will be spread over the system damping matrix and should therefore be constructed and evaluated accordingly.

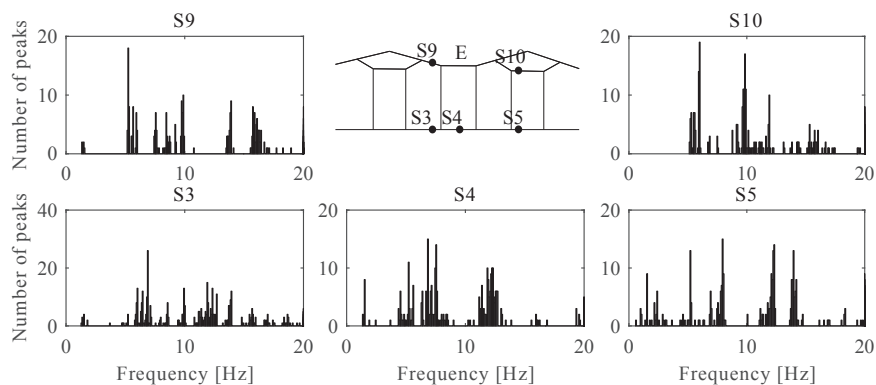


Figure 9. Histogram representation of the ten highest peaks at each passage for the relevant sensors (S3, S4, S5, S9 and S10 Figure 4) for all passages recorded at the Vålåsjø, vertical response.

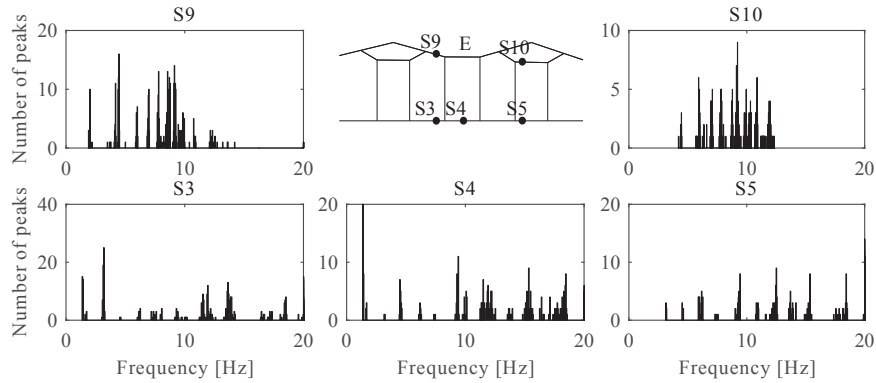


Figure 10. Histogram representation of the ten highest peaks at each passage for the relevant sensors (S3, S4, S5, S9 and S10 Figure 4) for all passages recorded at the Vålåsjø, lateral response.

### 5.3 Single sensor analysis by STFT

To further investigate the frequency content and position variations, three sensors are selected at the two locations. For the Soknedal section, S3, S4 and S9 are selected, and for the Vålåsjø section, S3, S5 and S9 are selected; the positions are shown in Figure 3 and Figure 4, respectively. These sensors capture similar positioning between the two sections and also the variation within each span. The analysis is conducted using the STFT and spectrogram representation. The time series and their accompanying spectrograms are shown in Figure 11, Figure 12, Figure 13 and Figure 14, which show the frequency characteristics during the passage of one train. From the diagrams, it is clear that during the short duration of the passage, the sensor time series acceleration will vary considerably and reach levels of several times gravity. To identify the major frequencies and the frequency transfer zone of the passage, the corresponding spectrograms are used. Numerical models of catenary systems [9] have shown that the catenary is a slender and flexible system with many similar frequency components, including small variations. This gives similar eigenvalues from the eigenvalue analysis, which can be observed to accumulate around given frequencies.

From the time series of the passages and the results from the spectrograms, the passage influence zone can be determined, which of course is equal for the two directions. This zone provides a good indication of the division into pre- and post-passage parts of the analysis, as previously conducted. The remaining part of the time series has less time-variance and fits better to any detailed operational modal analysis, such as determining mode shapes and modal updating of finite element models, rendering more distinct vertical and lateral results

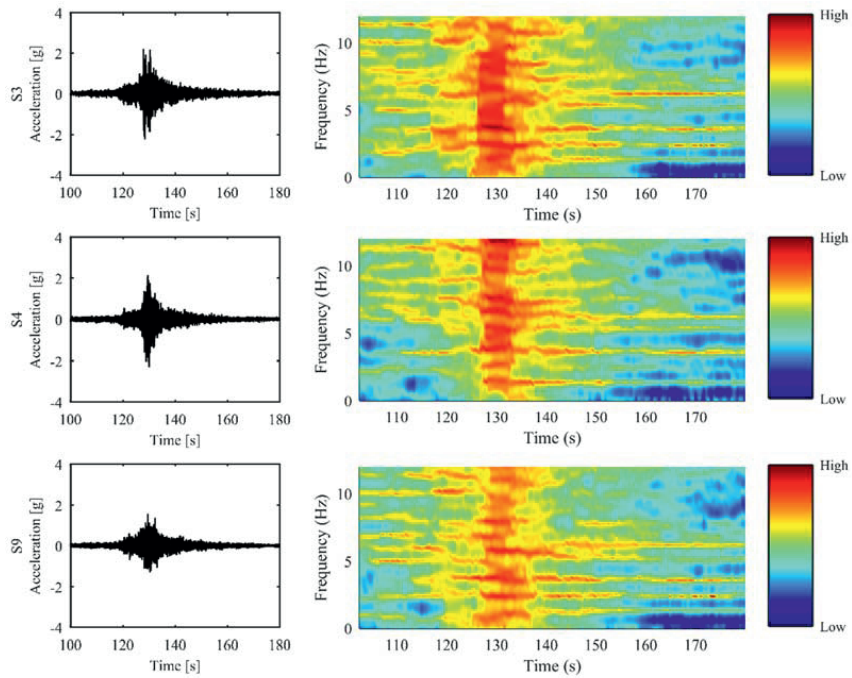


Figure 11. Vertical time series and spectrogram representation of the frequency content through a train passage; from top to bottom: sensors S3, S4 and S9 at Soknedal.

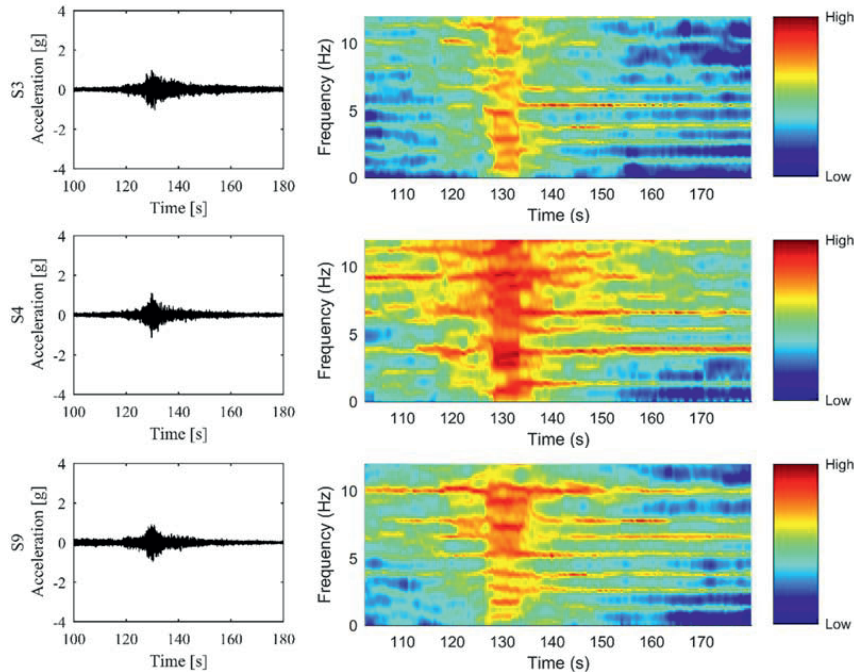


Figure 12. Lateral time series and spectrogram representation of the frequency content through a train passage; from top to bottom: sensors S3, S4 and S9 at Soknedal.

The vertical and lateral Soknedal sensor response analyses are shown in Figure 11 and Figure 12, respectively. It is interesting to observe the frequency change and the energy transfer between frequency components due to the train passage. Note that the fundamental modes are those modes that have a considerably longer duration. Furthermore, it is distinguishable that some are the same in both directions, representing spatial modes, whereas others are distinct in one of the two, representing single direction modes, all as previously shown in detail. That is, several frequency components are excited, but the energy converges to fundamental modes, rendering the other mode shapes with high damping, whereas the lasting fundamental modes typically have low damping characteristics. Note that, as expected, the pre-passage frequency distribution is different between the lateral and vertical directions because the large uplift caused by the passing pantograph is in the vertical direction. This difference can also be observed in the transition zone, especially for S3 and S9 in Figure 12. This result also shows the differences in the overall frequency interpretation in the two directions and why the lateral response in many cases is more pronounced, as previously stated.

Finally, the Vålåsjø vertical response spectrograms show even fewer distinct frequency components in the pre-passage part than that of the Soknedal section; see Figure 13. In addition, in the post-passage part, the frequency distribution is less harmonic than in the Soknedal section. That is, the Vålåsjø vertical spectrogram shows clusters of frequencies around a few central frequencies such as 2 Hz, 6 Hz

and 9 Hz. However, it is interesting to see the similarities in the messenger wire and the contact wire for sensors S3 and S9, which means that the motion engages more of the system than just individual wire segments in the given frequency range. . Though, this does not rule out that modes may have shapes where parts will coincide with segment lengths. This result can be observed by the difference in frequency distribution in the post-passage between sensors S5 and S9 and a few similarities between sensors S3 and S9. However, when evaluating the same passage in the lateral direction, as shown in Figure 14, the interpretation becomes clearer. In the lateral direction, there is less of a broadband pre-passage process, and the post-passage part gives easier detection of the frequency components. In fact, the clarity is such that several frequency components can be observed all the way through the transition zone, as expected, but are difficult to detect in the vertical response analysis. This fact emphasizes the importance of including the lateral response analysis when investigating the vertical dynamic behaviour of catenary systems in operation.

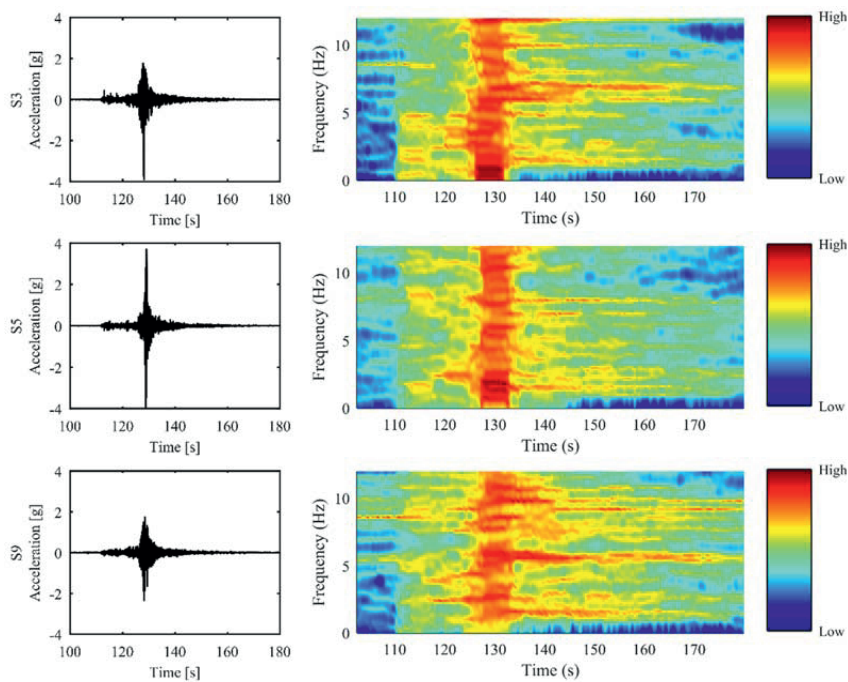


Figure 13. Vertical time series and spectrogram representation of the frequency content through a train passage; from top to bottom: sensors S3, S5 and S9 at Vålåsjø.

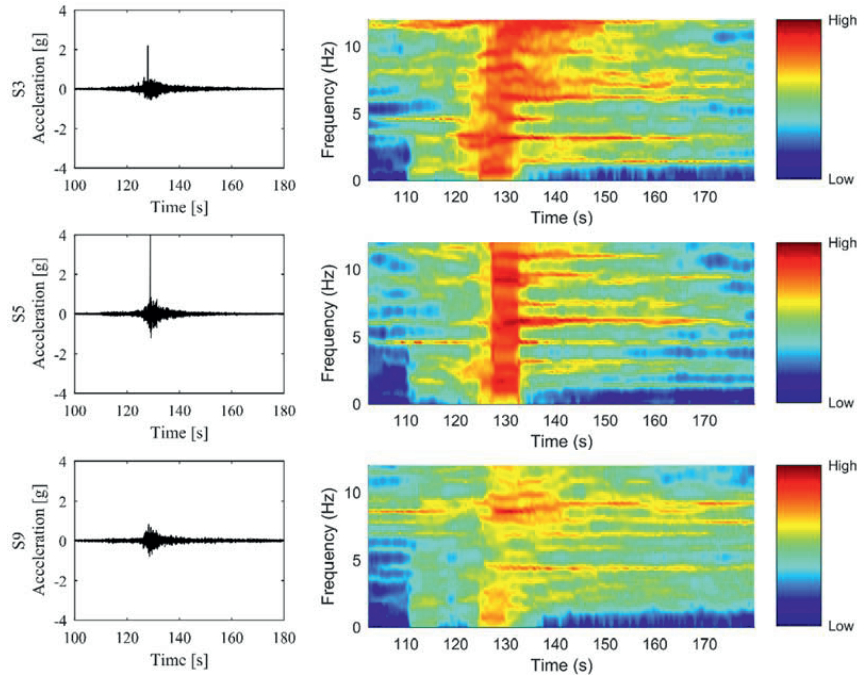


Figure 14. Lateral time series and spectrogram representation of the frequency content through a train passage; from top to bottom: sensors S3, S5 and S9 at Vålåsjø.

## 6 Conclusions

Railway catenary systems have been dynamically assessed by monitoring the structural acceleration in the catenary. Several sensors from a newly developed sensor system have been used to sample the field measurements of regular train traffic. The system has been applied at the Soknedal station and at Vålåsjø, two distinctly different but similarly soft Norwegian railway catenary systems. The first is an old system with challenging geometry, and the other is a special case of a modern system with fairly high tension in both wires for the given design. The collected data have been used to investigate the system behaviour within one span. This paper emphasizes the inclusion of the lateral and vertical response, which is used in comparing the system's dynamic behaviour to identify similarities and differences between the two locations and between segments within each span. This study includes the overall data collected and analysed using all collected data from a week of measurements to better verify the system characteristics, which is not as easy when investigating single passages. The investigation is, in its extension, also intended to estimate modal parameters to verify numerical models such that they can be used to optimize each catenary. It is clear from the power spectral analysis and the spectrograms that the lateral response can advantageously be used to clarify spatial modes with main motion in the vertical direction and separate the different modes in the two directions, even if they are closely spaced.



The two investigated systems show characteristics that have some common features but also show distinct differences. The Soknedal section has a more harmonic characteristic in the estimated response distribution. Vålåsjø, on the other hand, shows a distribution with clusters of frequency components. The results from all passages vary between pre- and post-passage, where for the pre-passage, the correlation between the PSD peak histogram and the actual PSD of all passages is good. The post-passage, however, shows that several of the peaks are represented in the histograms, but the energy distribution in the PSD is weighted towards a few fundamental frequencies of the response.

The individual sensor study reveals the frequency components that generally contribute to the response at each segment. They show that some frequencies represent the fundamental motions that engage the entire catenary span, whereas others are specific for the position. This is apparent when studying the skewness of the histograms and how this skewness varies within the different sensors in the span and between sensors in the two sections. The lateral histograms of each sensor are also helpful in clarifying the difference between structural components and their corresponding frequency content of interest. That is, together with the vertical results, the skew distributions and the lack of contributions in distinct ranges are clarified. The difference in the number of distinct frequency peaks in the lateral and vertical histograms was also noted.

Different setups of the sensors at the different locations and different types of excitation will be used to improve the soft catenary system characteristics. Changing the setup of the sensors, identifying mode shapes of the railway catenary section and validating finite element models are all based on the preliminary results from the operational monitoring. That is, the use of the identified and verified dynamic behaviour from a successful monitoring programme will be important in suggesting modifications and solutions to local problems and the overall system problems of existing catenary systems.

## References

- [1] P. Nåvik, A. Rønnquist, and S. Stichel, "A wireless railway catenary structural monitoring system: full-scale case study," *Case Stud. Struct. Eng.*, May 2016.
- [2] J. Ambrósio, J. Pombo, M. Pereira, P. Antunes, and a. Móscã, "Recent Developments in Pantograph-Catenary Interaction Modelling and Analysis," *Int. J. Railw. Technol.*, vol. 1, no. 1, pp. 249–278, Apr. 2012.
- [3] F. Kiessling, R. Puschmann, A. Schmieder, and E. Schneider, *Contact lines for electric railways : planning, design, implementation, maintenance*. Munich: Publicis, 2009.
- [4] G. A. Scott and M. Cook, "Extending the limits of pantograph/overhead performance," in *Better Journey Time - Better Business. I. Mech. E. Conference Transactions 1996-8*, 1996, vol. 8, pp. 207–218.
- [5] G. Poetsch, J. Evans, R. Meisinger, W. Kortüm, W. Baldauf, A. Veitl, and J. Wallaschek, "Pantograph/Catenary Dynamics and Control," *Veh. Syst. Dyn.*, vol. 28, no. 2–3, pp. 159–195, 1997.
- [6] J. Pombo and P. Antunes, "A Comparative Study between Two Pantographs in

Multiple Pantograph High-Speed Operations,” *Int. J. Railw. Technol.*, vol. 2, no. 1, pp. 83–108, 2013.

- [7] Z. Liu, P.-A. Jönsson, S. Stichel, and A. Rønnquist, “Implications of the operation of multiple pantographs on the soft catenary systems in Sweden,” *Proc. Inst. Mech. Eng. Part F J. Rail Rapid Transit*, Dec. 2014.
- [8] J. Pombo and J. Ambrósio, “Multiple Pantograph Interaction With Catenaries in High-Speed Trains,” *J. Comput. Nonlinear Dyn.*, vol. 7, no. 4, p. 041008, 2012.
- [9] A. Rønnquist and P. Nåvik, “Dynamic assessment of existing soft catenary systems using modal analysis to explore higher train velocities: A case study of a Norwegian contact line system,” *Veh. Syst. Dyn.*, vol. 53, no. 6, pp. 756–774, 2015.
- [10] L. Drugge, T. Larsson, and A. Stensson, “Modelling and simulation of catenary-pantograph interaction,” vol. 33, pp. 490–501, 1999.
- [11] P. Nåvik, A. Rønnquist, and S. Stichel, “Identification of system damping in railway catenary wire systems from full-scale measurements,” *Eng. Struct.*, vol. 113, pp. 71–78, 2016.
- [12] P. Nåvik, A. Rønnquist, and S. Stichel, “A wireless railway catenary structural monitoring system: Full-scale case study,” *Case Stud. Struct. Eng.*, vol. 6, pp. 22–30, 2016.
- [13] M. T. Stickland, T. J. Scanlon, I. A. Craighead, and J. Fernandez, “An investigation into the mechanical damping characteristics of catenary contact wires and their effect on aerodynamic galloping instability,” *Proc. Inst. Mech. Eng. Part F J. Rail Rapid Transit*, vol. 217, no. 2, pp. 63–71, Mar. 2003.
- [14] Y. H. Cho, J. M. Lee, S. Y. Park, and E. S. Lee, “Robust Measurement of Damping Ratios of a Railway Contact Wire Using Wavelet Transforms,” *Key Engineering Materials*, vol. 321–323, pp. 1629–1635, 2006.
- [15] C. Rainieri and G. Fabbrocino, *Operational Modal Analysis of Civil Engineering Structures*. New York: Springer, 2014.
- [16] J. P. Burg, “Maximum entropy spectral analysis,” Stanford University, 1975.
- [17] A. Rønnquist and P. Nåvik, “Exploring dynamic behaviour of soft catenaries subject to regular loading using full scale measurements,” in *Civil-Comp Proceedings*, 2016, vol. 110.
- [18] “Mekanisk systembeskrivelse av kontaktledningsanlegg.” [Online]. Available: [http://www.jernbanekompetanse.no/wiki/Mekanisk\\_systembeskrivelse\\_av\\_kontaktledningsanlegg](http://www.jernbanekompetanse.no/wiki/Mekanisk_systembeskrivelse_av_kontaktledningsanlegg). [Accessed: 02-Oct-2013].
- [19] “JD540 Teknisk regelverk, Kontaktledning.” [Online]. Available: <https://trv.jbv.no/wiki/Kontaktledning/Prosjektering/Kontaktledningssystemer>. [Accessed: 08-Feb-2016].
- [20] H. Nyquist, “Certain Topics in Telegraph Transmission Theory,” *American Institute of Electrical Engineers, Transactions of the*, vol. 47, no. 2, pp. 617–644, 1928.
- [21] P. Nåvik, A. Rønnquist, and S. Stichel, “The use of dynamic response to evaluate and improve the optimization of existing soft railway catenary systems for higher speeds,” *Proc. Inst. Mech. Eng. Part F J. Rail Rapid Transit*, Sep. 2015.

- [22] “EUROPAC European Optimised Pantograph Catenary Interface: Publishable Final Activity Report,” 2008.
- [23] J. S. Bendat and A. G. Piersol, *Random data: analysis and measurement procedures*, 2nd ed. New York: John Wiley & Sons, 1986.
- [24] L. R. Rabiner and J. B. Allen, “On the implementation of a short-time spectral analysis method for system identification,” *IEEE Trans. Acoust.*, vol. 28, pp. 69–78, 1980.





## Paper VII

Petter Nåvik, Anders Rønnquist, Sebastian Stichel

Variation in the prediction of pantograph-catenary interaction contact forces, numerical simulations and field measurements

Submitted for journal publication, 2016



## Variation in predicting pantograph-catenary interaction contact forces, numerical simulations and field measurements

Petter Nåvik<sup>a</sup>, Anders Rønquist<sup>a</sup> and Sebastian Stichel<sup>b</sup>

<sup>a</sup>Norwegian University of Science and Technology, Department of Structural Engineering, Trondheim, Norway

<sup>b</sup>KTH Royal Institute of Technology, Department of Aeronautical and Vehicle Engineering, Stockholm, Sweden

**Corresponding author:** Petter Nåvik, Department of Structural Engineering, Norwegian University of Science and Technology, Rich. Birkelandsvei 1A, 7491 Trondheim, Norway, [petter\\_r.navik@ntnu.no](mailto:petter_r.navik@ntnu.no), +47 73 59 47 00

Anders Rønquist, Department of Structural Engineering, Norwegian University of Science and Technology, Rich. Birkelandsvei 1A, 7491 Trondheim, Norway, [anders.ronnquist@ntnu.no](mailto:anders.ronnquist@ntnu.no), +47 73 59 47 00

Sebastian Stichel, Department of Aeronautical and Vehicle Engineering, Royal Institute of Technology, SE-100 44 Stockholm, Sweden, [stichel@kth.se](mailto:stichel@kth.se), +46-70-233 01 63

### Abstract

The contact force between the pantograph and the contact wire ensures energy transfer between the two. Too small of a force leads to arching and unstable energy transfer, while too large of a force leads to unnecessary wear on both parts. Thus, obtaining the correct contact force is important for both field measurements and estimates using numerical analysis. The field contact force time series is derived from measurements performed by a self-propelled diagnostic vehicle containing overhead line recording equipment. The measurements are not sampled at the actual contact surface of the interaction but by force transducers beneath the collector strips. Methods exist for obtaining more realistic measurements by adding inertia and aerodynamic effects to the measurements. The variation in predicting the pantograph-catenary interaction contact force is studied in this paper by evaluating the effect the force sampling location and the effects of signal processing such as filtering. A numerical model validated by field measurements is used to study these effects. First, this paper shows that the numerical model can reproduce a train passage with high accuracy. Second, this study introduces three different options for contact force predictions from numerical simulations. Third, this paper demonstrates that the standard deviation and the maximum and minimum values of the contact force are sensitive to a low-pass filter. For a specific case, an 80 Hz cut-off frequency is compared to a 20 Hz cut-off frequency, as required by EN 50317:2012; the results show an 11% increase in standard deviation, a 36% increase in the maximum value and a 19% decrease in the minimum value.

**Keywords:** The pantograph-catenary interaction, contact force, field measurements, finite element model, railway catenary system, numerical simulations.

### 1 Introduction

The most important property of an electrical railway is the interaction between the railway catenary systems and the pantograph. This contact ensures that the train receives power and is essential for a reliable supply of electrical energy (1). The complexity of this interaction increases with increasing speed (2) but is equally important at all speeds. The magnitude of the force is important for displacements in the cable system, wear, and maintaining electric power supply. Numerous studies have used the contact force as one of the main evaluation parameters (3–7). Control strategies are based on contact forces (8,9), and the assessment of numerical models is based on contact force measurements (10–12). The mechanical friction resulting from the magnitude of the contact force is one of the three main contributors to wear (13). Therefore, it is important to study not only the magnitude of the force but also the methods used to predict this magnitude and the effects of post-processing.

Numerical models of structures can perform tests and analyses that are not reasonable or even possible to perform on a real structure, either because too many tests are needed or because it is too expensive or simply not feasible. The latter is true for the contact pressure between the contact wire and the pan head. To achieve reliable results, a numerical model must represent the physical processes as accurately as possible. In particular, the variation of the contact force requires a detailed description of both the pantograph and the catenary. The higher the train speed used in the analysis is, the higher the sample frequency should be. Note that a simple clamp for a dropper can be as small as 2.5 cm long, and to be sure that the collector strips in the model hits it at a speed of only 130 km/h one needs a time increment of 0.00069 s, i.e., a frequency of 1444 Hz, and for a speed of 300 km/h, a time increment of 0.0003 s (i.e., 3333 Hz) is needed. However, important results can be obtained with a lower sampling frequency,



but it demonstrates that a very short time increment is required to study the contact force in detail. In contrast, the measurements with an overhead line recording train from the continuous load process contain response contributions that are also excited at much higher frequencies than the sampling frequency. Currently, the EN 50317:2012 (14) code requires a sampling rate of greater than 200 Hz for a time sampling of less than 0.4 m for distance sampling for on-line measurements; in addition, the contact forces should be low-pass filtered at 20 Hz, which has been followed by the literature (15). However, Collina and Bruni (16) state that numerical models should be validated up to at least 100 Hz to describe wear phenomena.

This study focuses on the variation in the predicted contact force of the pantograph-catenary interaction. Both field measurements and numerical results are included in this study. The contact force field measurements are obtained from a database containing measurements taken twice a year for the past five years; these data are sampled using an overhead line recording vehicle at every 0.5 m, and the values are taken from force transducers located just beneath the collector strips. This paper presents a finite element numerical model with geometry based on in-field mounting procedures. The model presented here is based on an earlier version of the model discussed in (17,18): it is a three-dimensional model where the train can be given displacements in all three directions and rotational movements about the longitudinal axis of the train and the axis perpendicular to the track. Thus, the track cant can be described along with the horizontal movement of the train. The model includes a contact description that gives the contact in the interface between the contact wire and the pan head and considers how the pantographs tilt with the train on curves. The penalty method is used to represent the sliding contact and is the most frequently used method in the literature (19). In this study, the numerical model is validated against geometry, elasticity, pre-sag, displacement time series, frequency content and statistical contact force values from field measurements. The validation shows that the model has sufficient accuracy; the methods used for validation and the sampling procedures for the field measurements are developed in (20–22).

This study focuses on variations in the predicted pantograph-catenary interaction contact force. First, the variation of the measured contact force time series is investigated by studying several passages at the same railway catenary section. The variation is found to be significant, demonstrating the importance of evaluating more than one train passage when conducting field measurements. Second, the effect of post-processing on the contact force prediction is studied using numerical simulations. The differences between three different methods for predicting the contact force are investigated by comparing their mean values, standard deviations, and maximum and minimum values. In addition, the effect of filtering is studied in more detail by comparing the statistical values obtained from a single contact force time series that has been low-pass filtered at varying cut-off frequencies. This study demonstrates that the method used for the low-pass filtering and the limit for the cut-off filter significantly affect the contact force estimations. Overall, this study shows significant variability in the contact force depending on individual train passages and post-processing.

## **2 Finite element modelling**

### **2.1 Catenary**

The finite element method (FEM) is used to numerically model railway catenary sections. This study uses the commercial FEM software Abaqus to create the models and run the simulations.

The first step in the modelling procedure is to obtain the correct geometry of a railway catenary section. Here, this process follows the actual mounting procedure used when installing these sections on site. First, the geometry of the section is defined using only the lengths of the components described in the design. The droppers are created with small geometrical imperfections to ensure lateral bending if exposed to pressure. Including dropper slackening is considered to substantially influence the accuracy of the model (19). The second step is to apply the tension forces used on the particular section and to apply gravity; it is important to apply the tension forces and gravity simultaneously to ensure a stable solution that includes geometrical nonlinearities in the process. The resulting geometry should be the same as the on-site geometry. Thus, this procedure ensures accurate geometry without needing further corrections. This procedure is critical when working with three-dimensional section models that have complex geometry and geometrical nonlinearities, considering different span lengths, curves and variable contact wire height. The tension forces in the wires are introduced using predefined temperatures; it is very important that these tension forces are correct in the model to ensure accurate results (17). The tension force in the stitch wires has been found to be essential for correctly describing the geometry; small variations in the tension force results in large variations in the vertical geometry and thus in the pre-sag and elasticity. This variation is particularly noticeable when modelling the geometrically varying sections, and iterations are therefore needed for each stitch wire to obtain the correct tension force. The iteration procedure is independent of the model and is only dependent on the designed tension force. It is also important to define local coordinate systems at each pole support to ensure correct boundary conditions; this is especially important in sections with curves where an incorrect description leads to erroneous boundary conditions, which in turn decreases the tension force in the

contact and messenger wire due to fixing the wires partly in the wrong direction. This issue does not occur on straight sections because the local coordinate system (CSYS) on the poles is the same as the global CSYS.

The contact wire, messenger wire, stitch wires and droppers are made using three-dimensional deformable beam elements. All wire components are modelled using Timoshenko beam elements, which is preferable for the numerical stability in this particular model, as described in (18), and the shortest wire element length used is 0.05 m. Every light steady arm is modelled with a spring and a point mass, and a point mass is included for every dropper clamp. Finally, a good damping description is very important, as shown in the recent numerical benchmark presented in (19). The Rayleigh damping coefficients estimated from the field measurements in Nåvik et al. (23) are used in this study. The mass and stiffness proportional damping coefficients are  $\alpha=0.062$  and  $\beta=6.13e-06$ , respectively.

The railway catenary section in the present study is located along the Dovre rail line and is named ‘‘Fokstua wire 21’’. This is a 1295 m long section of railway with a catenary system called System 20 C1 (24). The key properties of this section are presented in **Table 1** and **Table 2**.

**Table 1.** Key properties of the catenary section Fokstua wire 21

Section	Fokstua
Length	1295 m
Year of construction	2015
Catenary system	System 20 C1
Tension force in the contact wire	13 kN
Tension force in the messenger wire	13 kN
Cross-sectional area of the contact wire	120 mm <sup>2</sup>
Cross-sectional area of the messenger wire	70 mm <sup>2</sup>
Density of the wire material	8890 kg/m <sup>3</sup>
Wave propagation speed	435 km/h
Stitch wire (Yes/No)	Yes
Number of spans in contact with the pantograph	28

**Table 2.** Design properties of the Fokstua wire 21 span lengths and droppers

Span no.	1	2	3	4	5	6	7	8	9	10	11	12	13	14
Length [m]	44.27	44.98	45	49.45	45.51	45.65	44.88	45.03	45.1	44.54	45.28	44.76	45.34	48.87
No. of droppers	2	4	5	5	5	5	5	5	5	5	5	5	5	5
Span no.	15	16	17	18	19	20	21	22	23	24	25	26	27	28
Length [m]	49.02	48.77	50.8	52.23	51.95	52.1	51.87	52	52.06	42.48	39.95	30.99	39.54	42.55
No. of droppers	5	5	5	6	5	6	5	5	6	5	4	4	4	2

## 2.2 Pantograph

The numerical models of the pantograph used in this study have two degrees of freedom (DOF). The original mass-spring-damper system is obtained from the manufacturer, Schunk Nordiska AB, as presented in **Figure 1 a**). This model does not account for the fact that there are two collector strips with two attachment points each, four points in total, or the effect of the stagger. The model is therefore modified to account for these properties. The model includes two collector strips connected to the middle mass with two spring-dampers each. In addition, the original total pan head mass is divided into four, one in each attachment point to account for inertia. The new model is presented in **Figure 1 b**) and **Table 3**. The new model meets the requirements of EN 50318 (25).

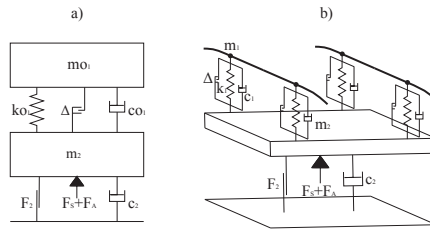


**Figure 1.** Schematics of the pantograph numerical models: a) the original model and b) the new model

**Table 3.** Parameters for the pantograph numerical models

Pantograph	WBL85	WBL88
$m_{01}$ [kg]	4.6	6.6
$m_1$ [kg]	1.15	1.65
$m_2$ [kg]	16.5	19.7
$ko_1$ [N/m]	6200	4400
$k_1$ [N/m]	1550	1100
$\Delta$ [m]	0.035	0.03
$co_1$ [Ns/m]	20	75.6
$c_1$ [Ns/m]	5	18.9
$c_2$ [Ns/m]	63.5	63.5
$F_2$ [N]	7	17
$F_S$ [N]	55	55
$F_A$ [N]	$0.0068*v(m/s)^2$	$0.0068*v(m/s)^2$

The movement of the train, or, more accurately, the movement of the pantograph, along the investigated sections must be described correctly. The pantograph tilts with the train in curves; due to the horizontal geometry of the contact wire, either stagger or curvature of the track results in the contact wire moving back and forth over the pan head. Two different CSYSs have been used to describe the true movement of the train as it runs along the rail line: one global CSYS (GCSYS) and one local CSYS (LCSYS) in the pantograph. The GCSYS is used to describe the position and rotation of the base of the train. Translational and rotational movements can be prescribed in and about three axes to ensure that the train can follow any track geometry. The train position also rotates to ensure that the pan head is perpendicular to the track at all times. Rotational movements about the longitudinal axis, accounting for the track cant, are introduced by applying the real cant angle described in the design of the rail track geometry. The LCSYS is mainly introduced to ensure that the pantograph moves correctly locally which means that it only experiences displacements along its normal axis and that the pan head can rotate about the longitudinal axis of the pantograph, as presented in the left of **Figure 2**, where arrows are used to illustrate the DOFs available in the local CSYS. An overview of both the GCSYS and the LCSYS is illustrated in the right of **Figure 2**.

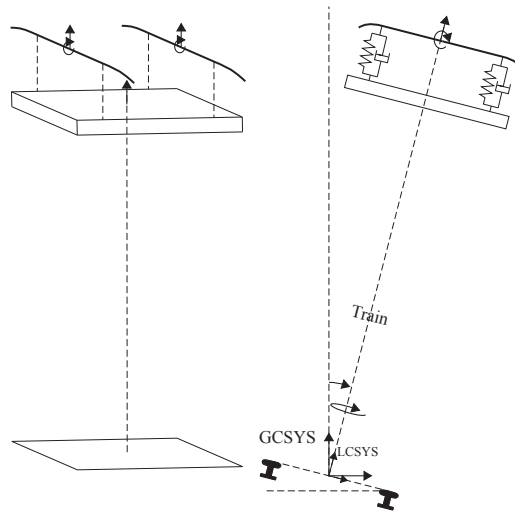


**Figure 2.** Illustration of the DOFs in the new pantograph model

### 2.3 Contact

One of the key properties in the catenary evaluation is the description of the contact between the pan head and the contact wire, which results in the important pantograph-catenary interaction. The contact force is dependent on several properties such as the catenary type and design, the pantograph type, the position of the contact wire on the pan heads, the horizontal geometry, and the train speed. Aerodynamic effects on the pantograph related to the train speed are included by adding a correction given by the pantograph manufacturer, as shown in **Table 3**. The importance of adding this is thoroughly shown in (26). Aerodynamic effects related to wind-induced vibration are not included, but their importance is acknowledged in (27).

This model uses a beam-to-beam general contact with hard contact that allows for separation after contact, and the penalty method is used as the constraint enforcement method, which is the default method for this type of contact in Abaqus (28). Ambrósio et al. (29) conclude that the penalty method is suitable for describing all relevant features of the pantograph-catenary interaction contact interface. Frictionless tangential behaviour is assumed.

### 2.4 Simulation of train passages

Simulating a train travelling along the numerical model is performed as a general nonlinear dynamic analysis and uses implicit time integration to calculate the dynamic response. The Hilbert-Hughes-Taylor  $\alpha$ -method is implemented in Abaqus for numerical integration, while Newton's method is used as the numerical technique for solving the nonlinear equilibrium equations. The default value for  $\alpha$  is -0.05 to ensure stable solutions with minimum influence on the dynamic system (28). The model uses an automatic incrementation with a maximum time increment size of 0.005 s and a sampling frequency of 200 Hz has been used for this study. An implicit scheme usually gives acceptable solutions with a time step that is typically one or two orders of magnitude larger than the time that an elastic wave uses to cross the smallest element in the model; in contrast, an explicit scheme is only conditionally stable with a step time limit equal to this time (28). At a wave propagation speed equal to the investigated section, which is 435 km/h, and an element length of 0.05 m, a time increment of 0.00041 s is needed to ensure a stable solution when using an explicit scheme.

### 2.5 Uncertainties/errors in geometric modelling

In the present study, the design values are used to create the numerical models, but it is important to acknowledge that these systems may have changed after they were mounted. This is shown by including both measured and designed contact wire heights from "Fokstua wire 21", as presented in **Figure 3**. This figure illustrates the possible differences between the design and actual geometry, and it clearly shows the variability in the existing structures. Due to these differences, it is easier to validate the geometry by validating the elasticity and pre-sag.

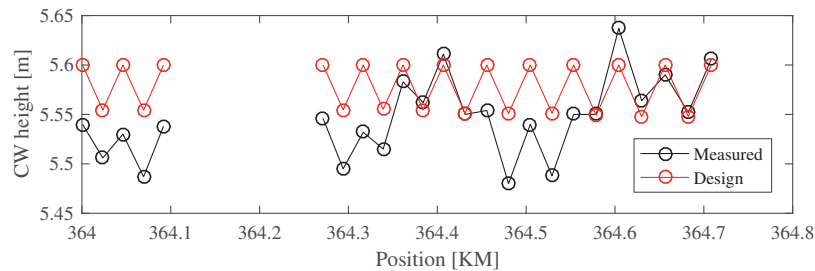


**Figure 3.** Measured and designed contact wire (CW) heights from Fokstua wire 21

The variability of each train passage, including variability in speed and static uplift force, is neither intended nor currently possible to include in the model. These variations are expected to cause deviations between the results from the model compared to the measured values.

### 3 Field measurements

In the present investigation, field measurements are used to ensure that the numerical model correctly represents the intended system rendering reliable results. Thus, several different field measurements are performed for comparison between reality and the models. The methods for obtaining these measurements are described in the following section.

#### 3.1 Accelerations

The Fokstua wire 21 was monitored with 10 three-axis wireless accelerometers at selected positions, as shown in **Figure 4**. All sampling is performed at 200 Hz, and the time series are 8 minutes long. The monitoring system used is presented in detail in Nāvik et al. (20). All measurements are sampled during normal scheduled train operation.

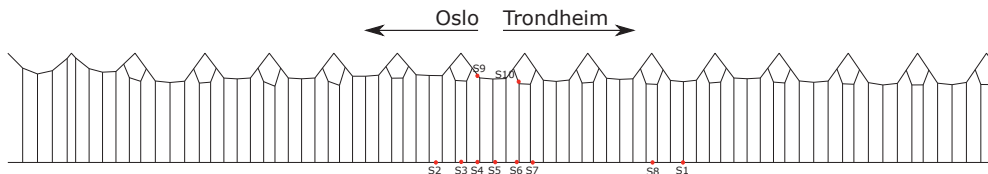


**Figure 4.** Instrumentation of the Fokstua wire 21, where the red dots illustrate the sensor positions

#### 3.2 Displacements

The estimated displacement time series used in this study is from close-range photogrammetry and from integrated acceleration time series; both methods are thoroughly described in (21). The camera setup for the photogrammetry is aimed at a target on sensor S1. The location of the sensor is in the middle of the span, as shown in **Figure 4**, and the distance between the camera setup and the target is approximately 6 metres. The details of the acceleration measurements are provided in section 3.1.

#### 3.3 Contact forces

All of the contact force field measurements are from scheduled routine measurements with the track and overhead line recording vehicle of the National Norwegian Rail Administration, Mermec Roger 1000 (30). The pantograph on the vehicle is a Schunk WBL85, and all sampling is performed every 0.5 metres along the tracks. The contact forces are measured directly from the force transducers; therefore, the inertia correction described in EN 50317:2012 is not included in the measurements.

#### 3.4 Geometry

The contact wire height and stagger are measured at selected positions along the sections and at positions along the track. The geometry is measured using a laser and a mount, as shown in **Figure 5**. The mount contains three parts: one beam that rests on the rails, one pole that is fastened normal to the beam and can slide along the length of the beam, and a mount on top of the pole for the laser. This setup ensures that the laser is normal to the rail, and thus, measuring the correct contact wire height. In addition, the stagger is read using a ruler on the beam.



**Figure 5.** Measuring contact wire heights on site

## **4 Results and discussion**

### **4.1 Parameters of the dynamic simulations**

All simulations are performed in the Fokstua wire 21 numerical model for a train running with a single pantograph. To calculate the total uplift force, the static force is set to 55 N, and the aerodynamic force is set according to the formula in the below equation:

$$F(v(\text{m/s})) = 55 + 0.0068 \times v^2 \text{ N}$$

Simulations are performed with two types of pantographs, WBL85 and WBL88, and with train speeds of 80 and 130 km/h, which give  $F = 58.36 \text{ N}$  and  $63.87 \text{ N}$ , respectively. Thus, four simulations are performed to represent the train speed on site that more or less falls between these two speeds and these two pantographs are the most commonly used at the investigated section.

### **4.2 Validation of the numerical model**

#### **4.2.1 Geometry and elasticity**

It is important to validate the geometry of the numerical models as well as the results they produce. This is challenging because, as mentioned, the geometry varies from span to span and from section to section and often differs considerably from the design, especially for older sections. Instead of comparing exact geometrical values, it is better to look at values such as pre-sag and elasticity. Pre-sag is easy to measure and compare, while elasticity is more time consuming to measure; however, calculated elasticity curves exist for most systems at some specified span length. The elasticity analyses are performed along the length of the numerical models by running a train along the section as a static rather than a dynamic step. A train speed of 80 km/h and a sampling rate of 200 Hz gave a spatial sampling of approximately 0.11 m. The elasticity curve is shown in **Figure 6**; the end spans are not displayed for clarity.

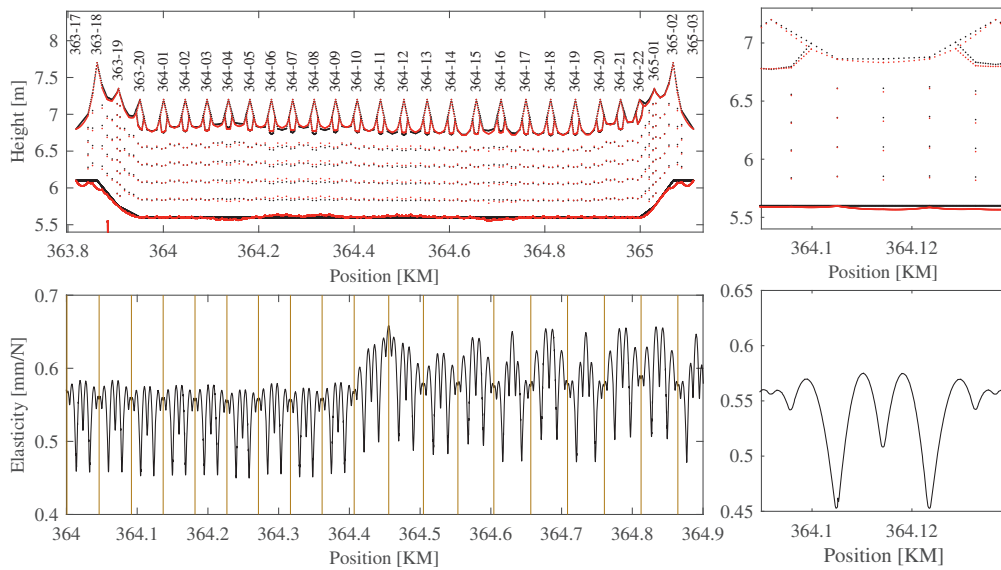


**Figure 6.** Vertical geometry and elasticity of the numerical model of the railway catenary section Fokstua wire 21. The elasticity of one 44.9 m long span is shown on the right for a clearer interpretation

The elasticity curve to the right in **Figure 6** is compared to an estimated elasticity curve for a 45 m long System 20 C1 span from Banverket's report (31). The elasticity from both of these analyses are approximately equal; the main difference is a slightly stiffer support for the developed numerical model. This difference could be due to the differences in the neighbouring span geometry and other properties.

#### 4.2.2 Dynamic comparison using acceleration and displacement results

A comparison of the measured and simulated displacement time series is performed to verify that the numerical model can produce a satisfactory time series. A displacement time series from the numerical simulation is compared with the displacement measurements from a train passage for further analysis. The numerical results are from an analysis using pantograph WBL88 running at 130 km/h, while the field results are from a typical passenger train passage that normally runs at the same speed of 130 km/h using WBL88. The field displacements are obtained as described in section 3.2. **Figure 7** shows that the displacement time series obtained from the numerical model describes the real response well, including both the displacement magnitude during the whole passage and the shape. The train pass the sampling position at approximately 127 s resulting in the maximum displacement seen in **Figure 7**.

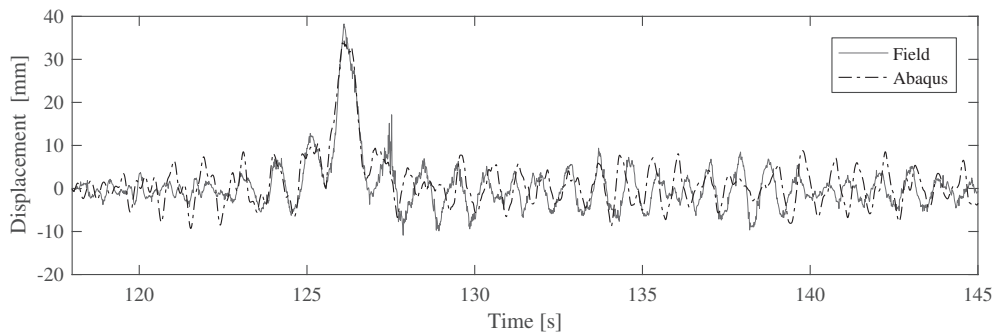


**Figure 7.** Displacement time series from position S1 with WBL88 at 130 km/h from a numerical simulation and a field displacement estimation for a passing passenger train. The train pass this position at approximately 127 s, as can be seen as a peak in the displacement time series

The frequency content in the dynamic process is also an important quantity that needs to be verified by comparing the results from the numerical simulation with pantograph WBL88 running at 130 km/h with the overall system

data from all measurements performed at the location, as described in (20,22). The numerical results are obtained by calculating the power spectral density (PSD) of the acceleration time series sampled at the corresponding locations to where the sensors were mounted during the field tests.

The mean PSD of the total setup is estimated by normalizing the sum of all sensor contributions by the number of sensors. Thus, a PSD is obtained that can be used to compare the energy magnitude of the process. The field results are obtained by the following procedure: 1) adding the PSDs from all time passages individually for each sensor and normalizing by the number of train passages, giving a mean PSD for each sensor and 2) adding these PSDs from each sensor together and dividing by the number of sensors to obtain a mean total PSD for the section. The result from each location then contributes equally to the section PSD. The frequency content is not expected to be identical due to the randomness in the natural process and because the results from the measured values are averages of many passages; each train passage may differ in terms of speed, pantograph type, wear of the collector strips, wind at the location at each point in time, and temperature. Therefore, the validation is performed through the similarities and the overall behaviour of the dynamic process. Many similar frequencies are expected, but with varying energy levels, as illustrated by the overall analysis in **Figure 8**, which clearly shows many similar frequencies with some deviating intensities. Furthermore, as expected, some frequency peaks are slightly shifted. Overall, though, taking the nature of the process into account, the comparison is satisfactory.

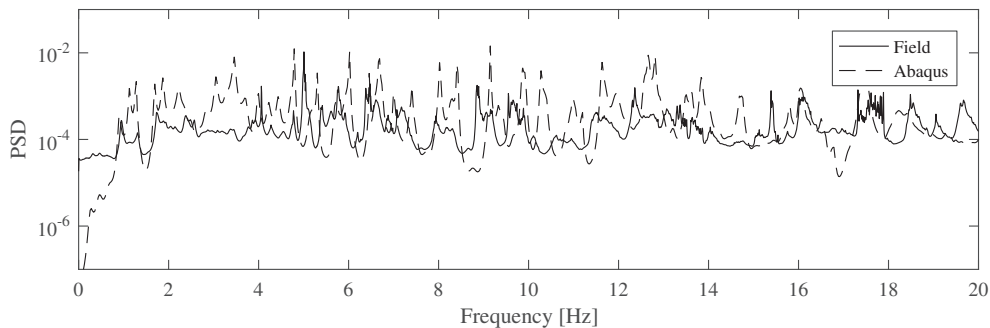


**Figure 8.** Comparison of the mean PSD from the numerical train passage using WBL88 at 130 km/h and the overall section PSD from the field measurements

### 4.3 Forces

#### 4.3.1 Measured forces and statistical values

First, it is important to establish the magnitude of the contact forces that are expected at the investigated section. The forces vary from train to train, so the contact forces measured over the past five years (measured approximately twice a year) are therefore used to evaluate the mean and standard deviations of the forces and the force variation over the years, as presented in **Figure 9**. The two most recent measurements were taken after a total update of the catenary system; the system changed from two System 35 sections to one System 20 C1 section. The numerical simulation results from an analysis taking pantograph WBL85 running at 130 km/h, denoted “Abaqus” in **Figure 9**, shows that the obtained values are within the expected range. The force varies among the measured train passages, which illustrates the expected random nature of the total process as these measurements are from the same train with the same WBL85 pantograph. This result demonstrates the difficulty of isolating one parameter in practical field testing to set specific values for expected contact forces.

The contact force measurements are from four different positions, and the two lower subfigures in **Figure 9** demonstrate the importance of studying the positions separately. In previous studies, the contact force has been split into rear and front collector force (32,33). In general, the front collector strip clearly experiences a higher contact force than the rear one. The magnitude difference has some variations, which highlights the difficulty of estimating this parameter. The variation between the forces on the front and rear collector strip is clearly not captured by the model, which is natural due to the lack of rotational stiffness perpendicular to the travel direction in the numerical model. A frequency study of the contact forces cannot be used for validation in this study because the sampling is spatial.



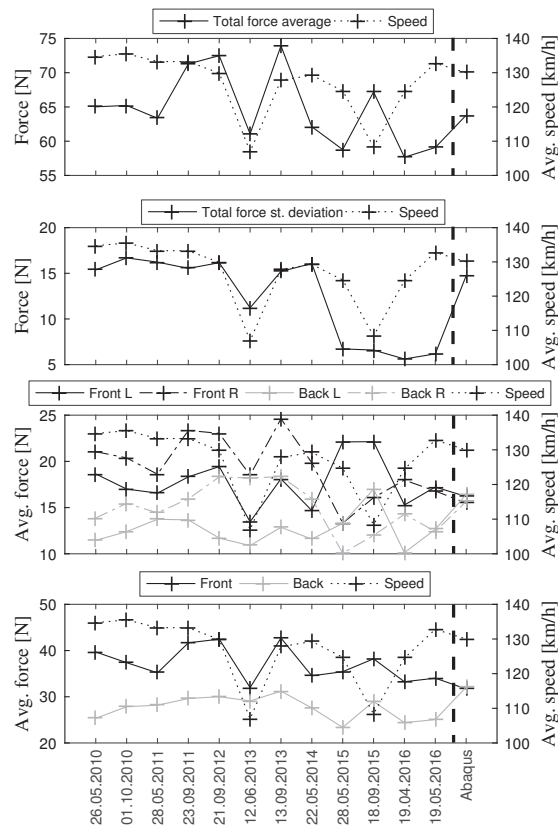


**Figure 9.** Contact force parameters extracted from twelve measurement runs with Roger 1000 and one numerical simulation

#### 4.3.2 Force variation in output and filtering

The methods used to predict and post-process the contact forces are very important. **Figure 10** shows three different contact force time series, all taken from the same analysis but estimated differently: 1) the force in the actual interface between the contact wire and the collectors strips; 2) the forces from the connectors connecting the pan head to the pan arm; and 3) the previously listed force with the inertia correction described in (14). The differences between these three forces indicate the variation in contact force estimations depending only on how the force is estimated.

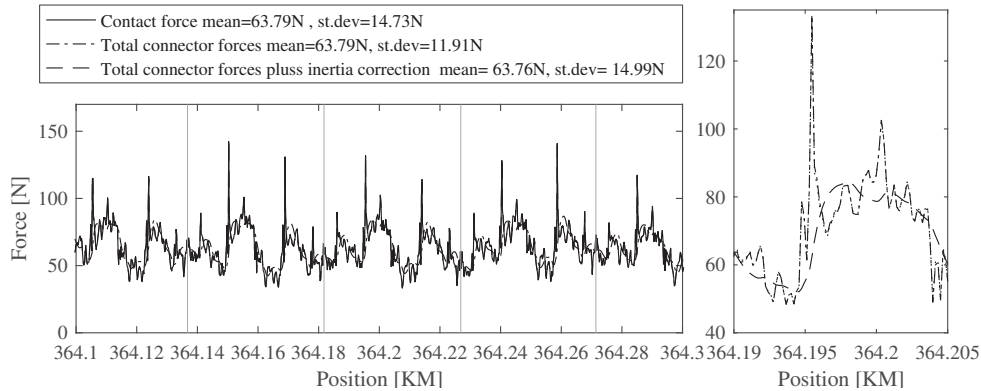


**Figure 10.** Contact forces from the numerical analysis at 130 km/h with pantograph WBL88. The right part of the figure shows the differences between the connector forces and contact forces on a small part of the section

To further study this effect, the results from the four different numerical simulations, WBL85 and WBL88 pantographs at 80 and 130 km/h, are listed in **Table 4**. This was chosen for presenting a range of different forces. First, “Contact force” is the force measured at the interface between the two collector strips in the model and the contact wire with 200 Hz sampling. Second, “Contact force, filter @ 20 Hz” is calculated as specified in (14), filtering the contact force at 20 Hz. Third, “Connector forces” is the total forces acting in the connectors between the collector strips and the pan arm. Fourth, “Connector forces and accelerations” is the sum of the forces acting in the connectors as well as the inertia correction from (14). Finally, “Connector forces and accelerations, filter @ 20 Hz” is the forces that (14) states should be computed.

In general, the mean values of the contact forces are the same for all of the methods used; the other parameters vary with the prediction method. The unfiltered contact forces and the inertia corrected connector forces give approximately the same results. In general, the inertia corrected forces have a slightly higher standard deviation and maximum values than the contact forces. A significant difference is shown when comparing these two forces to the connector forces. Compared with the unfiltered contact force, the 20 Hz filtered contact force for “Analysis 4” gives a 19% lower standard deviation, a 32% decrease in the maximum value, and a 57% increase in the minimum value. The same trends are clearly shown for all analyses and increase with speed.

**Table 4.** Tabulated results from the numerical analyses performed on Fokstua wire 21

Analysis	1	2	3	4
Pantograph type	WBL85	WBL88	WBL85	WBL88
Speed (km/h)	80	80	130	130
Max. displacement at S1 [mm]	26.38	26.95	34.53	34.57
1. Contact force, mean [N]	58.39	58.39	63.82	63.79
2. Contact force, filter @ 20 Hz, mean [N]	58.39	58.39	63.82	63.79
3. Connector forces, mean [N]	58.37	58.36	63.81	63.79
4. Connector forces + inertia correction, mean [N]	58.37	58.37	63.80	63.76
5. Connector forces + inertia correction, filter @ 20 Hz, mean [N]	58.37	58.37	63.79	63.76
1. Contact force, st. dev. [N]	7.12	7.32	13.93	14.73
2. Contact force, filter @ 20 Hz, st. dev. [N]	6.89	6.97	12.58	13.17
3. Connector forces, st. dev. [N]	6.68	6.45	12.25	11.91
4. Connector forces + inertia correction, st. dev. [N]	7.18	7.41	14.13	14.99
5. Connector forces + inertia correction, filter @ 20 Hz, st. dev. [N]	6.95	7.05	12.77	13.42
1. Contact force, min [N]	34.21	35.19	22.34	21.02
2. Contact force, filter @ 20 Hz, min [N]	34.37	37.46	26.54	25.85
3. Connector forces, min [N]	30.94	35.64	27.82	33.05
4. Connector forces + inertia correction, min [N]	33.53	35.20	22.39	20.89
5. Connector forces + inertia correction, filter @ 20 Hz, min [N]	33.69	36.67	26.57	25.76
1. Contact force, max [N]	85.40	90.00	148.54	154.88
2. Contact force, filter @ 20 Hz, max [N]	82.02	82.85	111.65	105.12
3. Connector forces, max [N]	81.74	81.22	108.77	104.98
4. Connector forces + inertia correction, max [N]	86.24	90.97	150.27	156.56
5. Connector forces + inertia correction, filter @ 20 Hz, max [N]	81.70	83.81	112.04	106.40

A more thorough study on the effect of filtering on the output contact forces is also conducted because of the substantial effects due to filtering on the predicted contact force. The time series from a 130 km/h train passage with a WBL88 pantograph is studied, and the contact force time series is filtered with different low-pass cut-off frequency limits. The selected parameters of this study are the mean, standard deviation, the minimum, and maximum of the contact force. The filtering shows clear effects on the contact force time series. The mean value is approximately unchanged, as expected, but the filtering significantly affects all other parameters. As the filter is set to higher frequencies, the standard deviation and the maximum value increase, while the minimum decreases. The relative change between a 20 Hz cut-off and an 80 Hz cut-off is an 11% increase in standard deviation, a 36% increase in maximum value, and 19% decrease in minimum value. The contact force parameters are presented in **Figure 11**, and the values relative to those found at a 20 Hz cut-off frequency are presented in **Figure 12**.

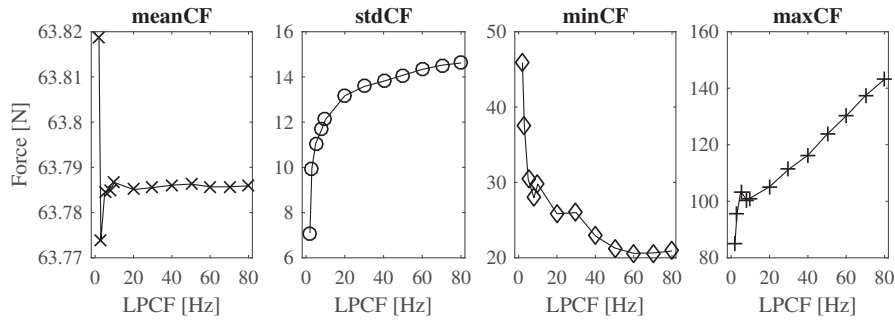


**Figure 11.** Mean, standard deviation, minimum and maximum of the contact force time series for a 130 km/h train passage with WBL88 pantograph filtered at different low-pass cut-off frequencies (LPCF)

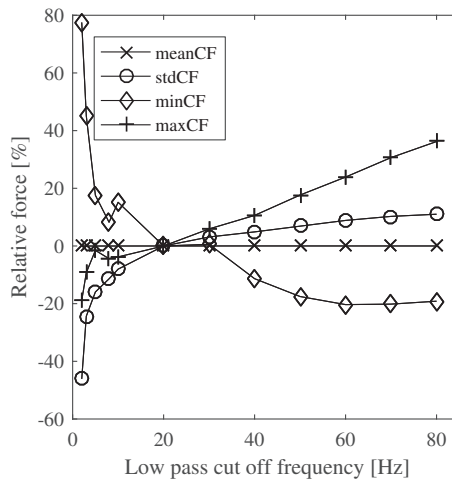


**Figure 12.** Relative changes in the mean, standard deviation, minimum and maximum of the contact force time series related to the low-pass cut-off frequency limit; the values at 20 Hz are set to 0%

## 5 Conclusion

This paper investigates the variation in predicting the pantograph-catenary interaction contact force. The investigation analyses both field measurements and numerical simulations. First, the numerical model is validated by comparing the geometry, elasticity, pre-sag, displacement time series, frequency content of the acceleration time series and the statistical contact force values with field measurements. In addition, a description of the numerical model is included. Second, the contact forces from field measurements are studied to demonstrate the variation among individual train passages. In addition, the variation between the front and rear collector strips are shown to be varying and substantial. Third, the variation in the contact force prediction is studied using numerical model results. The standard deviation is stated to be the most important quantity for defining the contact quality (34), which is generally true when regarding the contact quality along a whole section. However, the maximum and minimum values can help identify point wear, loss of contact, and other local effects that are very important

for the local contact quality and for lifetime estimations. The results of this study indicate that the maximum and minimum contact force are more sensitive to filtering than the standard deviation, which in turn is more sensitive than the mean value. The mean value is shown to be constant regardless of post-processing for all practical purposes. Comparing the results from an 80 Hz cut-off to the 20 Hz suggested in the standard EN 50317:2012 shows, for one of the analyses, an 11% increase in the standard deviation, a 36% increase in the maximum value and a 19% decrease in the minimum value. These results demonstrate the need for increasing the cut-off frequency limit to study local effects, such as point wear.

#### Acknowledgements

The authors are grateful to Jernbaneverket, the Norwegian National Rail Administration, for their assistance with field measurements and the funding of this research.

#### Bibliography

- [1] Poetsch G, Evans J, Meisinger R, et al. Pantograph/catenary dynamics and control. *Veh Syst Dyn.* 1997;28:159–195. doi: 10.1080/00423119708969353.
- [2] Kiessling F, Puschmann R, Schmieder A, et al. Contact lines for electric railways : planning, design, implementation, maintenance. 2nd ed. Erlangen: Publicis Publishing. 2012.
- [3] Wu TX, Brennan MJ. Dynamic stiffness of a railway overhead wire system and its effect on pantograph–catenary system dynamics. *J Sound Vib.* 1999;219:483–502. doi: 10.1006/jsvi.1998.1869.
- [4] Alberto A, Benet J, Arias E, et al. A high performance tool for the simulation of the dynamic pantograph–catenary interaction. *Math Comput. Simul.* 2008;79:652–667.
- [5] Mei G, Zhang W, Zhao H, et al. A hybrid method to simulate the interaction of pantograph and catenary on overlap span. *Veh Syst Dyn.* 2006;44:571–580:571–80. doi: 10.1080/00423110600875559.
- [6] Lee JH, Park TW, Oh HK, et al. Analysis of dynamic interaction between catenary and pantograph with experimental verification and performance evaluation in new high-speed line. *Veh Syst Dyn.* 2015;53:1117–1134. doi: 10.1080/00423114.2015.1025797.
- [7] Gerstmayr J, Shabana AA. Analysis of thin beams and cables using the absolute nodal Co-ordinate formulation. *Nonlin Dyn.* 2006;45:109–130. doi: 10.1007/s11071-006-1856-1.
- [8] Sanchez-Rebollo C, Jimenez-Octavio JR, Carnicero A. Active control strategy on a catenary–pantograph validated model. *Veh Syst Dyn.* 2013;51:554–569. doi: 10.1080/00423114.2013.764455.
- [9] Pappalardo CM, Patel MD, Tinsley B, et al. Contact force control in multibody pantograph/catenary systems. *Proc Inst Mech Eng E J Multi-Body Dyn.* 2015:1–22. doi: 10.1177/1464419315604756.
- [10] Ikeda M, Nagasaka S, Usuda T. A precise contact force measuring method for overhead catenary system. *Proceedings of World Congress on Railway Research.* Köln: UIC; 2001; Available from: <http://www.railway-research.org/IMG/pdf/015.pdf>.
- [11] Usuda T. The pantograph contact Force measurement method in overhead catenary system. *Proceedings of the 8th World Congress on Railway Research.* Seoul. South Korea: UIC; 2008. Available from: <http://www.railway-research.org/IMG/pdf/s.1.4.3.4.pdf>.
- [12] Zhang W, Shen Z, Zeng J. Study on dynamics of coupled systems in high-speed trains. *Veh Syst Dyn.* 2013;51(7):966–1016. doi: 10.1080/00423114.2013.798421.
- [13] Bucca G, Collina A. Electromechanical interaction between carbon-based pantograph strip and copper contact wire: A heuristic wear model. *Tribol Int.* 2015;92:47–56. doi: 10.1016/j.triboint.2015.05.019.
- [14] NEK. NEK EN 50317:2012 Railway applications - Current collection systems - Requirements for and validation of measurements of the dynamic interaction between pantograph and overhead contact line. 2012.
- [15] Ambrósio J, Pombo J, Rauter F, et al. A memory based communication in the co-simulation of multibody and finite element codes for pantograph-catenary interaction simulation multibody dynamics. In: Bottasso CL, editor. *Multibody dynamics computational methods and applications.* Netherlands: Springer Verlag; 2009. p. 231–252.

- [16] Collina A, Bruni S. Numerical simulation of pantograph-overhead equipment interaction. *Veh Syst Dyn.* 2002;38:261–291. doi: 10.1076/vesd.38.4.261.8286.
- [17] Nåvik P, Rønquist A, Stichel S. The use of dynamic response to evaluate and improve the optimization of existing soft railway catenary systems for higher speeds. *Proc Inst Mech Eng Part F J Rail Rapid Transit.* 2015;230:1388–96.
- [18] Rønquist A, Nåvik P. Dynamic assessment of existing soft catenary systems using modal analysis to explore higher train velocities: a case study of a Norwegian contact line system. *Veh Syst Dyn.* 2015;53:756–774. doi: 10.1080/00423114.2015.1013040.
- [19] Bruni S, Ambrosio J, Carnicero A, et al. The results of the pantograph–catenary interaction benchmark. *Veh Syst Dyn.* 2015;53:412–435. doi: 10.1080/00423114.2014.953183.
- [20] Nåvik P, Rønquist A, Stichel S. A wireless railway catenary structural monitoring system: full-scale case study. *Case stud. Struct Eng.* 2016;6:22–30.
- [21] Frøseth GT, Nåvik P, Rønquist A. Close Range Photogrammetry for Measuring the Response of a Railway Catenary System. *Proceedings of the Third International Conference on Railway Technology: Research, Development and Maintenance*, ed. J. Pombo. Civil-Comp Press, Stirlingshire, UK, Paper 102. 2016. doi: 10.4203/ccp.110.102.
- [22] Rønquist A, Nåvik P. Exploring Dynamic Behaviour of Soft Catenaries subject to Regular Loading using Full Scale Measurements. *Proceedings of the Third International Conference on Railway Technology: Research, Development and Maintenance*, ed. J. Pombo. Civil-Comp Press, Stirlingshire, UK, Paper 101. 2016. doi: 10.4203/ccp.110.101.
- [23] Nåvik P, Rønquist A, Stichel S. Identification of system damping in railway catenary wire systems from full-scale measurements. *Eng Struct.* 2016;113:71–78. doi: 10.1016/j.engstruct.2016.01.031.
- [24] Mekanisk systembeskrivelse av kontaktledningsanlegg [Internet]. The Norwegian National Rail Administration; [cited 2013 Oct 2]. Available from: [http://www.jernbanekompetanse.no/wiki/Mekanisk\\_systembeskrivelse\\_av\\_kontaktledningsanlegg](http://www.jernbanekompetanse.no/wiki/Mekanisk_systembeskrivelse_av_kontaktledningsanlegg).
- [25] NEK. NEK EN 50318:2002 Railway applications - Current collection systems - Validation of simulation of the dynamic interaction between pantograph and overhead contact line. 2002.
- [26] Carnevale M, Facchinetti A, Maggiori L, et al. Computational fluid dynamics as a means of assessing the influence of aerodynamic forces on the mean contact force acting on a pantograph. *Proc Inst Mech Eng Part F J Rail Rapid Transit.* 2016;230:1698-1713. doi: 10.1177/0954409715606748.
- [27] Song Y, Liu Z, Wang H, et al. Nonlinear analysis of wind-induced vibration of high-speed railway catenary and its influence on pantograph–catenary interaction. *Veh Syst Dyn.* 2016;54:723–747. doi: 10.1080/00423114.2016.1156134.
- [28] ABAQUS 6.14 Theory Manual. Dassault Systèmes; 2014
- [29] Ambrósio J, Pombo J, Pereira M, et al. Recent developments in pantograph-catenary interaction modelling and analysis. *Int J Railw Technol.* 2012;1:249–278. doi: 10.4203/ijrt.1.1.12.
- [30] ROGER 1000 [Internet]. [cited 2016 Jun 16]. Available from: <http://www.mermecgroup.com/inspect/recording-cars/104/roger-1000.php>.
- [31] BANVERKET. Analys av kontaktledningsdynamik vid flera verksamma strömvagtare Del 1, BKL 02/10. Banverket 2004.
- [32] Carnevale M, Collina A. Processing of collector acceleration data for condition-based monitoring of overhead lines. *Proc Inst Mech Eng Part F J Rail Rapid Transit.* 2016;230:472–85. doi: 10.1177/0954409714545637
- [33] Zhou N, Zhang W, Li R. Dynamic performance of a pantograph-catenary system with the consideration of the appearance characteristics of contact surfaces. *J Zhejiang Univ Sci A.* 2011;12:913–920. doi: 10.1631/jzus.A11GT015.
- [34] Ambrósio J, Pombo J, Pereira M. Optimization of high-speed railway pantographs for improving pantograph-catenary contact. *Theor Appl Mech Lett.* 2013;3:013006. doi:10.1063/2.1301306.

**DEPARTMENT OF STRUCTURAL ENGINEERING  
NORWEGIAN UNIVERSITY OF SCIENCE AND TECHNOLOGY**

N-7491 TRONDHEIM, NORWAY  
Telephone: +47 73 59 47 00    Telefax: +47 73 59 47 01

"Reliability Analysis of Structural Systems using Nonlinear Finite Element Methods",  
C. A. Holm, 1990:23, ISBN 82-7119-178-0.

"Uniform Stratified Flow Interaction with a Submerged Horizontal Cylinder",  
Ø. Arntsen, 1990:32, ISBN 82-7119-188-8.

"Large Displacement Analysis of Flexible and Rigid Systems Considering  
Displacement-Dependent Loads and Nonlinear Constraints",  
K. M. Mathisen, 1990:33, ISBN 82-7119-189-6.

"Solid Mechanics and Material Models including Large Deformations",  
E. Levold, 1990:56, ISBN 82-7119-214-0, ISSN 0802-3271.

"Inelastic Deformation Capacity of Flexurally-Loaded Aluminium Alloy Structures",  
T. Welo, 1990:62, ISBN 82-7119-220-5, ISSN 0802-3271.

"Visualization of Results from Mechanical Engineering Analysis",  
K. Aarnes, 1990:63, ISBN 82-7119-221-3, ISSN 0802-3271.

"Object-Oriented Product Modeling for Structural Design",  
S. I. Dale, 1991:6, ISBN 82-7119-258-2, ISSN 0802-3271.

"Parallel Techniques for Solving Finite Element Problems on Transputer Networks",  
T. H. Hansen, 1991:19, ISBN 82-7119-273-6, ISSN 0802-3271.

"Statistical Description and Estimation of Ocean Drift Ice Environments",  
R. Korsnes, 1991:24, ISBN 82-7119-278-7, ISSN 0802-3271.

"Properties of concrete related to fatigue damage: with emphasis on high strength  
concrete",  
G. Petkovic, 1991:35, ISBN 82-7119-290-6, ISSN 0802-3271.

"Turbidity Current Modelling",  
B. Brørs, 1991:38, ISBN 82-7119-293-0, ISSN 0802-3271.

"Zero-Slump Concrete: Rheology, Degree of Compaction and Strength. Effects of  
Fillers as Part Cement-Replacement",  
C. Sørensen, 1992:8, ISBN 82-7119-357-0, ISSN 0802-3271.

"Nonlinear Analysis of Reinforced Concrete Structures Exposed to Transient Loading",  
K. V. Høiseeth, 1992:15, ISBN 82-7119-364-3, ISSN 0802-3271.

"Finite Element Formulations and Solution Algorithms for Buckling and Collapse  
Analysis of Thin Shells",  
R. O. Bjærum, 1992:30, ISBN 82-7119-380-5, ISSN 0802-3271.

"Response Statistics of Nonlinear Dynamic Systems",  
J. M. Johnsen, 1992:42, ISBN 82-7119-393-7, ISSN 0802-3271.

"Digital Models in Engineering. A Study on why and how engineers build and operate  
digital models for decision support",  
J. Høyte, 1992:75, ISBN 82-7119-429-1, ISSN 0802-3271.

"Sparse Solution of Finite Element Equations",  
A. C. Damhaug, 1992:76, ISBN 82-7119-430-5, ISSN 0802-3271.

"Some Aspects of Floating Ice Related to Sea Surface Operations in the Barents Sea",  
S. Løset, 1992:95, ISBN 82-7119-452-6, ISSN 0802-3271.

"Modelling of Cyclic Plasticity with Application to Steel and Aluminium Structures",  
O. S. Hopperstad, 1993:7, ISBN 82-7119-461-5, ISSN 0802-3271.

"The Free Formulation: Linear Theory and Extensions with Applications to Tetrahedral  
Elements  
with Rotational Freedoms",  
G. Skeie, 1993:17, ISBN 82-7119-472-0, ISSN 0802-3271.

"Høyfast betongs motstand mot piggdekkslitasje. Analyse av resultater fra prøving i  
Veisliter'n",  
T. Tveter, 1993:62, ISBN 82-7119-522-0, ISSN 0802-3271.

"A Nonlinear Finite Element Based on Free Formulation Theory for Analysis of  
Sandwich Structures",  
O. Aamlid, 1993:72, ISBN 82-7119-534-4, ISSN 0802-3271.

"The Effect of Curing Temperature and Silica Fume on Chloride Migration and Pore  
Structure of High Strength Concrete",  
C. J. Hauck, 1993:90, ISBN 82-7119-553-0, ISSN 0802-3271.

"Failure of Concrete under Compressive Strain Gradients",  
G. Markeset, 1993:110, ISBN 82-7119-575-1, ISSN 0802-3271.

"An experimental study of internal tidal amphidromes in Vestfjorden",  
J. H. Nilsen, 1994:39, ISBN 82-7119-640-5, ISSN 0802-3271.

"Structural analysis of oil wells with emphasis on conductor design",  
H. Larsen, 1994:46, ISBN 82-7119-648-0, ISSN 0802-3271.

"Adaptive methods for non-linear finite element analysis of shell structures",  
K. M. Okstad, 1994:66, ISBN 82-7119-670-7, ISSN 0802-3271.

"On constitutive modelling in nonlinear analysis of concrete structures",  
O. Fyrrileiv, 1994:115, ISBN 82-7119-725-8, ISSN 0802-3271.

"Fluctuating wind load and response of a line-like engineering structure with emphasis  
on motion-induced wind forces",  
J. Bogunovic Jakobsen, 1995:62, ISBN 82-7119-809-2, ISSN 0802-3271.

"An experimental study of beam-columns subjected to combined torsion, bending and  
axial actions",  
A. Aalberg, 1995:66, ISBN 82-7119-813-0, ISSN 0802-3271.

"Scaling and cracking in unsealed freeze/thaw testing of Portland cement and silica  
fume concretes",  
S. Jacobsen, 1995:101, ISBN 82-7119-851-3, ISSN 0802-3271.

"Damping of water waves by submerged vegetation. A case study of laminaria  
hyperborea",  
A. M. Dubi, 1995:108, ISBN 82-7119-859-9, ISSN 0802-3271.

"The dynamics of a slope current in the Barents Sea",  
Sheng Li, 1995:109, ISBN 82-7119-860-2, ISSN 0802-3271.

"Modellering av delmaterialenes betydning for betongens konsistens",  
Ernst Mørtzell, 1996:12, ISBN 82-7119-894-7, ISSN 0802-3271.

"Bending of thin-walled aluminium extrusions",  
Birgit Søvik Opheim, 1996:60, ISBN 82-7119-947-1, ISSN 0802-3271.

"Material modelling of aluminium for crashworthiness analysis",  
Torodd Berstad, 1996:89, ISBN 82-7119-980-3, ISSN 0802-3271.

"Estimation of structural parameters from response measurements on submerged  
floating tunnels",  
Rolf Magne Larssen, 1996:119, ISBN 82-471-0014-2, ISSN 0802-3271.

"Numerical modelling of plain and reinforced concrete by damage mechanics",  
Mario A. Polanco-Loria, 1997:20, ISBN 82-471-0049-5, ISSN 0802-3271.

"Nonlinear random vibrations - numerical analysis by path integration methods",  
Vibeke Moe, 1997:26, ISBN 82-471-0056-8, ISSN 0802-3271.



“Numerical prediction of vortex-induced vibration by the finite element method”,  
Joar Martin Dalheim, 1997:63, ISBN 82-471-0096-7, ISSN 0802-3271.

“Time domain calculations of buffeting response for wind sensitive structures”,  
Ketil Aas-Jakobsen, 1997:148, ISBN 82-471-0189-0, ISSN 0802-3271.

"A numerical study of flow about fixed and flexibly mounted circular cylinders",  
Trond Stokka Meling, 1998:48, ISBN 82-471-0244-7, ISSN 0802-3271.

“Estimation of chloride penetration into concrete bridges in coastal areas”,  
Per Egil Steen, 1998:89, ISBN 82-471-0290-0, ISSN 0802-3271.

“Stress-resultant material models for reinforced concrete plates and shells”,  
Jan Arve Øverli, 1998:95, ISBN 82-471-0297-8, ISSN 0802-3271.

“Chloride binding in concrete. Effect of surrounding environment and concrete composition”,  
Claus Kenneth Larsen, 1998:101, ISBN 82-471-0337-0, ISSN 0802-3271.

“Rotational capacity of aluminium alloy beams”,  
Lars A. Moen, 1999:1, ISBN 82-471-0365-6, ISSN 0802-3271.

“Stretch Bending of Aluminium Extrusions”,  
Arild H. Clausen, 1999:29, ISBN 82-471-0396-6, ISSN 0802-3271.

“Aluminium and Steel Beams under Concentrated Loading”,  
Tore Tryland, 1999:30, ISBN 82-471-0397-4, ISSN 0802-3271.

"Engineering Models of Elastoplasticity and Fracture for Aluminium Alloys",  
Odd-Geir Lademo, 1999:39, ISBN 82-471-0406-7, ISSN 0802-3271.

"Kapasitet og duktilitet av dybelforbindelser i trekonstruksjoner",  
Jan Siem, 1999:46, ISBN 82-471-0414-8, ISSN 0802-3271.

“Etablering av distribuert ingeniørarbeid; Teknologiske og organisatoriske erfaringer fra en norsk ingeniørbedrift”,  
Lars Line, 1999:52, ISBN 82-471-0420-2, ISSN 0802-3271.

“Estimation of Earthquake-Induced Response”,  
Símon Ólafsson, 1999:73, ISBN 82-471-0443-1, ISSN 0802-3271.

“Coastal Concrete Bridges: Moisture State, Chloride Permeability and Aging Effects”  
Ragnhild Holen Relling, 1999:74, ISBN 82-471-0445-8, ISSN 0802-3271.

”Capacity Assessment of Titanium Pipes Subjected to Bending and External Pressure”,  
Arve Bjørset, 1999:100, ISBN 82-471-0473-3, ISSN 0802-3271.

- “Validation of Numerical Collapse Behaviour of Thin-Walled Corrugated Panels”,  
Håvar Ilstad, 1999:101, ISBN 82-471-0474-1, ISSN 0802-3271.
- “Strength and Ductility of Welded Structures in Aluminium Alloys”,  
Mirosław Matusiak, 1999:113, ISBN 82-471-0487-3, ISSN 0802-3271.
- “Thermal Dilation and Autogenous Deformation as Driving Forces to Self-Induced Stresses in High Performance Concrete”,  
Øyvind Bjøntegaard, 1999:121, ISBN 82-7984-002-8, ISSN 0802-3271.
- “Some Aspects of Ski Base Sliding Friction and Ski Base Structure”,  
Dag Anders Moldestad, 1999:137, ISBN 82-7984-019-2, ISSN 0802-3271.
- "Electrode reactions and corrosion resistance for steel in mortar and concrete",  
Roy Antonsen, 2000:10, ISBN 82-7984-030-3, ISSN 0802-3271.
- "Hydro-Physical Conditions in Kelp Forests and the Effect on Wave Damping and Dune Erosion. A case study on Laminaria Hyperborea",  
Stig Magnar Løvås, 2000:28, ISBN 82-7984-050-8, ISSN 0802-3271.
- "Random Vibration and the Path Integral Method",  
Christian Skaug, 2000:39, ISBN 82-7984-061-3, ISSN 0802-3271.
- "Buckling and geometrical nonlinear beam-type analyses of timber structures",  
Trond Even Eggen, 2000:56, ISBN 82-7984-081-8, ISSN 0802-3271.
- ”Structural Crashworthiness of Aluminium Foam-Based Components”,  
Arve Grønsund Hanssen, 2000:76, ISBN 82-7984-102-4, ISSN 0809-103X.
- “Measurements and simulations of the consolidation in first-year sea ice ridges, and some aspects of mechanical behaviour”,  
Knut V. Høyland, 2000:94, ISBN 82-7984-121-0, ISSN 0809-103X.
- ”Kinematics in Regular and Irregular Waves based on a Lagrangian Formulation”,  
Svein Helge Gjosund, 2000-86, ISBN 82-7984-112-1, ISSN 0809-103X.
- ”Self-Induced Cracking Problems in Hardening Concrete Structures”,  
Daniela Bosnjak, 2000-121, ISBN 82-7984-151-2, ISSN 0809-103X.
- "Ballistic Penetration and Perforation of Steel Plates",  
Tore Børvik, 2000:124, ISBN 82-7984-154-7, ISSN 0809-103X.
- "Freeze-Thaw resistance of Concrete. Effect of: Curing Conditions, Moisture Exchange and Materials",  
Terje Finnerup Rønning, 2001:14, ISBN 82-7984-165-2, ISSN 0809-103X

"Structural behaviour of post tensioned concrete structures. Flat slab. Slabs on ground",  
Steinar Trygstad, 2001:52, ISBN 82-471-5314-9, ISSN 0809-103X.

"Slipforming of Vertical Concrete Structures. Friction between concrete and slipform panel",  
Kjell Tore Fosså, 2001:61, ISBN 82-471-5325-4, ISSN 0809-103X.

"Some numerical methods for the simulation of laminar and turbulent incompressible flows",  
Jens Holmen, 2002:6, ISBN 82-471-5396-3, ISSN 0809-103X.

"Improved Fatigue Performance of Threaded Drillstring Connections by Cold Rolling",  
Steinar Kristoffersen, 2002:11, ISBN: 82-421-5402-1, ISSN 0809-103X.

"Deformations in Concrete Cantilever Bridges: Observations and Theoretical Modelling",  
Peter F. Takács, 2002:23, ISBN 82-471-5415-3, ISSN 0809-103X.

"Stiffened aluminium plates subjected to impact loading",  
Hilde Giæver Hildrum, 2002:69, ISBN 82-471-5467-6, ISSN 0809-103X.

"Full- and model scale study of wind effects on a medium-rise building in a built up area",  
Jónas Thór Snæbjörnsson, 2002:95, ISBN82-471-5495-1, ISSN 0809-103X.

"Evaluation of Concepts for Loading of Hydrocarbons in Ice-infested water",  
Arnor Jensen, 2002:114, ISBN 82-417-5506-0, ISSN 0809-103X.

"Numerical and Physical Modelling of Oil Spreading in Broken Ice",  
Janne K. Økland Gjølsten, 2002:130, ISBN 82-471-5523-0, ISSN 0809-103X.

"Diagnosis and protection of corroding steel in concrete",  
Franz Pruckner, 20002:140, ISBN 82-471-5555-4, ISSN 0809-103X.

"Tensile and Compressive Creep of Young Concrete: Testing and Modelling",  
Dawood Atrushi, 2003:17, ISBN 82-471-5565-6, ISSN 0809-103X.

"Rheology of Particle Suspensions. Fresh Concrete, Mortar and Cement Paste with Various Types of Lignosulfonates",  
Jon Elvar Wallevik, 2003:18, ISBN 82-471-5566-4, ISSN 0809-103X.

"Oblique Loading of Aluminium Crash Components",  
Aase Reyes, 2003:15, ISBN 82-471-5562-1, ISSN 0809-103X.

"Utilization of Ethiopian Natural Pozzolans",  
Surafel Ketema Desta, 2003:26, ISSN 82-471-5574-5, ISSN:0809-103X.

“Behaviour and strength prediction of reinforced concrete structures with discontinuity regions”, Helge Brå, 2004:11, ISBN 82-471-6222-9, ISSN 1503-8181.

“High-strength steel plates subjected to projectile impact. An experimental and numerical study”, Sumita Dey, 2004:38, ISBN 82-471-6282-2 (printed version), ISBN 82-471-6281-4 (electronic version), ISSN 1503-8181.

“Alkali-reactive and inert fillers in concrete. Rheology of fresh mixtures and expansive reactions.”

Bård M. Pedersen, 2004:92, ISBN 82-471-6401-9 (printed version), ISBN 82-471-6400-0 (electronic version), ISSN 1503-8181.

“On the Shear Capacity of Steel Girders with Large Web Openings”.

Nils Christian Hagen, 2005:9 ISBN 82-471-6878-2 (printed version), ISBN 82-471-6877-4 (electronic version), ISSN 1503-8181.

”Behaviour of aluminium extrusions subjected to axial loading”.

Østen Jensen, 2005:7, ISBN 82-471-6873-1 (printed version), ISBN 82-471-6872-3 (electronic version), ISSN 1503-8181.

”Thermal Aspects of corrosion of Steel in Concrete”.

Jan-Magnus Østvik, 2005:5, ISBN 82-471-6869-3 (printed version), ISBN 82-471-6868 (electronic version), ISSN 1503-8181.

”Mechanical and adaptive behaviour of bone in relation to hip replacement.” A study of bone remodelling and bone grafting.

Sébastien Muller, 2005:34, ISBN 82-471-6933-9 (printed version), ISBN 82-471-6932-0 (electronic version), ISSN 1503-8181.

“Analysis of geometrical nonlinearities with applications to timber structures”.

Lars Wollebæk, 2005:74, ISBN 82-471-7050-5 (printed version), ISBN 82-471-7019-1 (electronic version), ISSN 1503-8181.

“Pedestrian induced lateral vibrations of slender footbridges”,

Anders Rönnquist, 2005:102, ISBN 82-471-7082-5 (printed version), ISBN 82-471-7081-7 (electronic version), ISSN 1503-8181.

“Initial Strength Development of Fly Ash and Limestone Blended Cements at Various Temperatures Predicted by Ultrasonic Pulse Velocity”.

Tom Ivar Fredvik, 2005:112, ISBN 82-471-7105-8 (printed version), ISBN 82-471-7103-1 (electronic version), ISSN 1503-8181.

“Behaviour and modelling of thin-walled cast components”,

Cato Dørum, 2005:128, ISBN 82-471-7140-6 (printed version), ISBN 82-471-7139-2 (electronic version), ISSN 1503-8181.

- “Behaviour and modelling of selfpiercing riveted connections”,  
Raffaele Porcaro, 2005:165, ISBN 82-471-7219-4 (printed version), ISBN 82-471-7218-6 (electronic version), ISSN 1503-8181.
- ”Behaviour and Modelling og Aluminium Plates subjected to Compressive Load”,  
Lars Rønning, 2005:154, ISBN 82-471-7169-1 (printed version), ISBN 82-471-7195-3 (electronic version), ISSN 1503-8181.
- ”Bumper beam-longitudinal system subjected to offset impact loading”,  
Satyanarayana Kokkula, 2005:193, ISBN 82-471-7280-1 (printed version), ISBN 82-471-7279-8 (electronic version), ISSN 1503-8181.
- “Control of Chloride Penetration into Concrete Structures at Early Age”,  
Guofei Liu, 2006:46, ISBN 82-471-7838-9 (printed version), ISBN 82-471-7837-0 (electronic version), ISSN 1503-8181.
- “Modelling of Welded Thin-Walled Aluminium Structures”,  
Ting Wang, 2006:78, ISBN 82-471-7907-5 (printed version), ISBN 82-471-7906-7 (electronic version), ISSN 1503-8181.
- ”Time-variant reliability of dynamic systems by importance sampling and probabilistic analysis of ice loads”,  
Anna Ivanova Olsen, 2006:139, ISBN 82-471-8041-3 (printed version), ISBN 82-471-8040-5 (electronic version), ISSN 1503-8181.
- “Fatigue life prediction of an aluminium alloy automotive component using finite element analysis of surface topography”,  
Sigmund Kyrre Ås, 2006:25, ISBN 82-471-7791-9 (printed version), ISBN 82-471-7791-9 (electronic version), ISSN 1503-8181.
- ”Constitutive models of elastoplasticity and fracture for aluminium alloys under strain path change”,  
Dasharatha Achani, 2006:76, ISBN 82-471-7903-2 (printed version), ISBN 82-471-7902-4 (electronic version), ISSN 1503-8181.
- “Simulations of 2D dynamic brittle fracture by the Element-free Galerkin method and linear fracture mechanics”,  
Tommy Karlsson, 2006:125, ISBN 82-471-8011-1 (printed version), ISBN 82-471-8010-3 (electronic version), ISSN 1503-8181.
- “Penetration and Perforation of Granite Targets by Hard Projectiles”,  
Chong Chiang Seah, 2006:188, ISBN 82-471-8150-9 (printed version), ISBN 82-471-8149-5 (electronic version), ISSN 1503-8181.

“Deformations, strain capacity and cracking of concrete in plastic and early hardening phases”,

Tor Arne Hammer, 2007:234, ISBN 978-82-471-5191-4 (printed version), ISBN 978-82-471-5207-2 (electronic version), ISSN 1503-8181.

“Crashworthiness of dual-phase high-strength steel: Material and Component behaviour”, Venkatapathi Tarigopula, 2007:230, ISBN 82-471-5076-4 (printed version), ISBN 82-471-5093-1 (electronic version), ISSN 1503-8181.

“Fibre reinforcement in load carrying concrete structures”,

Åse Lyslo Døssland, 2008:50, ISBN 978-82-471-6910-0 (printed version), ISBN 978-82-471-6924-7 (electronic version), ISSN 1503-8181.

“Low-velocity penetration of aluminium plates”,

Frode Grytten, 2008:46, ISBN 978-82-471-6826-4 (printed version), ISBN 978-82-471-6843-1 (electronic version), ISSN 1503-8181.

“Robustness studies of structures subjected to large deformations”,

Ørjan Fyllingen, 2008:24, ISBN 978-82-471-6339-9 (printed version), ISBN 978-82-471-6342-9 (electronic version), ISSN 1503-8181.

“Constitutive modelling of morsellised bone”,

Knut Birger Lunde, 2008:92, ISBN 978-82-471-7829-4 (printed version), ISBN 978-82-471-7832-4 (electronic version), ISSN 1503-8181.

“Experimental Investigations of Wind Loading on a Suspension Bridge Girder”,

Bjørn Isaksen, 2008:131, ISBN 978-82-471-8656-5 (printed version), ISBN 978-82-471-8673-2 (electronic version), ISSN 1503-8181.

“Cracking Risk of Concrete Structures in The Hardening Phase”,

Guomin Ji, 2008:198, ISBN 978-82-471-1079-9 (printed version), ISBN 978-82-471-1080-5 (electronic version), ISSN 1503-8181.

“Modelling and numerical analysis of the porcine and human mitral apparatus”,

Victorien Emile Prot, 2008:249, ISBN 978-82-471-1192-5 (printed version), ISBN 978-82-471-1193-2 (electronic version), ISSN 1503-8181.

“Strength analysis of net structures”,

Heidi Moe, 2009:48, ISBN 978-82-471-1468-1 (printed version), ISBN 978-82-471-1469-8 (electronic version), ISSN 1503-8181.

“Numerical analysis of ductile fracture in surface cracked shells”,

Espen Berg, 2009:80, ISBN 978-82-471-1537-4 (printed version), ISBN 978-82-471-1538-1 (electronic version), ISSN 1503-8181.

“Subject specific finite element analysis of bone – for evaluation of the healing of a leg lengthening and evaluation of femoral stem design”,  
Sune Hansborg Pettersen, 2009:99, ISBN 978-82-471-1579-4 (printed version), ISBN 978-82-471-1580-0 (electronic version), ISSN 1503-8181.

“Evaluation of fracture parameters for notched multi-layered structures”,  
Lingyun Shang, 2009:137, ISBN 978-82-471-1662-3 (printed version), ISBN 978-82-471-1663-0 (electronic version), ISSN 1503-8181.

“Modelling of Dynamic Material Behaviour and Fracture of Aluminium Alloys for Structural Applications”  
Yan Chen, 2009:69, ISBN 978-82-471-1515-2 (printed version), ISBN 978-82-471-1516-9 (electronic version), ISSN 1503-8181.

“Nanomechanics of polymer and composite particles”  
Jianying He 2009:213, ISBN 978-82-471-1828-3 (printed version), ISBN 978-82-471-1829-0 (electronic version), ISSN 1503-8181.

“Mechanical properties of clear wood from Norway spruce”  
Kristian Berbom Dahl 2009:250, ISBN 978-82-471-1911-2 (printed version) ISBN 978-82-471-1912-9 (electronic version), ISSN 1503-8181.

“Modeling of the degradation of TiB<sub>2</sub> mechanical properties by residual stresses and liquid Al penetration along grain boundaries”  
Micol Pezzotta 2009:254, ISBN 978-82-471-1923-5 (printed version) ISBN 978-82-471-1924-2 (electronic version) ISSN 1503-8181.

“Effect of welding residual stress on fracture”  
Xiabo Ren 2010:77, ISBN 978-82-471-2115-3 (printed version) ISBN 978-82-471-2116-0 (electronic version), ISSN 1503-8181.

“Pan-based carbon fiber as anode material in cathodic protection system for concrete structures”  
Mahdi Chini 2010:122, ISBN 978-82-471-2210-5 (printed version) ISBN 978-82-471-2213-6 (electronic version), ISSN 1503-8181.

“Structural Behaviour of deteriorated and retrofitted concrete structures”  
Irina Vasililjeva Sæther 2010:171, ISBN 978-82-471-2315-7 (printed version) ISBN 978-82-471-2316-4 (electronic version) ISSN 1503-8181.

“Prediction of local snow loads on roofs”  
Vivian Meløysund 2010:247, ISBN 978-82-471-2490-1 (printed version) ISBN 978-82-471-2491-8 (electronic version) ISSN 1503-8181.

“Behaviour and modelling of polymers for crash applications”  
Virgile Delhaye 2010:251, ISBN 978-82-471-2501-4 (printed version) ISBN 978-82-471-2502-1 (electronic version) ISSN 1503-8181.

“Blended cement with reduced CO<sub>2</sub> emission – Utilizing the Fly Ash-Limestone Synergy”,  
Klaartje De Weerd 2011:32, ISBN 978-82-471-2584-7 (printed version) ISBN 978-82-471-2584-4 (electronic version) ISSN 1503-8181.

“Chloride induced reinforcement corrosion in concrete” Concept of critical chloride content – methods and mechanisms.  
Ueli Angst 2011:113, ISBN 978-82-471-2769-9 (printed version) ISBN 978-82-471-2763-6 (electronic version) ISSN 1503-8181.

“A thermo-electric-Mechanical study of the carbon anode and contact interface for Energy savings in the production of aluminium”.  
Dag Herman Andersen 2011:157, ISBN 978-82-471-2859-6 (printed version) ISBN 978-82-471-2860-2 (electronic version) ISSN 1503-8181.

“Structural Capacity of Anchorage Ties in Masonry Veneer Walls Subjected to Earthquake”. The implications of Eurocode 8 and Eurocode 6 on a typical Norwegian veneer wall.  
Ahmed Mohamed Yousry Hamed 2011:181, ISBN 978-82-471-2911-1 (printed version) ISBN 978-82-471-2912-8 (electronic ver.) ISSN 1503-8181.

“Work-hardening behaviour in age-hardenable Al-Zn-Mg(-Cu) alloys”.  
Ida Westermann , 2011:247, ISBN 978-82-471-3056-8 (printed ver.) ISBN 978-82-471-3057-5 (electronic ver.) ISSN 1503-8181.

“Behaviour and modelling of selfpiercing riveted connections using aluminium rivets”.  
Nguyen-Hieu Hoang, 2011:266, ISBN 978-82-471-3097-1 (printed ver.) ISBN 978-82-471-3099-5 (electronic ver.) ISSN 1503-8181.

“Fibre reinforced concrete”.  
Sindre Sandbakk, 2011:297, ISBN 978-82-471-3167-1 (printed ver.) ISBN 978-82-471-3168-8 (electronic ver.) ISSN 1503-8181.

“Dynamic behaviour of cablesupported bridges subjected to strong natural wind”.  
Ole Andre Øiseth, 2011:315, ISBN 978-82-471-3209-8 (printed ver.) ISBN 978-82-471-3210-4 (electronic ver.) ISSN 1503-8181.

“Constitutive modeling of solargrade silicon materials”  
Julien Cochard, 2011:307, ISBN 978-82-471-3189-3 (printed ver.) ISBN 978-82-471-3190-9 (electronic ver.) ISSN 1503-8181.

“Constitutive behavior and fracture of shape memory alloys”  
Jim Stian Olsen, 2012:57, ISBN 978-82-471-3382-8 (printed ver.) ISBN 978-82-471-3383-5 (electronic ver.) ISSN 1503-8181.



“Field measurements in mechanical testing using close-range photogrammetry and digital image analysis”

Egil Fagerholt, 2012:95, ISBN 978-82-471-3466-5 (printed ver.) ISBN 978-82-471-3467-2 (electronic ver.) ISSN 1503-8181.

“Towards a better understanding of the ultimate behaviour of lightweight aggregate concrete in compression and bending”

Håvard Nedrelid, 2012:123, ISBN 978-82-471-3527-3 (printed ver.) ISBN 978-82-471-3528-0 (electronic ver.) ISSN 1503-8181.

“Numerical simulations of blood flow in the left side of the heart”

Sigrid Kaarstad Dahl, 2012:135, ISBN 978-82-471-3553-2 (printed ver.) ISBN 978-82-471-3555-6 (electronic ver.) ISSN 1503-8181.

“Moisture induced stresses in glulam”

Vanessa Angst-Nicollier, 2012:139, ISBN 978-82-471-3562-4 (printed ver.) ISBN 978-82-471-3563-1 (electronic ver.) ISSN 1503-8181.

“Biomechanical aspects of distraction osteogenesis”

Valentina La Russa, 2012:250, ISBN 978-82-471-3807-6 (printed ver.) ISBN 978-82-471-3808-3 (electronic ver.) ISSN 1503-8181.

“Ductile fracture in dual-phase steel. Theoretical, experimental and numerical study”

Gaute Gruben, 2012:257, ISBN 978-82-471-3822-9 (printed ver.) ISBN 978-82-471-3823-6 (electronic ver.) ISSN 1503-8181.

“Damping in Timber Structures”

Nathalie Labonnote, 2012:263, ISBN 978-82-471-3836-6 (printed ver.) ISBN 978-82-471-3837-3 (electronic ver.) ISSN 1503-8181.

“Biomechanical modeling of fetal veins: The umbilical vein and ductus venosus bifurcation”

Paul Roger Leinan, 2012:299, ISBN 978-82-471-3915-8 (printed ver.) ISBN 978-82-471-3916-5 (electronic ver.) ISSN 1503-8181.

“Large-Deformation behaviour of thermoplastics at various stress states”

Anne Serine Ognedal, 2012:298, ISBN 978-82-471-3913-4 (printed ver.) ISBN 978-82-471-3914-1 (electronic ver.) ISSN 1503-8181.

“Hardening accelerator for fly ash blended cement”

Kien Dinh Hoang, 2012:366, ISBN 978-82-471-4063-5 (printed ver.) ISBN 978-82-471-4064-2 (electronic ver.) ISSN 1503-8181.

“From molecular structure to mechanical properties”

Jiayang Wu, 2013:186, ISBN 978-82-471-4485-5 (printed ver.) ISBN 978-82-471-4486-2 (electronic ver.) ISSN 1503-8181.

“Experimental and numerical study of hybrid concrete structures”

Linn Grepstad Nes, 2013:259, ISBN 978-82-471-4644-6 (printed ver.) ISBN 978-82-471-4645-3 (electronic ver.) ISSN 1503-8181.

“Mechanics of ultra-thin multi crystalline silicon wafers”

Saber Saffar, 2013:199, ISBN 978-82-471-4511-1 (printed ver.) ISBN 978-82-471-4513-5 (electronic ver.) ISSN 1503-8181.

“Through process modelling of welded aluminium structures”

Anizahyati Alisibramulisi, 2013:325, ISBN 978-82-471-4788-7 (printed ver.) ISBN 978-82-471-4789-4 (electronic ver.) ISSN 1503-8181.

“Combined blast and fragment loading on steel plates”

Knut Gaarder Rakvåg, 2013:361, ISBN 978-82-471-4872-3 (printed ver.) ISBN 978-82-4873-0 (electronic ver.) ISSN 1503-8181.

“Characterization and modelling of the anisotropic behaviour of high-strength aluminium alloy”

Marion Fourmeau, 2014:37, ISBN 978-82-326-0008-3 (printed ver.) ISBN 978-82-326-0009-0 (electronic ver.) ISSN 1503-8181.

“Behaviour of threated steel fasteners at elevated deformation rates”

Henning Fransplass, 2014:65, ISBN 978-82-326-0054-0 (printed ver.) ISBN 978-82-326-0055-7 (electronic ver.) ISSN 1503-8181.

“Sedimentation and Bleeding”

Ya Peng, 2014:89, ISBN 978-82-326-0102-8 (printed ver.) ISBN 978-82-326-0103-5 (electric ver.) ISSN 1503-8181.

“Impact against X65 offshore pipelines”

Martin Kristoffersen, 2014:362, ISBN 978-82-326-0636-8 (printed ver.) ISBN 978-82-326-0637-5 (electronic ver.) ISSN 1503-8181.

“Formability of aluminium alloy subjected to prestrain by rolling”

Dmitry Vysochinskiy, 2014:363,, ISBN 978-82-326-0638-2 (printed ver.) ISBN 978-82-326-0639-9 (electronic ver.) ISSN 1503-8181.

“Experimental and numerical study of Yielding, Work-Hardening and anisotropy in textured AA6xxx alloys using crystal plasticity models”

Mikhail Khadyko, 2015:28, ISBN 978-82-326-0724-2 (printed ver.) ISBN 978-82-326-0725-9 (electronic ver.) ISSN 1503-8181.

“Behaviour and Modelling of AA6xxx Aluminium Alloys Under a Wide Range of Temperatures and Strain Rates”

Vincent Vilamosa, 2015:63, ISBN 978-82-326-0786-0 (printed ver.) ISBN 978-82-326-0787-7 (electronic ver.) ISSN 1503-8181.

“A Probabilistic Approach in Failure Modelling of Aluminium High Pressure Die-Castings”

Octavian Knoll, 2015:137, ISBN 978-82-326-0930-7 (printed ver.) ISBN 978-82-326-0931-4 (electronic ver.) ISSN 1503-8181.

“Ice Abrasion on Marine Concrete Structures”

Egil Møen, 2015:189, ISBN 978-82-326-1034-1 (printed ver.) ISBN 978-82-326-1035-8 (electronic ver.) ISSN 1503-8181.

“Fibre Orientation in Steel-Fibre-Reinforced Concrete”

Giedrius Zirgulis, 2015:229, ISBN 978-82-326-1114-0 (printed ver.) ISBN 978-82-326-1115-7 (electronic ver.) ISSN 1503-8181.

“Effect of spatial variation and possible interference of localised corrosion on the residual capacity of a reinforced concrete beam”

Mohammad Mahdi Kioumarsi, 2015:282, ISBN 978-82-326-1220-8 (printed ver.) ISBN 978-82-1221-5 (electronic ver.) ISSN 1503-8181.

“The role of concrete resistivity in chloride-induced macro-cell corrosion”

Karla Horbostel, 2015:324, ISBN 978-82-326-1304-5 (printed ver.) ISBN 978-82-326-1305-2 (electronic ver.) ISSN 1503-8181.

“Flowable fibre-reinforced concrete for structural applications”

Elena Vidal Sarmiento, 2015:335, ISBN 978-82-326-1324-3 (printed ver.) ISBN 978-82-326-1325-0 (electronic ver.) ISSN 1503-8181.

“Development of chushed sand for concrete production with microproportioning”

Rolands Cepuritis, 2016:19, ISBN 978-82-326-1382-3 (printed ver.) ISBN 978-82-326-1383-0 (electronic ver.) ISSN 1503-8181.

“Withdrawal properties of threaded rods embedded in glued-laminated timber elements”

Haris Stamatopoulos, 2016:48, ISBN 978-82-326-1436-3 (printed ver.) ISBN 978-82-326-1437-0 (electronic ver.) ISSN 1503-8181.

“An Experimental and numerical study of thermoplastics at large deformation”

Marius Andersen, 2016:191, ISBN 978-82-326-1720-3 (printed ver.) ISBN 978-82-326-1721-0 (electronic ver.) ISSN 1503-8181.

“Modeling and Simulation of Ballistic Impact”

Jens Kristian Holmen, 2016:240, ISBN 978-82-326-1818-7 (printed ver.) ISBN 978-82-326-1819-4 (electronic ver.) ISSN 1503-8181.

“Early age crack assessment of concrete structures”

Anja B. Estensen Klausen, 2016:256, ISBN 978-82-326-1850-7 (printed ver.) ISBN 978-82-326-1851-4 (electronic ver.) ISSN 1503-8181.

